To my parents

Kathleen and Jack

APPLICATIONS OF LASER PRODUCED CONTINUUM RADIATION

A THESIS FOR THE DEGREE OF

MASTER OF SCIENCE

PRESENTED TO THE NATIONAL COUNCIL FOR EDUCATIONAL AWARDS

By

James Brilly

SCHOOL OF PHYSICAL SCIENCES

NATIONAL INSTITUTE FOR HIGHER EDUCATION DUBLIN

RESEARCH SUPERVISOR

Dr Eugene T Kennedy

TABLE OF CONTENTS.

CHAPTER THREE EXPERIMENTAL RESULTS. PAGE

LIST OF FIGURES.

CHAPTER ONE PAGE

CHAPTER TWO PAGE

CHAPTER THREE PAGE

APPENDIX ONE PAGE

LIST OF TABLES PAGE

ABSTRACT

High density high temperature plasmas produced in the foci of powerful pulsed laser beams have many applications and have been the subject of intensive investigations since high power lasers first became available

The work described in this thesis is largly concerned with one particular application of laser generated plasmas that of photoabsorption spectroscopy of ionized species The first chapter provides an introduction to the subject by reviewing the work done to date in this area and the various techniques which have been used to obtain absorption spectra The usefulness of results obtained from VUV absorption spectra is also dealt with Recent work on the laser produced continuum source and the various applications which the source has found is also reviewed

A detailed description of the experimental method used to create two laser produced plasmas on separate targets and study the resulting absorption spectrum which is observed when continuum radiation emitted from one plasma is absorbed by the second plasma is given

New absorption spectra of magnesium aluminium and silicon plasmas are discussed and results are presented for the third fourth and fifth members of the neon-like isoelectronic sequence Mg III Al IV and Si V The VUV absorption spectra of these ions have been recorded in the wavelength range 250 - 60Å This is the first recorded observation of absorption features along an extended isoelectronic sequence The wavelengths of the principal $2s^2 2p^6\ {}^1S_0 - 2s^2 2p^5 ns$ nd transitions have been measured Also the autoionizing levels due to inner 2s shell excitation $2s^2 2p^6\ {}^1S_0 - 2s\ 2p^6 np\ {}^1P_1$ have been recorded and wavelengths for these features are given

Many new lines particularly in the spectra of aluminium and silicon plasmas are reported in this work for the first time Extensive atomic structure calculations have been carried out in an attempt to assign these features Calculations have also been carried out for the autoionizing levels of the neon-like sequence from Na II to Si V

The Xenon isoelectronic sequence has also been studied in absorption and results are presented for the absorption spectrum of a lanthanum plasma The 4d photoabsorption spectrum of La IV has been recorded for the first time in this work and this spectrum is discussed in terms of the previously observed 4d photoabsorption spectrum of Ba III

Progress on the evaluation of neutron scintillating glasses as new detector materials for the VUV spectral region is reported in Appendix 1 This application of laser produced continua is discussed and tentative results for cerium doped glass scintillators are presented

In Appendix 2 computer programs written over the course of this work are described Examples of input and output data are given

CHAPTER ONE INTRODUCTION

1 1 PLASMAS IN GENERAL

In general terms a plasma (sometimes described as the fourth state of matter) is matter in a state of *ionization* a gas *ionized sufficiently* so that the charge separation which can take place in it is small when compared to its macroscopic charge density On a macroscopic scale therefore a plasma is approximately neutral although its principal constituents are electrons and charged ions

This condition of overall neutrality is given by

$$N_e = \sum_z N_z Z \qquad (1\ 1)$$

where N_e is the electron number density and N_Z is the number density of ions of charge Z In order to produce and maintain such a medium a sufficient amount of energy is required to dissociate and ionize the initially neutral matter and to give the ions and electrons sufficient kinetic energy to prevent immediate reattachment and recombination over the cycle of the plasma

The reactions between particles in a neutral gas are both weak and short ranged whereas in a plasma reactions occur between charged particles and the Coulomb forces involved in these reactions are both relatively strong and act over a considerably longer range Thus plasma reactions are entirely different from those of the original neutral gas

One of the distinguishing features of a plasma is the exhibition of collective behaviour Some of the criteria necessary for a plasma to show collective behaviour are discussed below and can be summarised in the following four expressions relating the main plasma parameters

$$N_e \simeq N_i \qquad (1\ 2)$$

$$\lambda_D \ll L \qquad (1\ 3)$$

$$\frac{4\pi}{3}\lambda_D^3 N_e \gg 1 \qquad (1\ 4)$$

$$\frac{2\pi}{\omega_p} < \frac{1}{\nu_c} \qquad (1\ 5)$$

The condition fulfilled by eq(1 2) is the overall charge neutrality of the plasma N_e and N_i are the electron and ion number densities respectively The range of values of N_e and N_i for both laboratory and astrophysical plasmas are extensive as can be seen by reference to fig(1 1) In eq(1 3) λ_D is known as the Debye length and is given by

$$\lambda_D = \left[\frac{\epsilon_0 kT_e}{N_e e^2} \right]^{\frac{1}{2}} \qquad (1\ 6)$$

λ_D is a shielding distance defined as the distance over which N_e can differ appreciably from $N_e Z$ In eq(1 6) ϵ_0 is the permittivity of free space k is Boltzmanns constant T_e is the electron temperature and e the charge on the electron When discussing collective effects in plasmas λ_D is an important parameter in that it measures the minimum size of a system in which collective effects are dominant when compared with single particle effects Again reference to fig(1 1) shows the range of λ_D values for the different types of plasma

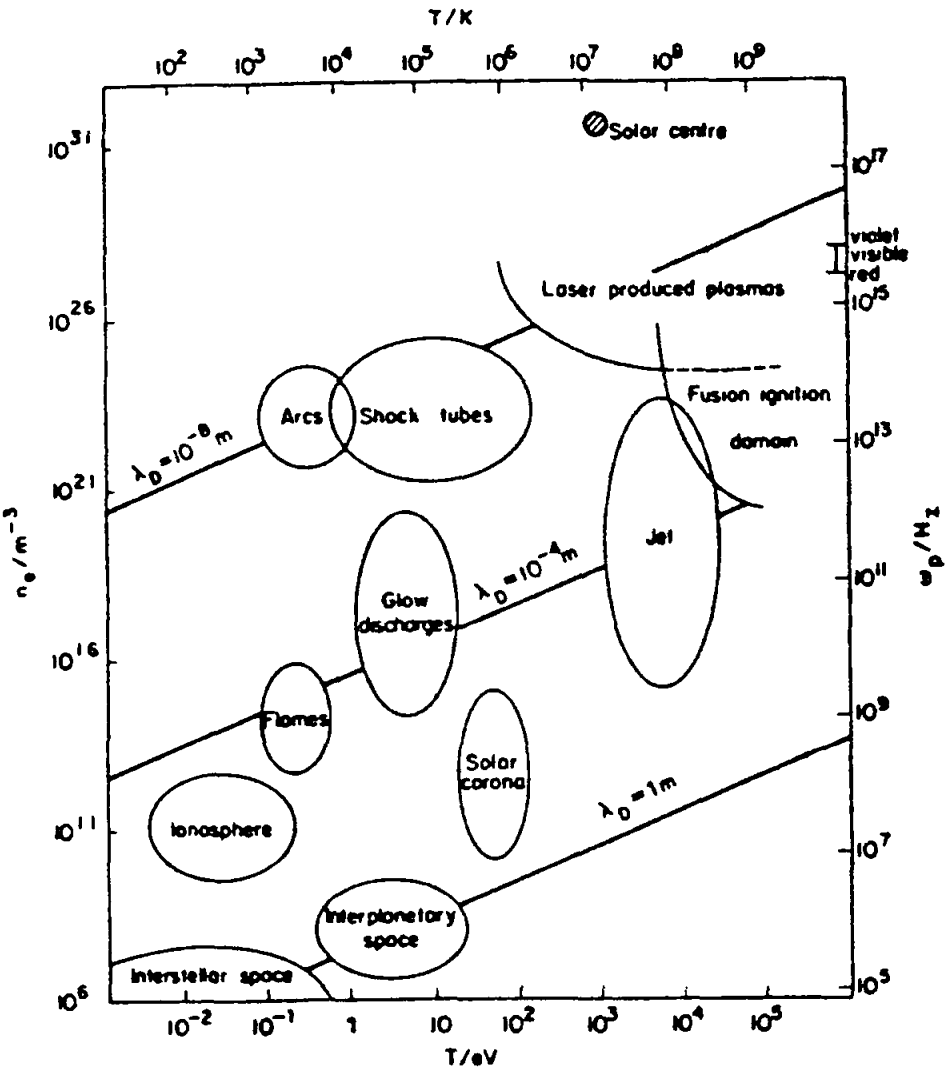

Fig (1 1) Shows the various types of plasma both laboratory and astrophysical together with typical temperature and density ranges, and carrisponding values of λ_D Jet represents the Joint European Torus (After Carroll and Kennedy (1981))

In order to obtain an expression for λ_D one assumes a smooth change in electric field in the region of the particle under consideration This necessarily assumes a large number of particles in the neighbourhood The third criterion given in eq(1 4) ensures that this is so The plasma frequency ω_p is defined by the equation

$$\omega_p = \left[\frac{Ne\ e^2}{m_e\ \epsilon_0} \right]^{\frac{1}{2}} \qquad (1\ 7)$$

where m_e is the electron mass The plasma frequency ω_p is one of the main paramoters used in describing collective oscillations in the plasma ω_p is the cut-off frequency for the transmission of electromagnetic waves through a plasma In order that collective oscillations can develop collisional damping must be small, this will be so when eq(1 6) is satisfied The dependence of ω the frequency of the incident waves on the propagation constant $k = 2\pi/\lambda$ can be shown from the solution of Maxwells equations for an ionized medium to be given by

$$\omega^2 = \omega_p^2 + c^2k^2 \qquad (1\ 8)$$

and the phase and group velosities of such waves in the plasma are found to be given in terms of the plasma frequency as,

$$v_p = \frac{\omega}{k} = c \left[1 - \frac{\omega_p^2}{\omega^2} \right]^{-\frac{1}{2}} \qquad (1\ 9)$$

$$v_g = \frac{d\omega}{dk} = c \left[1 - \frac{\omega_p^2}{\omega^2} \right]^{\frac{1}{2}} \qquad (1\ 10)$$

The subject of waves in plasmas is to say the least complex and is not dealt

with further in this work This area of plasma physics may however be pursued in a number of general references (see for example Hughes (1975) or Hora (1980)) given at the end of this chapter

Any account of the fundamental concepts of plasma physics however brief would be incomplete without reference to the various atomic processes which occur within plasmas Atomic processes govern the way in which photons electrons, ions and neutral atoms within the plasma interact with one another Processes such as collisional excitation and de-excitation collisional ionization and recombination photoexcitation and de-excitation, photoionization and recombination are largely self-explanatory They involve interactions between photons and electrons on the one hand and ions and neutral atoms within the plasma on the other This results in a loss or gain of kinetic energy for free electrons and a resulting excitation, de-excitation or ionization/recombination of the electronic structure of an ion or neutral atom The process of Bremsstrahlung involves free free transitions within an electronic structure composed of an electron of charge e and an ion of charge Ze The resulting transitions within the compound system of charge (Z-1)e give rise to continuum radiation when a transition from a higher to a lower continuum state of the system results in the emission of a photon It should be noted here that both Bremsstrahlung and the inverse of the process known simply as inverse Bremsstrahlung (which involves an electron in such a system making a transition to a higher state with a resulting increase in its kinetic energy) together play a very important part over the cycle of a laser produced plasma A comprehensive review of atomic processes in plasmas is given by Cooper (1966) the subject is also covered more recently in the list of general references provided at the end of this chapter

The atomic processes determine the macroscopic state of the plasma The criterion of equilibrium in plasmas is used to describe this macroscopic state The ideal plasma is described as being in a state of **complete thermodynamic equilibrium.** for such a plasma the following would hold (a) all particles neutral atoms ions, and electrons would possess Maxwellian velocity distributions characterized by the same temperature. (b) all population distributions over the states of atoms and ions would obey the Boltzmann formula (c) the fraction of ions in state Z relative to those in state (Z-1) would be given by the Saha equation and finally (d) the intensity distribution of the radiation as a function of frequency and temperature in such an ideal thermodynamic enclosure would be given by the Planck formula Such conditions do not of course obtain in real plasmas the fact that a plasma radiates energy prevents condition (d) from being fulfilled However, plasmas are found to obey other less complete, models of equilibrium For high density plasmas by which is meant that the plasma obeys the density condition

$$N_e \geq 1.6X10^{18} T_e^{0.5} \chi^3 \qquad (1.11)$$

(Where χ is the excitation energy in eV of the transition under consideration) the equilibrium model applied is that of **local thermodynamic equilibrium** (LTE) in which electron collisional processes are assumed to dominate At lower densities the **coronal model** applies and for intermediate plasmas the **collisional radiative model** is said to hold The various models of plasma equilibrium and the conditions under which each applies are discussed in more detail in the general references or for a brief account see Knot (1971) or Carroll and Kennedy (1981)

1 2 LASER PRODUCED PLASMAS

High density high temperature plasmas produced in the foci of powerful (>MW) pulsed laser beams have many applications and have been the subject of prolonged and very intensive investigations since the early to mid sixties when powerful lasers first became available

Laser produced plasmas have in recent years found a number of interesting uses One of the major goals of laser plasma physics is the possibility of extracting useful quantities of nuclear power indeed there appears to be a very definite possibility of producing useful amounts of nuclear fusion energy by the use of lasers At low to medium intensities (10^{16}–10^{17}Wcm^{-2}) all materials are heated vaporized and ionized At high intensities (10^{20}–10^{22}Wcm^{-2}) the relativistic change in the electron mass when quivering in the strong laser field (10^{12}volts cm^{-1}) results in relativistic optical constants which cause quick shrinking of the laser beam to one wavelength diameters this has resulted in the detection of ions with energies in excess of 10MeV flying against the laser beam (see for example Hora 1980) Also the excitation of nuclei by lasers has been reported. (Izawa et al (1979)) Laser produced plasmas have also been used to achieve compression of matter to extremely high densities and as sources of both hard and soft x-rays neutrons, and highly charged ions

Also of current interest is the possibility of achieving laser action at short wavelengths (in the VUV/soft x-ray regime) The major problem here is the obtainment of a significant degree of population density inversion between the

lasing states Recently there have been several reports of population inversions in laser produced plasmas Among the more interesting has been the observation and measurement of population inversions between the upper n=4 5, 6 and the lower n=3 levels in C^{4+} and C^{5+} ions for potential quasi-cw lasing in tho $\lambda = 35-76$ nm wavolength range. (Dixon et al (1977 and 1978)) Hydrogen helium and neon like ions are important as laser media as they provide metastable levels which can be populated by either collisional excitation or *recombination* in laser produced plasmas. and much work is underway in this field Calculations for XUV gain in laser produced aluminium plasmas have been carried out by Pert and Tallents (1981) and show promising results with predictions of significant small signal gain from the hydrogen like Al XIII Balmer α 38 7A transition More recently Silfvast et al (1982) have observed some fifty new laser transitions in the visible and near infrared in difforont metal vapours in the recombination phase of an expanding laser produced plasma and suggest that all of the reported transitions offer possible candidates for the long sought after x-ray laser when isoelectronically scaled to higher ion stages Boiko et al (1983) reported the observation of stimulated emission due to Be II transitions in a recombining laser produced plasma The stimulated emission was observed as a result of transitions in the Be II ion for λ = 467 and 436 nm in an expanding laser produced plasma 2cm long and approximately 200 μm wide formed on a solid target by a 20J 10nsec Nd-glass laser There have also been the recent reports of substantial progress in x-ray lasor technology reported at the Lawrence - Livermore Laboratory (see Matthews etal (1985))

A roview of progress and tronds in x-ray laser research with particular attention to the hydrogen like ion approach is given by Elton (1981) and Pert (1981) has reviewed the current state of research in EUV laser action in plasmas in

which he describes the many proposals outlined for the production of sufficient gain at short wavelengths, and the various avenues by which laser action in plasmas has been explored with particular attention given to the recombination scheme.

The lasers used in the high intensity experiments described above are mostly of the Neodymium doped glass variety the output powers of which usually lie in the 1GW — 1TW range. This output is then focused with an aspheric lens of usually f = 10cm onto a solid target situated in a vacuum, and results in focused power densities of between 10^{13} and $10^{16}Wcm^{-2}$ achieved for pulse durations ranging from 100psec to 6nsec. In such plasmas temperatures approaching 1KeV can be generated and electron densities of 10^{19} to 10^{22} cm^{-1}, are typical and as a result both high and low energy levels are substantially populated. In such fast expanding plasmas population inversions may result in the recombination phase.

A useful review of laser produced plasmas is that of Carroll and Kennedy (1981), and for plasmas in the high intensity regime see Kennedy (1984). A general review of the subject of laser produced plasmas has been given by De Michelis and Matioli (1981) in which they discuss soft x—ray diagnostics of laboratory plasmas in general and also discuss laser produced plasmas as soft x—ray sources. Nagel (1984) describes the characteristics and uses of x—radiation from laser heated plasmas created on solid targets, and discusses recent x-ray measurements obtained with laser repetition rates of up to 10 Hz. The possible applications of the laser produced plasma as an x-ray source in research and industry are outlined. Morgan (1983) gives a brief account of the salient characteristics of laser produced plasmas and outlines some of the principal processes which are responsible for their formation.

The literature on the subject of laser produced plasmas is extensive the intention here has been to give a brief account of laser produced plasmas In the next section particular attention is given to the spectroscopic applications ie the use of laser produced plasmas as sources of continuum radiation in the VUV and as a versatile ion source

1 3 THE LASER PRODUCED PLASMA AS A LIGHT SOURCE IN THE VUV

The first report of continuum emission from a laser produced plasma was published by Ehler and Weissler (1966) Using the output of a 100MW ruby laser focused onto various metal target surfaces, they found that the spectral output of the resulting plasmas contained both discrete and continuum emission but when high Z targets such as tungsten, platinum and tantalum were used the emission lines were only slightly more intense than the continuum and that the spectral output from plasmas produced on low Z targets contained a much more intense line emission The continua from tungsten tantalum and platinum plasmas were found though not accurately to peak at around 200Å and to extend to about 120Å

Williams (1973) using a photoelectric detector rather than the photographic plates used by Ehler and Weissler examined the spectrum of a laser produced uranium plasma and found the continuum to peak at around 750Å He also concluded that no significant continuum emission from uranium existed between 250 and 130A this result was later found by Damany and Esteva (1975) to be in error Studies of continuum emission were also carried out by Breton and Papoular (1973) who examined the emission, from high Z metal targets between 1000 and 2000Å Among the general results they reported were observations that the continuum emission per pulse increased almost linearly with target irradiance but more slowly with laser pulse length and wavelength They also reported on the effect of ambient pressure on continuum emission and found that with an ambient pressure of about 10^{-1} torr the continuum was reduced considerably However the continua were found to be less sensitive to laser focusing and angle of observation a result also

observed by Dewhurst Khan and Pert (1975)

The laser produced plasma was investigated primarily as a source of VUV continuum emission to provide a background for absorption experiments by Kennedy (1977) and Carroll et al (1980) In a series of experiments they investigated the spectral output of various metal targets between 30 and 2000 A The results of their experiments revealed the existence of strong usable continua throughout this spectral region The elements studied were all of high Z ($57 < Z < 74$) and strong continua were reported for uranium hafinum, tungsten, and for the rare earths in both the normal and grazing incidence regions The continua produced from the rare earths and other high Z elements were found to possess the following properties which specifically recommend them for use in VUV absorption spectroscopy as backlighting sources

EASE OF PRODUCTION the only requirement being simple focusing of a Q-switched laser on a suitable metal target

EASE OF LOCATION since the target is simply a piece of metal, the plasma position is therefore completely controllable by manipulation of the focusing optics

SPECTRAL PURITY This is dependent on the purity of the target material Spectroscopically pure materials are readily available with purities of better than 99 99% so that line free continua are normally obtained

NOISELESS since the laser producing the plasma can be operated from a remote position thus avoiding unwanted electrical noise

SPECTRAL EXTENT the continuua were found to be strong in the wavelength range 30-2000Å depending on the choice of target

PULSE DURATION this was found to be on the same time scale as the laser

pulse used to generate the continuum (typically ≈30ns)

SYNCHRONIZATION by splitting the laser beam two-plasma experiments could be performed, a time delay could be introduced by redirecting one portion of the beam using an optical delay line Thus time delays of up to 100nsec could be achieved quite easily For longer time delays electronic delay circuitry would need to be employed

SPATIAL EXTENT. the region of continuum emission was found to be very small almost point like (typically ≈ μm)

AMBIENT PRESSURE the source was found to be quite insensitive to ambient pressure and as a demonstration of this Kennedy (1977) presented absorption studies of the rare gases in the VUV and O'Sullivan (1982 a b) reported on experiments involving VUV absorption of low molecular weight organic compounds

REPRODUCABILITY the continua were also found not to suffer seriously from pulse to pulse variations in laser output

The results of these experiments were reported in a series of publications which followed Carroll Kennedy and O'Sullivan (1978) Carroll Kennedy and O'Sullivan (1980), O'Sullivan Carroll Mc'Ilrath and Ginter (1981) and later a design for a "table top VUV source" based on the laser produced plasma was proposed (Carroll Kennedy and O'Sullivan (1983)) The usefulness of the laser produced plasma as a backlighting source for absorption experiments in the VUV was also established by the same authors for LiII (Carroll and Kennedy (1977)) and for Be II (Kennedy and Carroll (1977))

Other workers have also investigated the VUV emission of laser produced plasmas, Heckenkamp, Heinzmann and Schonhznse (1981) studied the

feasability of using laser generated plasmas as VUV continuum sources for photoelectron spectroscopy and measured the spectral intensity distribution in the wavelength region from 43 - 79nm by energy analysis of the photoelectrons ejected from argon atoms Their results showed a shift in the emission maximum to lower wavelengths with increasing laser energy Fischer and Kuhne (1983) carried out studies into the time duration of the VUV emission from laser produced plasmas as a function of pulse length and observation wavelength and noted a wavelength dependent correlation between laser pulse length and the time duration of the vuv emission from the plasma They found the vuv emission to be on the same time scale as the laser pulse length and that by increasing the laser pulse length longer wavelength vuv emission was observed

Sinha and Gopi (1980) have studied x-ray and vuv continuum emission from a copper target Jannitti Nicolosi and Tondello (1983) have reported an experiment in which an "extremely clean and intense ($\simeq 5X10^{7}$ Wcm^{-2} Sr^{-1} $Å^{-1}$)" continuum between 20 and 80Å was emitted by a plasma also produced on a copper target Other applications of laser produced continuua besides the investigation of atomic structure have recently been studied Vinogradov et al (1982) carried out an investigation of laser produced plasmas as a soft x-ray source operating at laser power densities of $5X10^{11} - 2X10^{14}$ Wcm^{-2} They studied the conversion efficiency of laser radiation into x-rays emitted by plasmas over a wide range of power densities and atomic number of target materials (4 - 92) The studies were carried out with a view to obtaining a suitable soft x-ray source for use in x-ray photolitography of resists More recently Caro et al (1984) used a laser produced plasma as a soft x-ray continuum source to generate metastable ions By focusing a laser beam through Li vapor onto a massive target inside the vapor a population of

$Li^+(1s2s)$ ions in excess of $10^{15}cm^{-3}$ was measured $Li^+(1s2s)$ population measurements were made for different target materials including thallium iron nickel and lithium. the authors also discussed their work with respect to possible applications to various proposed extreme ultraviolet laser systems

1 4 OTHER SOURCES OF CONTINUUM VUV/SOFT X-RAY RADIATION

There are several ways in which continuum vuv radiation may be produced Before the advent of laser produced plasmas the major sources of continuum VUV were synchrotrons and various types of gas and vacuum spark discharges Synchrotrons have been used for vuv spectroscopy since the first absorption experiments carried out in the early 1960's (Madden and Codling (1963 1964) and Codling and Madden (1964)) Comprehensive reviews of synchrotron radiation and its applications to atomic spectroscopy and other areas have been given by Codling (1973) and more recently by Wuilleumier (1981) and Williams (1983) The major disadvantages of synchrotron radiation are that since sychrotrons are large and expensive facilities they are generally unavailable to the "average spectroscopist" although this is changing as many synchrotron facilities have been built specifically for use as radiation sources whereas previously spectroscopists only had access to synchrotrons as parasitic users The requirement of an ultra high vacuum environment for synchrotron use can impose restrictions on certain types of experiment such as absorption experiments involving gases or vapors (or absorption experiments on laser produced plasmas which have not as yet been carried out) There are also the effects of hard x-rays produced by the machine which impose the further restriction that experiments must be carried out remotely Clearly the experiments must also be carried out at the site of the storage ring or synchrotron and not in the users own laboratory Lastly an important factor concerning the nature of the radiation is that synchrotron radiation is highly polarized and possesses only small emittance in the plane vertical to the electron orbit

Because of the above reasons a substantial effort has been put into the development of other bright VUV radiation sources. The two potential candidates to fulfil this role are the laser produced plasma, which has been discussed above, and the vacuum spark discharge which is discussed below.

Balloffet (1960), while studying the spectral emission of spark discharges in vacuo, observed a continuum which was only present when electrodes of high atomic number such as tungsten or platinum were used. In a further report Balloffet et al (1961) used a uranium anode and observed continuum radiation in the range 80 - 2000Å. The discharge conditions were typically 0.05μF, 22kV, 0.08μH, with a peak current of 55kA and a pulse duration of 1.25μsec. Further study by Balloffet et al (1962) of Laue diffraction patterns formed by a crystal of NaCl revealed that soft x-rays were also present in the discharge. Spatial studies which were carried out indicate that the origin of the continuum is located around the high density plasma sheath produced by the high current densities. It is thought (Lotte et al (1963)) that the deceleration of electrons within this plasma sheath produces bremsstrahlung radiation. Thus with the extremely high current densities present in spark discharges a strong continuum might be expected. Free bound transitions must also be present but to what extent is not known. However, the observations show that the anode must be a high Z element and that when low Z anodes are used only line spectra are observed.

A modern version of this BRV source, as it is now generally known, is commercially available from Chelsea Instruments, U.K. The source consists of a cylindrical uranium rod which serves as the anode, the brass cathode has a central bore and contains a third trigger electrode which initiates the main discharge by means of a sliding spark between this trigger electrode and the

cathode The main discharge produces a hot dense uranium plasma in front of the anode, which is viewed end-on through the hole in the cathode The source has the following operating paramaters an operating voltage of 20KV, capacitance of 0 05μF, stored electrical energy of 10J The anode cathode discharge is approximately 3mm The source operates in a pressure of $< 10^{-3}$ torr and has a repetition rate of 0 1Hz

A radiometric comparision of the above BRV source with a laser produced plasma has been carried out in the normal incidence region by Kuhne (1982) His main conclusions were that although both sources have a similar distribution of time-integrated spectral radiance the laser produced plasma is much more reproducible and has a more precisely defined radial distribution Also the radiation output of the laser produced plasma is not very sensitive to de-focusing or to changes in laser output energy

Another novel source of soft x-ray continuum radiation is the exploding wire In this case a large current is passed through a thin wire (diameter $\simeq$ 0 5mm), if the current is sufficiently large ($\simeq$ kA) then the wires explode and pinch on axis radiating a short pulse ($\simeq$ nsec) of continuum soft x-ray radation One particular example of this type of source has been used by Riordan and Pearlman (1981) to obtain an absorption spectrum of an aluminium plasma

1 6 PHOTOABSORPTION SPECTROSCOPY OF FREE IONS IN THE VUV

To obtain the absorption spectrum of a medium requires a background source with an intensity in the spectral range of interest which is greater than that of the absorption cell This is best achieved by a source the characteristics of which resemble those of a black body i e a source which is optically thick For neutral species this is readily attainable in the visible part of the spectrum

Based on the above considerations the absorption spectra of ionized species would appear to present a serious degree of dificulty since the intense sources required to observe absorption in ions would lie in the VUV The associated problems however have been overcome by a number of different workers utilizing a number of different techniques, all of which are based on the use of two plasmas one of which serves as the light source and another which serves as the absorbing medium It is the intention here to review this research and to give an historical perspective to the various methods employed in the study of photoabsorption of ionized species

Phenomena related to excitation and ionization of manifoldly charged ions provide a wide field of study for theoretical and experimental investigations which are of importance to present and future applications such as thermo-nuclear fusion and x-ray lasers

Until relatively recently emission spectroscopy in the visible, ultraviolet and x-ray regions was the only way to carry out experimental studies on the properties of ions From emission data it is possible to deduce energies of outer unoccupied levels of ions, the ionization potentials of the occupied

shells, and in some cases (if satellite lines are observed) binding energies of the first electronic inner shell In the recent past much theoretical effort has gone into numerical calculations of crossections of radiative and non-radiative excitation de-excitation and recombination processes in highly charged ions this is however only an indirect approach since emission spectroscopy of manifoldy charged ions is almost entirely carried out using plasmas or spark discharges which contain ions only as an intricate mixture of different species with a large range of processes contributing to the macroscopically observable behaviour It would therefore appear that any improvement in this situation by new techniques which would allow the measurement of xuv photoabsoption would be welcome However despite this no major effort has been put into the study of photoabsorption of ions in the VUV until relatively recently, although since about 1968 many successful methods have been developed which enable VUV spectra of free ions to be recorded Much valuable knowledge has been obtained by the use of these methods all of which require two plasmas Some of these methods are discussed in what follows

Huber and Tobey (1968) obtained gf values for lines in Fe I Cr I and Cr II and in a later publication Grasdalen Huber and Parkinson (1969) measured gf values for lines in Fe I and Fe II They used as an absorption medium a shock-heated gas which contained Fe and as a light source they made use of a coaxial flash tube with a large aperture which provided a usable continuum over the spectral region 3150-3780Å

Hildum and Cooper (1972) reported an experiment in which a Z-pinch discharge was used as an absorption medium to generate the ionized species and a modified theta-pinch plasma formed the background light source, fig(1 2) shows the experimental arrangement

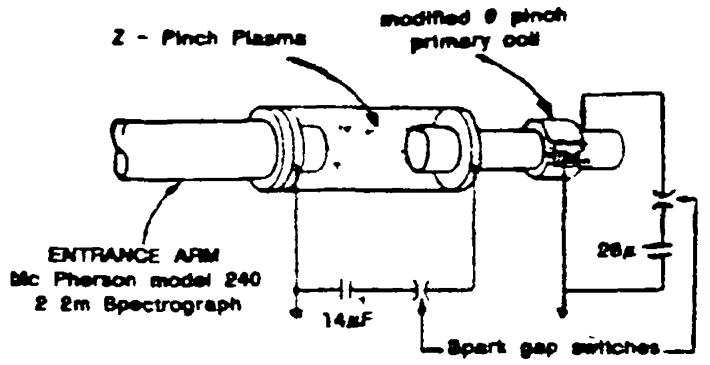

Fig (1 2) Shows a schematic view of the windowless system used to obtain VUV absorption spectra using a Z-pinch plasma as the absorbing medium together with a modified θ-pinch plasma providing the background source (After Hildum and Cooper (1972))

They obtained a brightness temperature for the theta pinch plasma in excess of 35 000K in the region 1100 - 2000Å and illustrated the technique by obtaining absorption in known lines of Si II Si III and C II The continuum was found to extend from 1100Å out to the visible

Mehlman Balloffet and Esteva (1969) reported an experimental tecnnique by which two BRV spark discharges one serving as the ion source while the other provided the vuv continuum background were used to study the absorption spectra of beryllium and magnesium The experimental arrangement used by them is shown in fig(1 3) below

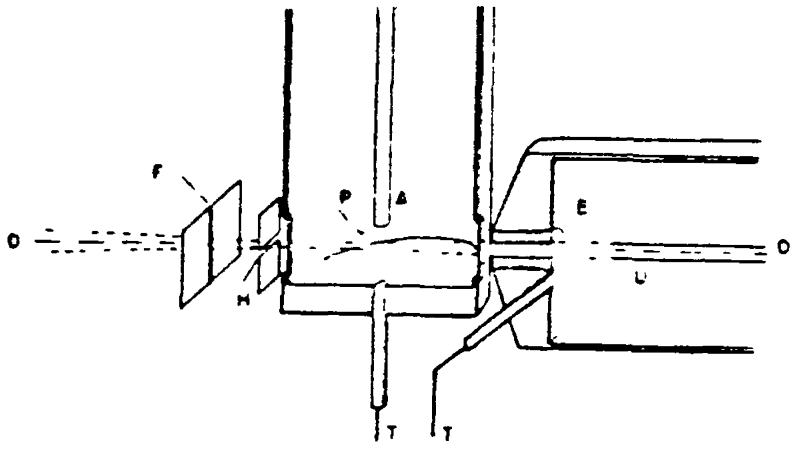

Fig (1 3) Shows the experimental arrangement used to obtain a VUV absorption spectrum using two synchronised spark discharges See text (After Esteva et al (1974))

The plasma P which contains the ions of interest is generated in a modified BRV spark device simply by replacing the uranium anode used to generate the continuum with a beryllium or magnesium rod The uranium anode producing the background light is seen end-on The distance between ions and light source is about 3 5cm and no focusing of the background source was used Experiments were performed to find the parameters which influenced the values of the absorption coefficient in order to obtain maximum absorption and largest variation of the absorption coefficient Electricial circuits were selected which gave maximum peak current, i, together with a maximum value of di/dt at breakdown Both circuits were identical each having capacitors of 0 5μF charged to 22kV and discharged over a period of 1 2μsec It was found necessary to operate the system with a time delay between both discharges With a time delay of 1 μsec the spectra obtained showed strong absorption of both continous and discrete nature The technique was used to study autoionized line series and other features in the spectra of ionized beryllium and magnesium In a later publication (Esteva and Mehlman (1974)) autoionization spectra of magnesium (Mg I, II and III) were recorded in the 50-110 eV energy range They identified some 68 resonances including the observation of the neon like series $1s^2 2s^2 2p^6 - 1s^2 2s^2 2p^5 ns, nd$, and several inner shell autoionizing resonances of the type $1s^2 2s^2 2p^6 - 1s^2 2s 2p^6$ np in Mg III

Carillon, Jaegle and Dhez (1970) reported an experiment involving two laser produced plasmas which allowed the absorption of radiation from one plasma by another to be observed this was the first time that two laser produced plasmas had been combined in this way The experimental arrangement is shown in fig (1 4) below The experiment consisted of having two target rods (I and II) one of which (I) was placed at a fixed distance from the entrance slit of a spectrograph the other (II) was placed between the spectrograph slit and

(I) in such a way that its distance from the optic axis of the spectrograph could be varied Thus plasma (II) formed the absorbing medium and plasma (I) the radiating source Movement of target (II) together with the use of optical delay lines allowed different regions of the absorbing plasma to be studied The experiment used a two concave grating spectrograph and a Nd-glass laser which delivered approximately 25 MW of power to each target The radiation was detected using a gas flow proportional counter

The point of the experiment as stated above was to observe the absorption of radiation from plasma (I) by plasma (II) To do this, intensity measurements were taken in the following manner at a given wavelength λ three sucessive measurements of intensity were taken Firstly that of the emission from plasma (I) secondly that of plasma (II), and as a final measurement the emission of target (I) behind target (II) was examined the experiment was repeated a number of times to eliminate fluctuations in laser output power If no absorption by target (II) took place then the last measurement would on average be the sum of the first two however this was not the case and the conclusion drawn by the authors was that absorption of part of the radiation from one plasma by the other did in fact take place A mean value was obtained over the duration of the source continuum which was about 40 nsec The relative timing of the arrival of the two laser pulses at their respective targets could be adjusted by an optical delay line Fig (1 5) shows the transmittance of the plasma at 98 Å as a function of the distance z' from the hottest part of the plasma along the laser axis The hottest region of the plasma was found to occur at a distance of about 0 5mm from the target surface For a delay time of 12nsec the transmittance increased monotonically with distance d (see fig(1 5)) but for a delay of 27 nsec the transmittance had a minimum at 0 8mm The authors interpreted this minimum as being due to the presence

as a result of recombination of significant numbers of ions with sufficiently low ionization potentials to be photoionized by the 98Å radiation (with $\chi \simeq 12.5$eV) and concluded that such radiative transfer processes appear to be important in these types of plasmas

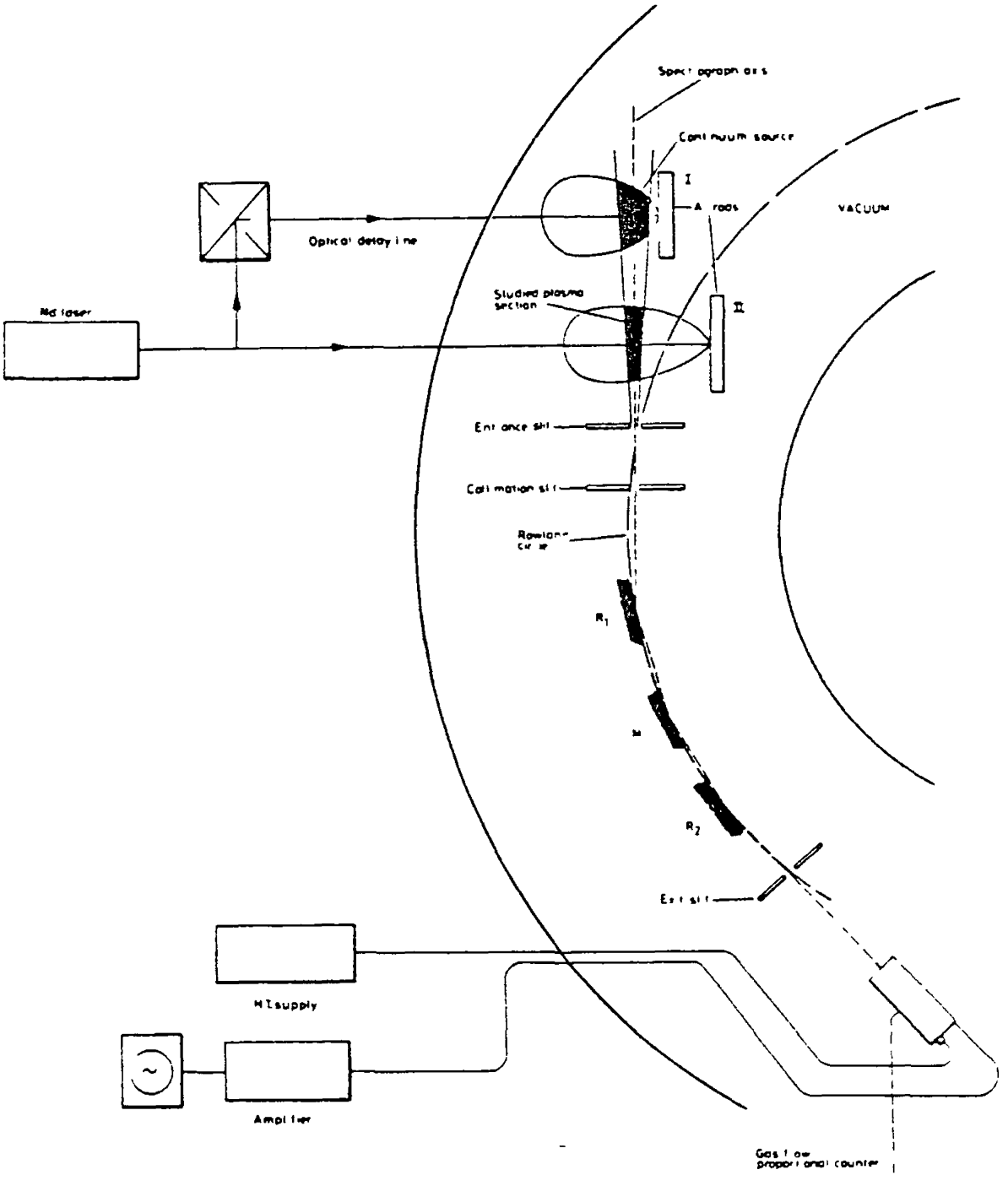

Fig (1 4) The experimental arrangement used to measure the far ultravoilet absorption spectrum of a laser generated aluminium plasma R_1 and R_2 are concave gratings and M is a concave mirror (After Carillon et al (1970))

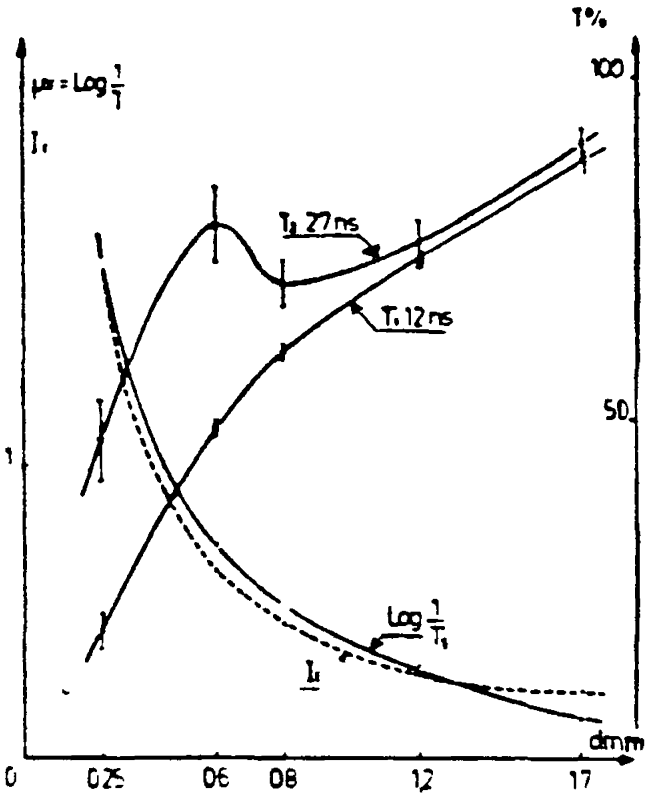

Fig (1 5) Transmittance T and absorption μx of EUV radiation through a laser produced plasma d is the distance from the observed zone to the hottest part of the plasma which was found to be about 0 5mm from the target surface See text (After Carillon et al (1970))

In a later publication Jaegle Carillon Dhez, Jamelot Sureau and Cukier (1971) reported on evidence for the possible existence of a stimulated emission in the extreme ultraviolet from an aluminium plasma They used the same two laser plasma technique and suggested that observed intensity anomalies in the absorption spectrum of an aluminium plasma implied the existence of a population inversion between the $2p^6\ ^1S_0$ and the $2p^5 4d\ ^1P_1$ levels in Al IV They attributed this population inversion to an interchannel interaction between nd states and the continuum i e that the $2p^5 4d\ ^1P_1$ level was populated by the recombination of the Al V ion with free electrons

In two further reports (Carillon Jamelot Sureau and Jaegle (1972) and Jamelot Sureau and Jaegle (1972)) identifications and measurements of the autoionizing series in the neon like Al IV ion were made Also they reported on

the observation of lines of the type $2p^6\ {}^1S_0 - 2p^5\ nd\ {}^3D_1, {}^1P_1$ Again this was related back to the earlier reports of laser action in the vacuum ultraviolet

Valero (1974) repeated the experiments of Carillon et al in an attempt to explain the reported intensity anomolies He repeated the experiment using higher power ($\simeq$ 600MW) and used photographic rather than photoelectric detection Valero also used a cylindrical lens in conbination with a spherical lens to generate both the *absorbing and continuum producing* plasmas respectively from the same target This was done to create a greater path length and so make any intensity anomalies more evident By making observations of relative intensities of lines of various ion stages in the plasma he concluded that the observed intensity anomalies were in fact due to self absorption and hence a relative increase in lines having lower transition probabilities He also concluded that the alleged observation by Carillon et al (1972) of a Beutler-Fano profile was in fact due to a low resolution detector system These results relating to the report of laser action in the extreme ultraviolet were, at the time of publication the subject of considerable controversy, and in further publications, (Jaegle, Jamelot, Carillon, Sureau and Dhez (1974) and Jamelot Carillon Jaegle and Sureau (1975)), the same group carried out further calculations in support of their claim One of these publications Carillon et al (1974) is of interest here as it describes a "technical device" and a "practical method" for the study of photoabsorption in ionized species This device employs a "split lens" to focus the laser output onto the target (whether a single spherical lens or two separate half spherical lenses are used is not clear from the original publication) As can be seen by reference to fig (1 6) below By this technique the two plasmas are produced close together on the same target, the distance between them being (according to Carillon etal (1974)) on average approximately 0 4mm using a two half-optical lens

system However it is also clear from fig(1 6) that such a division of a single spherical lens will cause the incident laser beam to be focused to the same region of the target from both sides of the lens division This will result in the production of a single point plasma If two separate half spherical lenses are used then two point plasmas will be created however they would be so close together that the experiment would be confined to a single target surface So it is clear that if the arrangement proposed by Carillon and shown in fig (1 6) is used then the experiment would be essentially confined to a single target and thus preclude the use of a second high z continuum emitting target The goal of this device was acording to the authors to atempt to measure a "negative absorption" for the transition $2p^5 4d\,^3P_1 - 2p^6\,{}^1S_0$ which is almost forbidden in the neon like ion Al IV

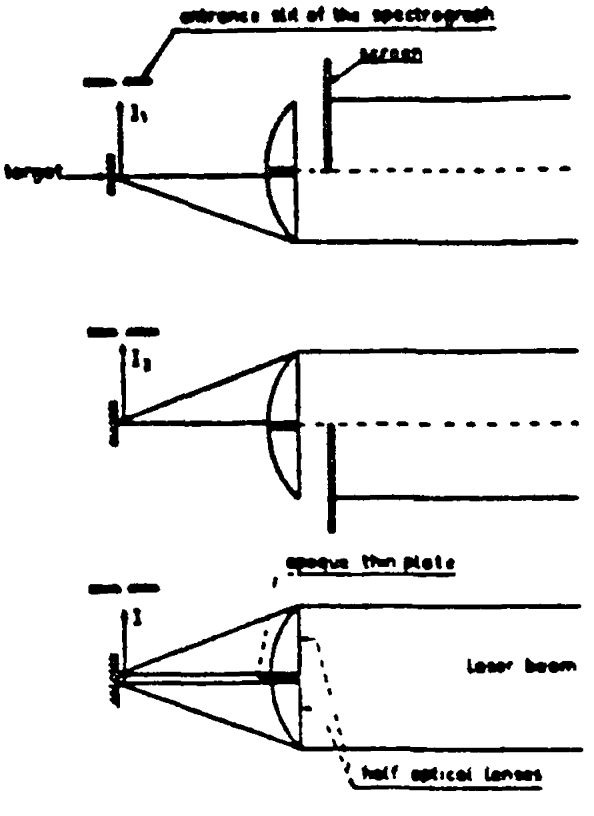

Fig (1 6) Shows a simpler form of the technique originally developed by Carillon etal (1970) This version uses two half-optical spherical lenses to produce both of the plasmas on the same flat target directly in front of the spectrograph entrance slit (After Carillon et al (1974))

Another method which has been used to study ionized species in the VUV involves the use of tunable lasers to create the ions The tunable laser has proven to be a powerful tool in the investigation of atomic structure using the various spectroscopic methods made possible by their development The application of the tunable laser to the absorption spectroscopy of *ionized* species was first demonstrated by Lucatorto and McIlrath (1976), when they were able, using a 1MW pulsed laser tuned to the $\lambda = 5896\mathring{A}$ $^2S_{1/2} - {}^2P_{1/2}$ resonance transition in sodium to produce nearly complete ionization of a one cm diameter column of sodium vapor

The absorption spectrum of the column of ionized vapor was obtained using the apparatus shown in fig (1 7) The continuum background used in this experiment was provided by a BRV vacuum spark The output of the laser was made to traverse a heat pipe which contained the sodium vapor between two plugs of helium buffer gas all at a pressure of about 1 torr The continuum produced by the BRV source was reflected using a toroidal mirror and transmitted through the capillary arrays used to separate the vacuum of the spark chamber from that of the heat pipe The small mirror placed near to the entrance slit of the 3m grazing incidance spectrograph, allowed for almost colinear illumination of the sodium vapor by both the laser and the BRV source

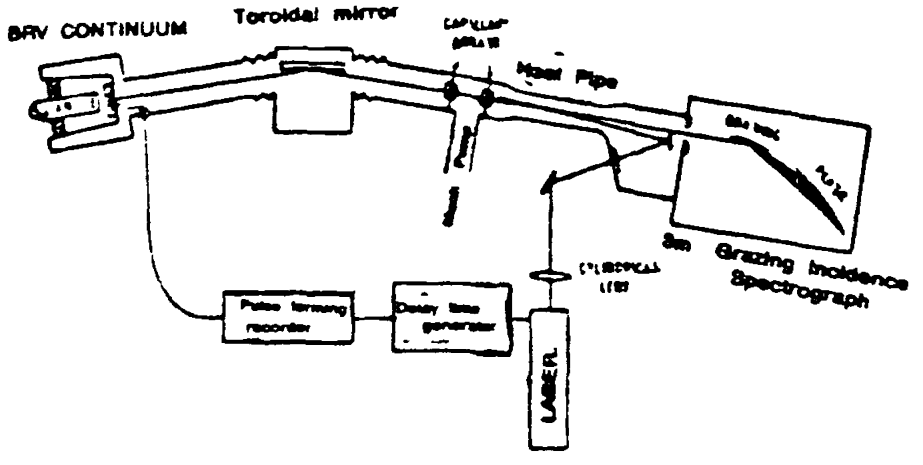

Fig (1 7) Schematic diagram illustrating the technique used to ionize a column of vapor and subsequently obtain its VUV absorption spectrum (After Lucatorto and McIlrath (1980))

The results of the experiment described above allowed measurements of the Na^+ photoionization continuum to be made The experiment also resulted in the observation of the neon like series $2s^22p^6\ {}^1S_0 - 2s^22p^5ns$ nd and six members of the autoionizing series $2s^22p^6\ {}^1S_0 - 2s2p^6np\,{}^1P_1$

This technique of resonant laser-driven ionization has since been applied to other vapors and ionization of Li Ca Sr and Ba vapor columns have been observed

In a further modification of the technique to include a second tunable laser Lucatorto, McIlrath Sugar and Younger (1981) observed for the first time the discrete 4d photoabsorption spectrum of Ba^{++} The experiment employed essentially the same technique with a 1MW pulsed dye laser tuned to the

5537Å resonance line in Ba which completley ionized a 12cm long column ($\simeq$ 2 $5X10^{15}cm^{-3}$) of Ba vapor which allowed the VUV absorption spectrum of Ba II to be observed A second laser tuned to the 4935A resonance line in Ba II further ionized the column and allowed the absorption spectrum of Ba III to be recorded The resulting redistribution of oscillator strength observed in the spectrum of Ba III, when compared with the spectrum of Ba II in the same energy region has generated considerable theoretical interest

At the time of the first experiment with sodium vapor the mechanism for the production of ions by this technique was not well understood Further experimental work by the same group (Lucatorto and McIlrath (1980)) has explained the phenomenon of resonant laser-driven ionization in dense vapors by a combination of several effects including multi-photon ionization dimer ionization associative ionization and stimulated Raman scattering

The technique has proved to be a very useful one for photoabsorption studies of neutrals, and for singly and doubly ionized species The same group has also suggested that the technique has wider applications beyond pure spectroscopy such as the use of ion columns as non linear media for up conversion into the ultraviolet by four-wave mixing Also possible using this technique are studies of recombination lasers as well as studies on the chemistry of ion-neutral reactions The technique is however limited by lack of crystals suitable for frequencey doubling into the VUV so that photoabsorption spectra of ionized species higher than III cannot be atempted with this technique at this time

Another technique which was used for photoabsorption studies on ionized species at about the same time was the technique of flash pyrolysis In this

technique metal vapors are heated in a glass or quartz absorption tube which is connected onto a spectrograph at one end and a vacuum chamber containing a continuum light source (usually a BRV) at the other The absorption tube is surrounded by a helical flashlamp working at voltages of up to 10kV, and capable of emitting a luminious flux of about $50Jcm^{-2}$ on a time scale of about $1\mu sec$ Using this technique Cantu, Parkinson Tondello, and Tozzi (1977) were able to obtain the absorption spectrum of Lithium (Li I and Li II) in the 215 – 160Å region Using a toroidal mirror to focus the backlighting BRV source they were able to obtain spectra in a single shot They reported on the observation and measurement of thirteen lines of singly ionized lithium together with the continious absorption at the limit of the series Absorption lines from inner shell excitations in neutral lithium were also observed and tentatively identified

The technique of using two laser produced plasmas to obtain absorption spectra of ions in the VUV first used by Carillon et al (1970) was (after incorporating several important modifications) successfully used by Carroll and Kennedy (1977) to obtain the VUV absorption spectrum of Li^+ from 200 to 50Å They reported the observation of three members of the doubly excited resonances $1s^2\ {}^1S_0 - 2snp\ {}^1P_1$ and were able to obtain measurements of the Fano parameters q and Γ for the first member They also observed the principal series together with its adjoining photoionization continuum The essential differences between this experiment and the experiments of Carillon et al (1970) and Valero (1974) are discussed below The technique utilised the continuum producing properties of high Z element plasmas discussed in section 1 3 The crossed target configuration (in which the laser beams entered the target chamber at right angles to each other.) shown in fig (1 8) was used

The single laser beam (1J in 30 - 40nsec) entered a beam splitter which directed half of the beam via an optical delay line to the continuum producing target (in this case tungsten) and the remainder of the beam to the ion producing lithium target This was an advance on the earlier two laser produced plasma techniques in that for the first time the backlighting source behind the absorbing plasma was a continuum producing plasma Also the spectra obtained with this variation were spatially resolved i e information about the structure of the absorbing plasma was revealed

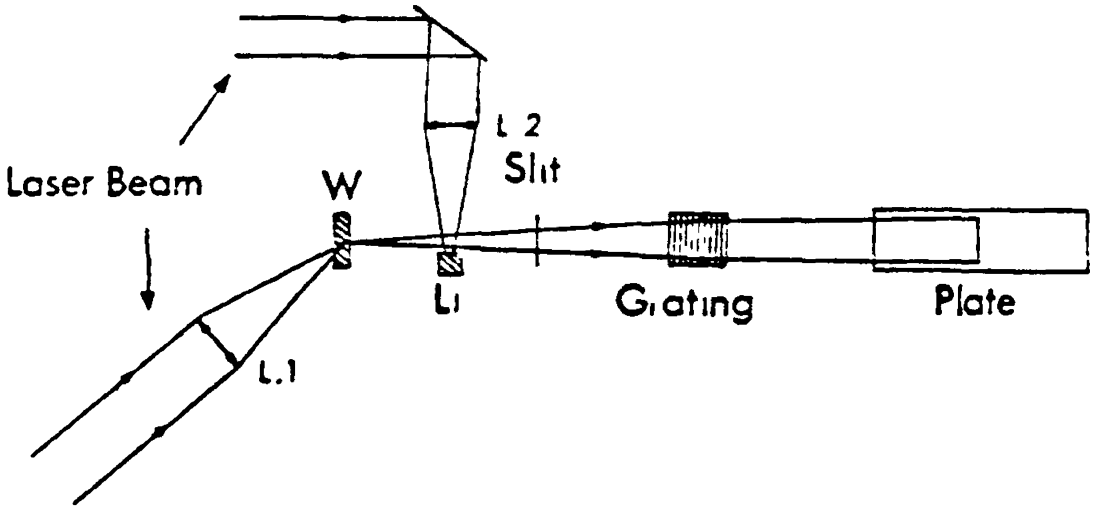

Fig(1 8) The target configuration used by Carroll and Kennedy (1977) to study the VUV absorption absorption spectrum of a Li laser produced plasma L 1 and L 2 are lenses (After Carroll and Kennedy (1977))

In a later publication Kennedy and Carroll (1977) reported absorption from excited states of Be^{+} also observed in a laser produced plasma In this case no backlighting continuum source was used Instead the single laser beam was directed to a Beryllium oxide target which contained some other elements of

higher atomic number, and these elements produced sufficient continuum radiation to allow the observation of absorption features

The technique of using two laser produced plasmas one as an ion source the other as a continuum source to obtain absorption spectra has more recently been used successfully by Jannitti, Nicolosi and Tondello (1983) in a modification of the arrangement first reported by Santi, Jannitti Nicolosi and Tondello (1981) The method employed involves the division of a Q-switched ruby laser beam ($\simeq$ 85J in 15nsec) between two targets, one of which produces the continuum radiation and the other the absorbing ions The experimental arangement, shown in fig (1 9), is relatively complicated when compared with that of Carroll and Kennedy (1977)

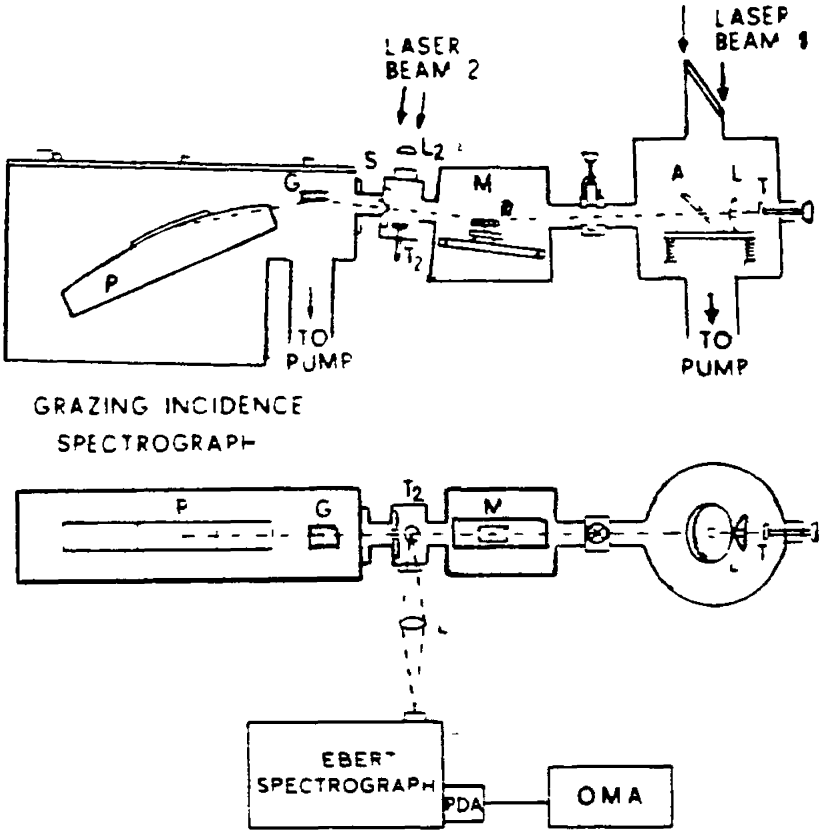

Fig (1 9) A modified version of the two laser produced plasma technique used to study absorption of ionized species (After Jannitti et al (1981))

The first beam laser beam 1 in fig (1 9) carries most of the energy (70-90%) and after deflection by mirror A, is *focused* by lens L_1 to produce the continuum radiating plasma on target T_1 Beam 2 which contains the rest of the laser pulse is brought to a focus on target T_2 using a sphero-cylindrical or spherical lens, L_2. This produces the absorbing plasma The continuum radiation generated on target T_1 is seen through two small holes in mirror A and in lens L_1 by the toroidial mirror M which collects and focuses the continuum radiation The radii of the mirror M are such as to produce a first astigmatic image on the entrance slit S of the two metre grazing incidence spectrograph As well as removing the astigmatism the mirror M also helps by filling the aperture of the spectrograph

With this arrangement the authors have produced absorption spectra of ions of low atomic number and have also reported on continuum measurements made on targets of low Z Nicolosi, Jannitti and Tondello (1981) concluded that plasmas produced on targets of low Z using lasers of moderate power (3 - 10J) can produce strong ($\approx 10^{8} Wcm^{-2} Sr^{-1} Å^{-1}$) continua in the soft x-ray (10 -100Å) region Absorption spectra of the He-like and Li-like stages of beryllium, boron and carbon have been obtained (Jannitti Nicolosi, and Tondello (1983)) Recently Jannitti, Nicolosi, and Tondello (1984) have measured the Fano parameters q and Γ for the $1s^2\ ^1S_0 - 2s2p\ ^1P_1$ autoionizing resonance in He-like beryllium Be III

Another method which has recently been used to obtain absorption spectra of ionized species in plasmas also deserves mention because of its relevance to work which is reported in chapter 3 Riordan and Pearlman (1981) have produced an absorption spectrum of a backlighted aluminium plasma, using the exploding wire technique shown in fig (1 10) below The technique utilises

a backlighting source which consists of a cylindrical array of fine stainless-steel wires strung across the diode of a 1-TW pulsed power generator Current passing through the wires cause them to explode radiating an intense 25nsec FWHM pulse of soft x-rays

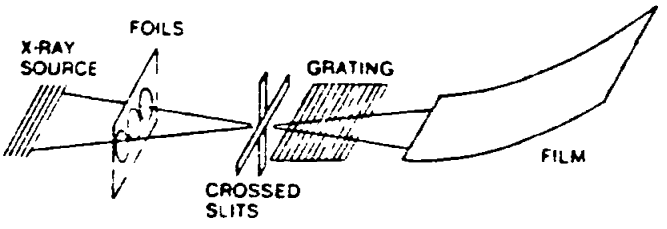

Fig (1 10) Schematic of the exploding wire technique used to record the absorption spectrum of an aluminium plasma (After Riordan and Pearlman (1981))

The plasma under investigation in this case aluminium was created by irradiating thin foils with the same soft x-ray source used for backlighting though it would also be possible to create the absorbing plasma independently of the backlighting source The foils used are placed over holes in a foil support one hole being left uncovered to measure the wire source The spectra were recorded using a 1m grazing incidence spectrograph The investigation showed that when the foils received an irradiance of $\simeq 1 Jcm^{-2}$ a spectrum of neutral aluminium was obtained The foils were found to be opaque below 170Å due to the $L_{11\ 111}$ edge in neutral aluminium However when the backlighting flux is increased "markedly" (to what extent is not clear in the original publication) the foils are completely ionized The authors report the observation of Ne-like Al IV states also satellite lines from Al II and Al III and a single absorption line from Al V The spectra were recorded over the

range 200 - 80Å The observation of the Rydberg series of autoionization resonances $2s^2 2p^6\ {}^1S_0 - 2s2p^6 np\ {}^1P_1$ were not reported In conclusion the authors suggest that this technique might also be useful in the diagnosis of warmer plasmas such as those produced by lasers

REFERENCES

Balloffet G Am Phys 5 1256 (1960)

Balloffet G Romand J and Vodar B Compt Rend 252 4139 (1961)

Balloffet G Romand J and Kieffer J Spectrochemica Acta 18 791 (1962)

Bioko VA Bryonetkin BA Bunkin FV Derzhiev VI Dyakin VM Duvanov BN Lysov VD Skobelev YYa Sulakuelidze VS Faenov AYa Fedosimov AI and Yakoulenko SI Sov J Quant Electron 10 5 (1983)

Breton C and Papoular R J Opt Soc Am 63 1225 (1973)

Cantu AM Parkinson WH Tondello G and Tozzi GP J Opt Soc Am 67 8 (1977)

Carillon A Jaegle P and Dhez P Phys Rev Lett 25 3 (1970)

Carillon A Jamelot G Sureau A and Jaegle P Phys Lett 38 2 (1972)

Carillon A Jamelot G Jaegle P and Sureau A Proc of the 4th conference on vacuum ultraviolet radiation physics Hamburg Germany (1974) PP 50 - 52

Caro RG Wang JC Yang JF and Norris SE Phys Rev A 30 3 (1984)

Carroll PK Kennedy ET and O'Sullivan G Opt Lett 2 PP 72 - 74 (1978)

Carroll PK Kennedy ET and O'Sullivan G Appl Opt 19 PP 1454 - 1462 (1980)

Carroll PK and Kennedy ET Phys Rev Lett 38 PP 1068 - 1071 (1977)

Carroll PK and O'Sullivan G Phys Rev A 25 PP 275 - 286 (1982)

Carroll PK and Kennedy ET Contemp Phys 22 61 (1981)

Carroll PK Kennedy ET and O'Sullivan G IEEE J Quant Elect 19 12 (1983)

Codling K Rep Prog Phys 36 541-624 (1973)

Codling K and Madden RP Phys Rev Lett 12 106 (1964)

Cooper J Rep Prog Phys 29 35 (1966)

Damany N and Esteva JM Opt Commun 13 383 (1975)

De Miclelis C and Mattioli M Nucl Fusion 21 6 (1981)

Dewhurst RJ Khan MA and Pert GJ J Phys B 8 2301 (1975)

Dixon RH Seeley JF and Elton RC Phys Rev Lett 38 1072 (1977)

Dixon RH Seeley JF and Elton RC Phys Rev Lett 40 122 (1978)

Ehler AW and Wissler GL App Phys Lett 889 (1966)

Elton RC Proc S P I E Int Soc Opt Eng 279 (1981)

Esteva JM and Mehlman G Astro Phys J 193 1 (1974)

Fischer J and Khune M Appl Phys B 1332 (1983)

Grasalden GL Huber M and Parkinson WH Astro Phys J 156 1153 (1969)

Heckinkamp C Hienzmann U and Schonhznse G J Phys D 14 12 (1981)

Hildum JS and Coooper J J Quant Spec Rad Trans 12 1453 (1972)

Hora H "Physics of laser driven plasmas " John Wiley and Sons Inc (1980)

Huber M and Tobey FL Astro Phys J 152 609 (1968)

Hughes TP "Plasmas and laser light " Adam Hilger (1975)

Izawa Y Otani H and Yamanaka C In Laser Interactions and Related Plasma Phenomena HJ Schwartz and H Hora Eds (Plenum New York) Vols 5 (1980).

Jaegle P Carillon A Dhez P Jamelot G Sureau A and Cukier M Phys -

Lett 36 3 (1971)

Jaegle P Jamelot G Carillon A Sureau A and Dhez P Phys Rev Lett 33 18 (1974)

Jamelot G Sureau A and Jaegle P Phys Lett 41A2 (1972)

Jamelot G Carillon A Jaegle P and Sureau A J De Phys (Lett) 36 PP293-295 (1975)

Jannitti E Nicolosi P and Tondello G AIP Conf Proc (USA) No 90 PP 243 - 253 (1982)

Jannitti E Nicolosi P and Tondello G J Phys (France) 43 7 (1982)

Jannitti E Nicolosi P and Tondello G Physica C 124 5 (1984)

Kennedy ET Ph D Thesis University College Dublin (1977) Unpublished

Kennedy ET and Carroll PK Phys Lett 64A 1 (1977)

Kennedy ET Contemp Phys 25 1 (1984)

Knot RGA Contemp Phys 12 1 (1971)

Kuhne M Appl Opt 21 12 (1982)

Lotte B Bon M and Romand J J DePhys Rad 24 346 (1963)

Lucatorto TB and McIlrath TJ Phys Rev Lett 37 7 (1976)

Lucatorto TB and McIlrath TJ App Opt 19 23 (1980)

Lucatorto TB McIlrath TJ Sugar J and Younger SM Phys Rev Lett 47 16 (1981)

Madden RP and Codling K Phys Rev Lett 10 516 (1963)

Madden RP and Codling K J Opt Soc Am 54 268 (1964)

Matthews DL Hagelstein PL Rosen MD Eckart MJ Ceglio NM Hazi AU Medecki H MacGowan BJ Trebes JE Whitten BL Campbell EC Hatcher CW Hawryluc AM Kauffman RL Plesence LD Ramback G Scofield JH Stone G and Weaver TA Phys Rev Lett 54 110 (1985)

Mehlman G. Balloffet G. and Esteva JM. Astro. Phys. J 157 PP 945 - 956 (1969)

Mehlman G and Esteva JM Astro Phys J 188 15 (1974)

Morgen CG Proceedings of the XVIth international conference on phenomena in ionized gases Dusseldorf Germany Univ Dusseldorf Press PP 36 - 44 (1983)

Nagel DJ Proc S P I E Int Soc Opt Eng 448 (1984)

Nicolosi P Jannitti E and Tondello G Appl Phys B (Germany) B26 2 (1981)

O'Sullivan G Ph D Thesis University College Dublin (1980) Unpublished

O'Sullivan G and Carroll PK J Opt Soc Am 71 PP 227-230 (1981)

O'Sullivan G Carroll PK McIlrath TJ and Ginter ML Appl Opt 20 PP 3043 - 3046 (1981)

O'Sullivan G J Phys B 15 L237 - 230 (1982)

O'Sullivan G J Phys B 15 2385 - 2390 (1982)

Pert GJ Philos Trans R Soc 300 1456 (1981)

Pert GJ and Tallents GJ J Phys B 14 9 (1981)

Riordan JC and Pearlman JS Appl Phys Lett 39 7 (1981)

Santi D Jannitti E Nicolosi P and Tondello G Il Nuvo Cimento 65B 1 (1981)

Silfvest WT Wood OR II and Holmdel NJ Opt Lett 7 11 (1982)

Sinha BK and Gopi N Phys Fluids 23 8 (1980)

Valero FPJ Appl Phys Lett 25 1 (1974)

Vinogradov AV Galichii AA Kalashnikov MP Kantsyres VL Kozyrev YuP Mazor MYu Mikhailov YuA Puzyrev VP Rsde AV Sklizkov GV and Frondzei IYa Sov J Quant Elect 12 8 (1982)

Williams GP Vacuum 32 6 (1983)

Williams MD J Opt Soc Am 63 383 (1973)

Wuilleumier FJ Atomic Physics VII Proceedings of the seventh international conference on atomic physics Phenum (1981)

GENERAL REFERENCES FOR CHAPTER ONE

Bekefi G Ed "Principles of laser plasmas " John Wiley and Sons Inc (1976)

Hora H "Physics of laser driven plasmas " John Wiley and Sons Inc (1980)

Hughes TP "Plasmas and laser light " Adam Hilger (1975)

Huddlestone RH and Leonard SL Ed's "Plasma diagnostic techniques " Academic Press (1965)

Krall NA and Trivelpiece AW "Principles of plasma Physics " McGraw Hill Book Company (1973)

Schmidt G "Physics of high temperature plasmas " Academic Press (1979)

CHAPTER TWO EXPERIMENTAL.

2 1 INTRODUCTION

The intention in this chapter is to describe the apparatus and experimental arrangement used to obtain the absorption spectra of ionized species which are reported in chapter three

The laser used in these experiments is a commercially available instrument and its general characteristics are outlined The spectrograph used to record the spectra is described and some details relevant to grazing incidence spectrographs in general are also discussed briefly

The experimental method employed is discussed in relation to alignment of the spectrograph so that best use is made of the instrument Details of photographic tests used in alignment of both plasmas with each other and with the spectrograph are described Also dealt with here is the method of target construction which has been found during the course of this work to be an important factor influencing the outcome of the experiments reported in chapter three

The intention throughout this section is to provide a clear and concise description of a series of experiments which have been highly successful in providing absorption spectra (in the VUV / soft x-ray wavelength region) of transient ionized species produced in laser generated plasmas

2.1 THE LASER.

The laser used for all of the experiments reported here was a commercially available ruby (series 2000) laser, supplied by J K LASERS The laser output which is linearly polarized occurs at a wavelength of 694 3nm The laser consists of a single oscillator which can deliver approximately 1 5 J of optical energy in a single pulse of 30 to 40 nsec (FWHM) duration when operated in the Q-switched mode as it was throughout these investigations

It is not the intention here to discuss the physics of ruby lasers as many texts exist on the subject. (see general references at the end of this chapter) However some details pertaining to the operation of this particular laser are discussed below A schematic diagram which shows the basic construction of the laser is shown in fig(2 1) The Pockels cell which makes Q-switching possible is located in the cavity just in front of the rear mirror and operates at a voltage of 2 7kV which can be varied by adjusting the controls on the Pockels cell unit This unit also controls the double pulse facility of the laser this allows the laser to be fired in a double pulse mode with a time delay between the pulses variable from one to several hundred micro seconds The output of the laser is monitored on an energy monitor which takes a portion of the output beam and directs it to a photo diode The integrated output from the photo diode is converted into a voltage which is proportional to the laser output and can be read from the energy monitor

Ruby is quite sensitive to variations in temperature its lasing efficiency rising with a reduction in temperature The coolant temprature is generally controlled

at approximately 20^{0}C The cooling medium used for this laser is distilled water As a further precaution the repetition rate of the laser was restricted to thirty shots per minute although it could be run at twice this rate

When operating at full aperture a laser generally oscillates in several transverse modes simultaneously By reducing the aperture (which in the case of this laser is located in the cavity behind the output mirror see fig(2 1)) the number of modes is progressively restricted untill the laser is only operating in single transverse mode (TEM_{00}) This mode generally known as the uniphase mode gives very good spatial coherence, and the lowest attainable beam divergence and hence a high energy density capability due to its good focusability Throughout these experiments the laser was used with the aperture set to its lowest value i e the smallest aperture was used and although the laser is not exactly operating in the TEM_{00} mode (even with the smallest aperture in place) most of the higher order modes are however eliminated by the inclusion of the aperture and hence the power output is optimised

Routine maintenance is largely confined to the Pockels cell which is a sealed unit (located in the cavity between the rod and the rear reflector see fig(2 1)) with anti-reflection coated windows at each end the void between the windows and the crystal is filled with FC104 index-matching fluid to minimise transmission losses The Pockels cell is checked at regular intervals to ensure that the fluid level is correct

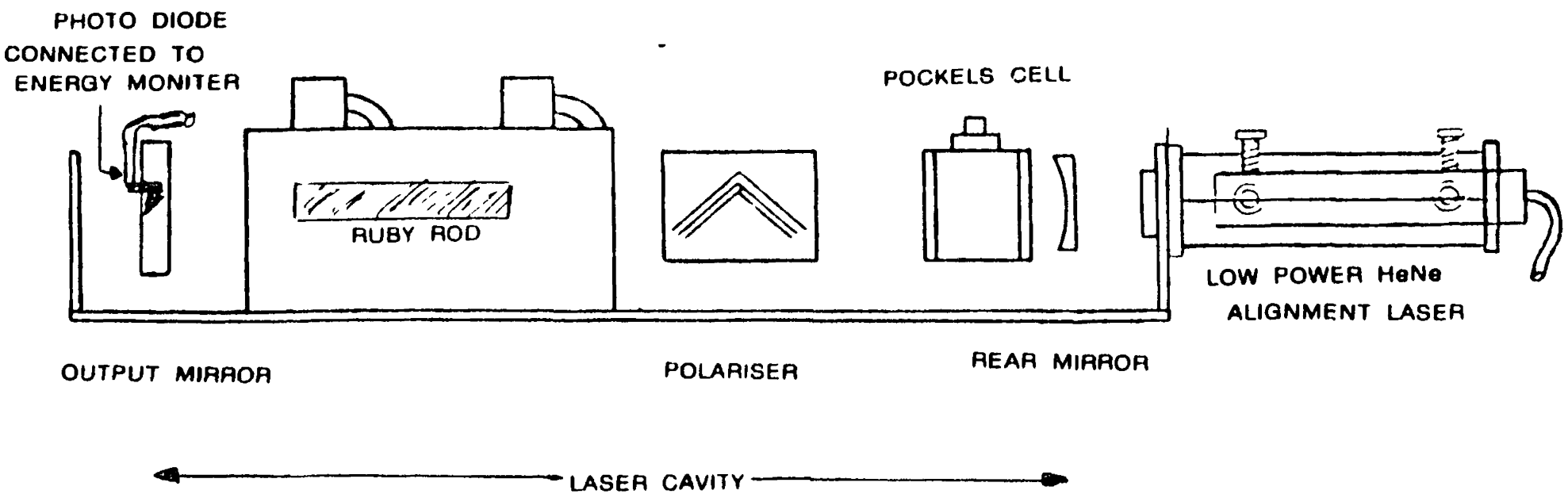

Fig (2 1) Schematic diagram showing the construction of the ruby laser system which was used throughout the work reported here Also shown is the low power HeNe alignment laser which is aligned along the optic axis of the ruby laser

Care must also be taken to ensure that there is nothing in the path of the beam which can return direct reflections into the laser It is important to ensure that any lenses in the optical train do not produce back-reflections which come to a point focus anywhere near another component, for example plano- convex lenses can produce focusing back-reflections from their flat or curved surfaces

To facilitate alignment a low power HeNe laser beam is passed through the optical system of the ruby laser as seen in fig(2 1) This second laser is used to fix precisely the position of optical components used in plasma production

2 2 THE TARGET CHAMBER

Most of the experimental work reported here involved a series of two plasma experiments carried out in vacuo in target chambers attached to the spectrograph just in front of the entrance slit Two target chambers were used for the experiments The first of these was constructed of 3mm mild steel plate and is of a construction similar to those reported by Kennedy (1977) and O'Sullivan (1980) This chamber was such that the plasmas were located approximately 10cm from the entrance slit of the spectrograph An alternative target chamber was constructed, also of mild steel, which allowed the plasmas to be formed approximately 5cm in front of the spectrograph entrance slit thus increasing the intensity of the light incident on the grating This chamber shown in fig(2 2) was constructed to allow maximum observation of the plasmas formed on the surface of the targets during the course of an experiment and to facilitate alignment

An attachment for holding a HeNe laser at the rear of the chamber was also

constructed the HeNe laser was aligned along the optic axis of the spectrograph and was used in coarse alignment of the plasmas with the entrance slit The top plate of the chamber contains the target holder and allows the target to be moved such that the optimum position in front of the entrance slit is obtained Both top and bottom plates of the chamber are approximately 2 5cm thick and are hollowed out to allow the target holder the greatest possible vertical motion within the chamber. this allowed relatively long (approximately 6cm) targets to be constructed The chamber was also differentially pumped this was accomplished by a small 1" diffusion pump connected to the base of the chamber This was felt to be necessary as the entrance slit of the spectrograph was normally set between 5-20μ and a typical plate required in excess of 300 shots This together with the fact that the target rod extends through a vacuum seal (which is quite easy to break while the target rod is being moved) into atmosphere and was constantly being moved during the experiment (every 5-10 shots) made differential pumping essential

To avoid the problem of the backlighting plasma being obscured and to ensure that maximum absorption be observed it was found that the targets had to be rotated and held at an angle of between 2 and 5 degrees to the spectrograph optic axis This was accomplished by a small piece of brass which was machined so as to be circular but with a small lip (as shown in fig(2 3 a)) This piece of brass fitted over the target rod and was held onto it with a small screw The machined lip which moved in a vertical groove cut in a hollow brass tube made to fit over the target holder allowed the target to be held at the predetermined angle Thus any angle which was set between the target holder and the spectrograph axis could be easily maintained The entire construction is shown in fig(2 3)

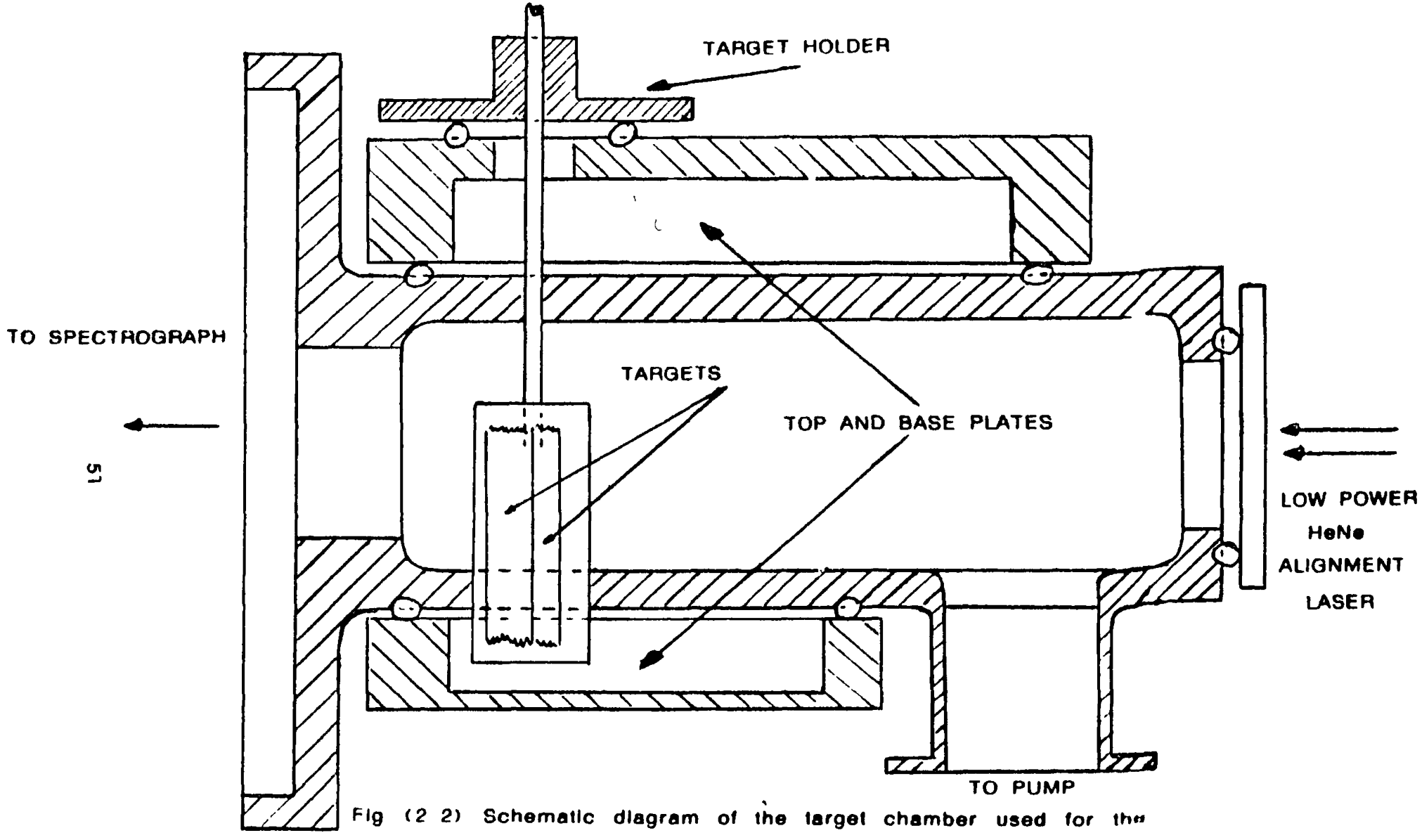

Fig (2 2) Schematic diagram of the target chamber used for the absorption experiments reported in chapter three The diagram shows a section taken along the optic axis of the spectrograph, and shows the target holder design

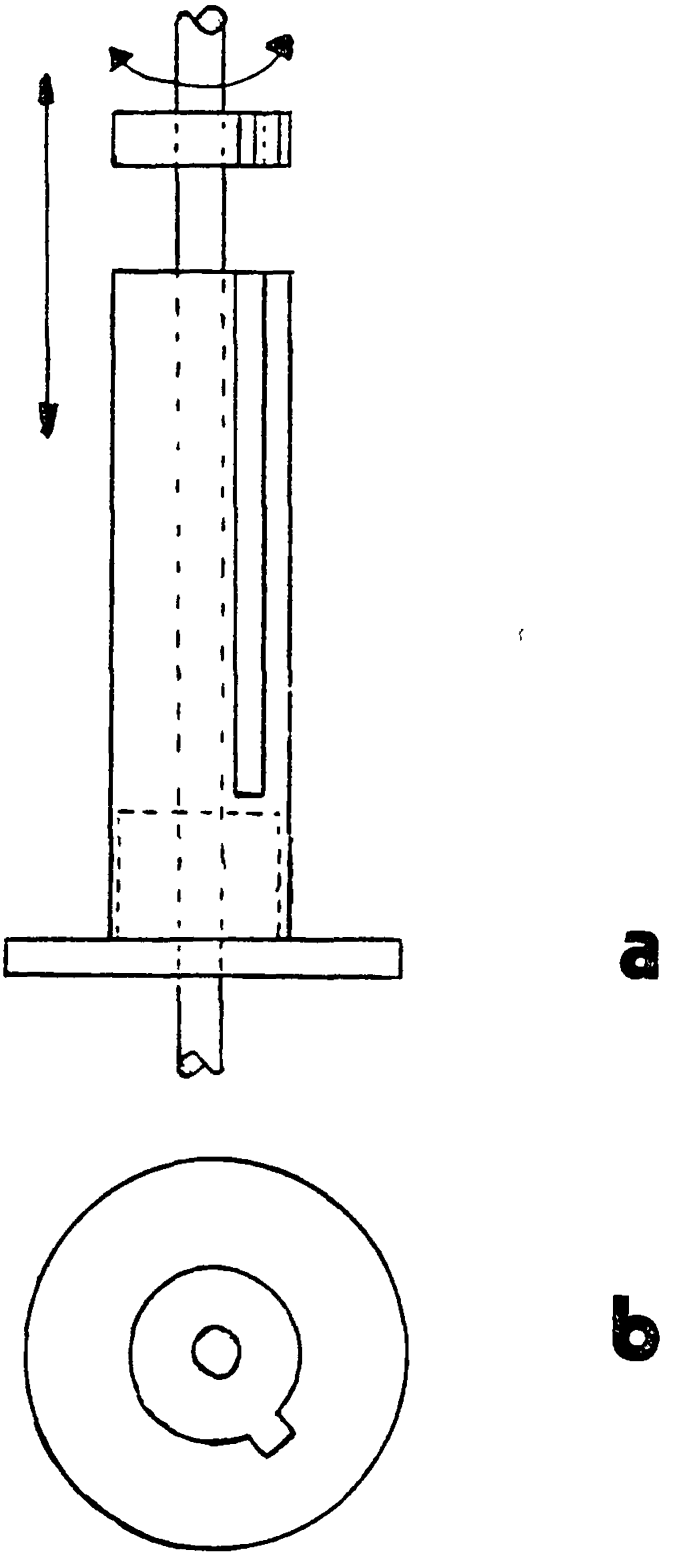

Fig (2 3) Shows an elevation and plan view of the cylindrical construction used to set and maintain the angle between the targets and the optic axis of the spectrograph during the experiment

2 3 THE SPECTROGRAPH.

The photoabsorption studies reported here, (chapter three) were all carried out in the extreme ultraviolet/soft x-ray region of the spectrum below 300Å In this wavelength region the decrease in reflectance of all materials with decreasing wavelength necessitates the use of grazing incidence spectrographs to obtain usable grating efficiency and, in general, the closer the incident angle α approaches 90^0 the lower will be the cut-off wavelength of the instrument For example, a platinum coated grating as used with the spectrograph discussed here has a critical wavelength (in angstroms) of approximately equal to 2 64 times the grazing angle in degrees, therefore at an angle of 4^0 (which was the angle of incidence used throughout this work) the wavelength cut-off should be approximately 11 3 angstroms However due to scattered light this theoretical cut-off minimum is never in fact achieved, in practice and for the spectrograph discussed here the minimum observable wavelength was about 36A This cutoff is also due to the fact that none of the sources used in this work emit strongly below about 40Å

The theory and construction of spectrographs is well known and is dealt with in a number of texts see for example Samson (1967) There are however some important points relating to grazing incidence spectrographs in general which should be mentioned here

Astigmatism is the major abberation in concave mirrors and this imperfection is inherited by the concave diffraction grating The theory of astigmatism was first developed by Rung and Mankopf (1927) and has since been dealt with in

detail by Beutler (1945) and Namioka (1961) Astigmatism results in a point on the slit being imaged into a vertical line, that is, focusing is achieved only in the horizontal plane The length z of the astigmatic image is given by,

$$z = \frac{l\cos\beta}{\cos\alpha} + L[\ \sin^2\alpha + \sin\alpha\tan\alpha\cos\beta\ ] \qquad (2\ 1)$$

where α is the angle of incidence, and β is the angle of the diffracted ray The first term gives the contribution due to the entrance slit of finite vertical length l and the second term is the astigmatism produced by a point on the entrance slit L represents the length of the ruled lines illuminated It can be seen from eq(2 1) that the image becomes more stigmatic for near normal incidence and quite stigmatic for $\alpha=\beta=0^0$ The astigmatic image also has an associated curvature which was studied by Beutler (1945) who identified two types of curvature, astigmatic curvature due to the astigmatism of a point source at the entrance slit and enveloping curvature caused by the finite length of the entrance slit when illuminated

Astigmatism can be tolerated in spectroscopy since only horizontal focusing is required to separate the various wavelengths However at grazing angles it is considered a major disadvantage since it reduces the light intensity per unit area of the image and imposes strict focusing conditions to produce maximum resolution, also spatial information from the source is lost Techniques for the reduction or elimination of astigmatism were not employed during this work and will not be discussed here

Dispersion expresses the way in which the various wavelengths are distributed over the Rowland circle Angular dispersion is defined as $d\beta/d\lambda$ and for a fixed

angle of incidence we have

$$\frac{d\beta}{d\lambda} = \frac{m}{d\cos\beta} \qquad (2\ 2)$$

We are usually more interested in the actual number of angstroms per mm dispersed along the Rowland circle This quantity the reciprocal of the linear dispersion $dx/d\lambda$ is called the plate factor and is given by

$$\frac{dx}{d\lambda} = \frac{d\cos\beta}{mR} \qquad (2\ 3)$$

whare R is the radius of curvature of the grating

While dispersion determines the separation of wavelenghts along the Rowland circle the resolving power determines whether this separation can be distinguished Resolving power is defined as $\lambda/\Delta\lambda$ and depends (if diffraction limited) on the order number m and the number of ruled lines N exposed to the incident radiation. it is usually written,

$$R = \frac{\lambda}{\Delta\lambda} = mN \qquad (2\ 4)$$

The resolving limit of a grazing incidence instrument is. in practice limited by the slit width if the slit width is small then resolving power is good but with wide slits poor resolution is obtained In the work presented in later chapters the slit width was varied between 5 and 30μm Typical values for resolution of the spectrograph used here are given below The influence of slit width on resolution has been discussed by Mack etal (1932)

Also of considerable importance is the grating efficiency. this can be defined

as the percentage of the incident radiation flux returned by the grating into a given spectral order The groove shape is important in determining how much radiation is concentrated into a given order also the type of reflective coating used in this case platinum The groove shape is described by the blaze angle θ blazed gratings are designed to have maximum efficiency over a certain wavelength region The grating used in this work had a blaze angle of $\theta = 1^{0}47'$ and is most efficient in the 60Å wavelength region

The instrument used for the investigations reported here was a two metre grazing incidence spectrograph model E580 supplied by HILGER ANALYTICAL and has specifications summarised in table(2 1) The grating was supplied by BAUSCH & LOMB and has the parameters, also listed below in table(2 1)

TABLE 2 1
Summary of the spesifications of the 2m grazing incidence spectrograph used throughout this work

Range	5 - 950Å - depending upon grating fitted
Grating	BAUSCH & LOMB Radius of curvature 2 metres Ruling 1200 grooves per mm Ruled area 25 X 35 mm Blank size 35 X 45 X 10mm Blaze angle $1^{0}47'$ Minimum grazing angle 40 minutes Angles of incidence 86 88 or 89^{0} Plates 2" X 25" (max) Working pressure 10^{-3} - 10^{-5}torr Slit widths used 10 - 50μm

Three interchangeable entrance slit assemblies giving angles of incidence of 86^0, 88^0 and 89^0 respectively were also supplied The plate holder used with this instrument takes 2" plates with a maximum length of 25", the curved surface of the plate holder (on which the plates are positioned) is machined to a positional accuracy of 0 0002", (0 005mm) The plate holder can be replaced with a tracking slit assembly which converts the spectrograph into a grazing incidence monochrometer thus photographic or photoelectric detection may be employed

The spectrograph is pumped by a 5" water cooled diffusion pump coupled to a rotary pump which together can evacuate the spectrograph from atmospheric pressure to a working pressure of 10^{-3} to 10^{-5}torr in approximately fourteen minutes Fig(2 4 a) shows the spectrograph in crossection The slit jaws are lapped onto their mount so that they are effectively vacuum sealed The only gas leak between the spectrograph and the target chamber is then the flow between the slit jaws and with slit widths of up to 10μm this leak is considered insignificant However it was found that the slit jaws needed to be cleaned regularly to remove debris from the plasma This was due to the close proximity of the plasma to the slit Cleaning of the slit jaws was carried out by simply removing the lower jaw from the assembly and removing the debris by drawing a match stick across the edges of the slit jaws

The walls of the spectrograph vacuum tank are constructed from a magnesium-zirconium alloy casting this alloy offers good vacuum properties is extremely stable and is very light in weight The base of the tank is shaped to reduce the internal volume and the sides are ribbed externally to reduce distortion under vacuum The top of the tank is a removable lid made from 12mm aluminum alloy plate and is sealed with an o-ring The plate holder

also shown in fig(2 4 a), consists of two main parts both constructed of the same material as the tank Fig (2 4 b) shows the way in which the plate A is held against the main body B by means of a shaped back C, assisted by two cord strips D The entire plate holder is supported kinematically within the tank Two points are located at the top end and a third at the lower end The cassette is held down on these supports by spring loaded lugs which engage in grooves in the side of the main tank A maximum plate length of 25" can be used The addition of a moveable baffle between the entrance slit and the plate holder allowed for multiple exposure of the same photographic plate by dividing the plate into sections

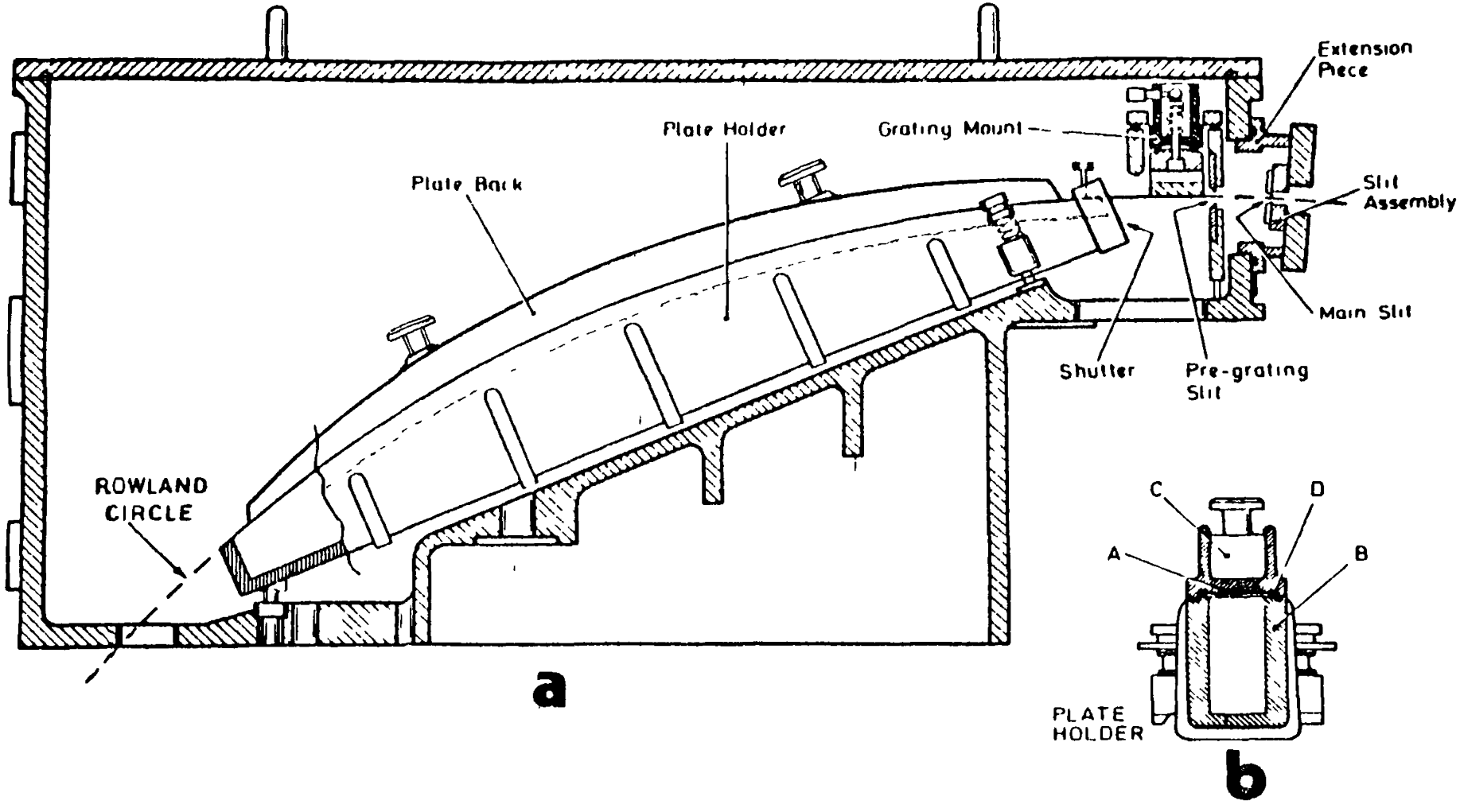

Fig (2 4 a b) Shows in section the vacuum tank plateholder and slit and grating assemblies of the two metre grazing incidence spectrograph used to record the spectra reported in chapter three (b) shows the plateholder in crosection

2 4 PHOTOGRAPIC PLATES

The plates used to record the spectra reported in later chapters were KODAK SWR plates These plates are slow when compared to other plates used in the VUV for example KODAK SC5 or 101 01 plates however SWR plates were found over the course of this work to produce clean measurable spectrograms

The processing technique followed simply consists of using four trays two of water one of developer (KODAK D-19), and one of fixer (KODAFIX) The temperature was that of the room and varied between 20 and 24^{0}C The plates were placed first in a tray of distilled water for 2-3 minutes they were then transfered to the developer tray (the developer being changed for each plate) for 2 minutes After washing in the third tray for a further 2 minutes the plates were transfered to the final tray and fixed for 5 minutes However despite following this procedure for each plate differences in plate density were found even between plates of identical exposure Scattered light from the spectrograph was also found to present problems This is however to be expected when one considers that the average exposure required for an absorption spectrum was of the order of 300 shots This number of shots can be set in perspective when one considers that to record a reference emission spectrum (which is usually aluminium or silicon) for a typical plate required on average only 15-20 shots The reasons for this difference in the number of shots required for the two spectra will be discussed in chapter 3 This therefore sets a practical limit on the minimum wavelength which can be recorded photographically in absorption with this instrument this was found to be about 60 angstroms The use of SWR and other plates have been described together

with developing procedures by Hoag and Miller (1969) and measurements of sensitivities and characteristic curves etc are given by Burton Hatter and Ridgely (1973) SWR plates as with all plates used in the VUV are extremely sensitive to abrasion and must be handled with care

Each absorption spectrum recorded had overlaying a section of it, an emission spectrum which was used as an external reference (internal references were also used where possible) with known lines from which positions on the plate of unknown features could easily be measured The following procedure was used in measuring the wavelengths of spectral features The plates were measured on the photoelectric comparator in the Physics department at University College Dublin This instrument is operated by hand and esentially allows the accurate determination of the positions of spectral lines along a photographic plate, and is accurate to about 1μm The transducer used on the comparator is interfaced to a micro computer and the positions of both known and unknown features are recorded on a printed output To compute final wavelengths of unknown features a computer program was written to read the data in the form of a series of x y points (x(position), y(wavelength)) The program used a least squares subroutine taken from the NAG numerical subroutine library to fit an N^{th} order polynomial to the data This program allows interpolation to be carried out so that the positions of unknown features can be converted into wavelengths The program together with sample input-/output data is listed in appendix two Wavelengths for the reference lines usualy from Al or Si were taken from Kelly and Palumbo (1973) Final errors in wavelength measurements using this technique are normally no more than ± 0.03Å

2 5 OPTICS AND ALIGNMENT TESTS

Fig (2 5) shows schematically the arrangement used to obtain the absorption spectra of a number of different laser produced plasmas The method employed used two lenses usually one a half-optical spherical lens and the other cylindrical or in some cases whare two point plasmas were used, one half-optical spherical and the other three-quarters-optical spherical lens (The term half-optical lens is taken to mean a lens that was cut along a diameter of its circular face so that two half-optical lenses were obtained and similarly for the term threequarter-optical) Both had the same focal length (typically f=6cm) One half-optical spherical lens was used to create the continuum backlighting source by focusing a portion (typically between 30 and 70%) of the laser output to a point focus on a high z metal target usually tungsten or hafnium The remaining portion of the beam was then focused by the second lens to a line focus on the second target to create the absorbing ions As can be seen in fig (2 5) the laser beam is directly split along the laser axis which means that optical delay lines were not required by this method, that is, all of the available energy in the beam was utilised for plasma production

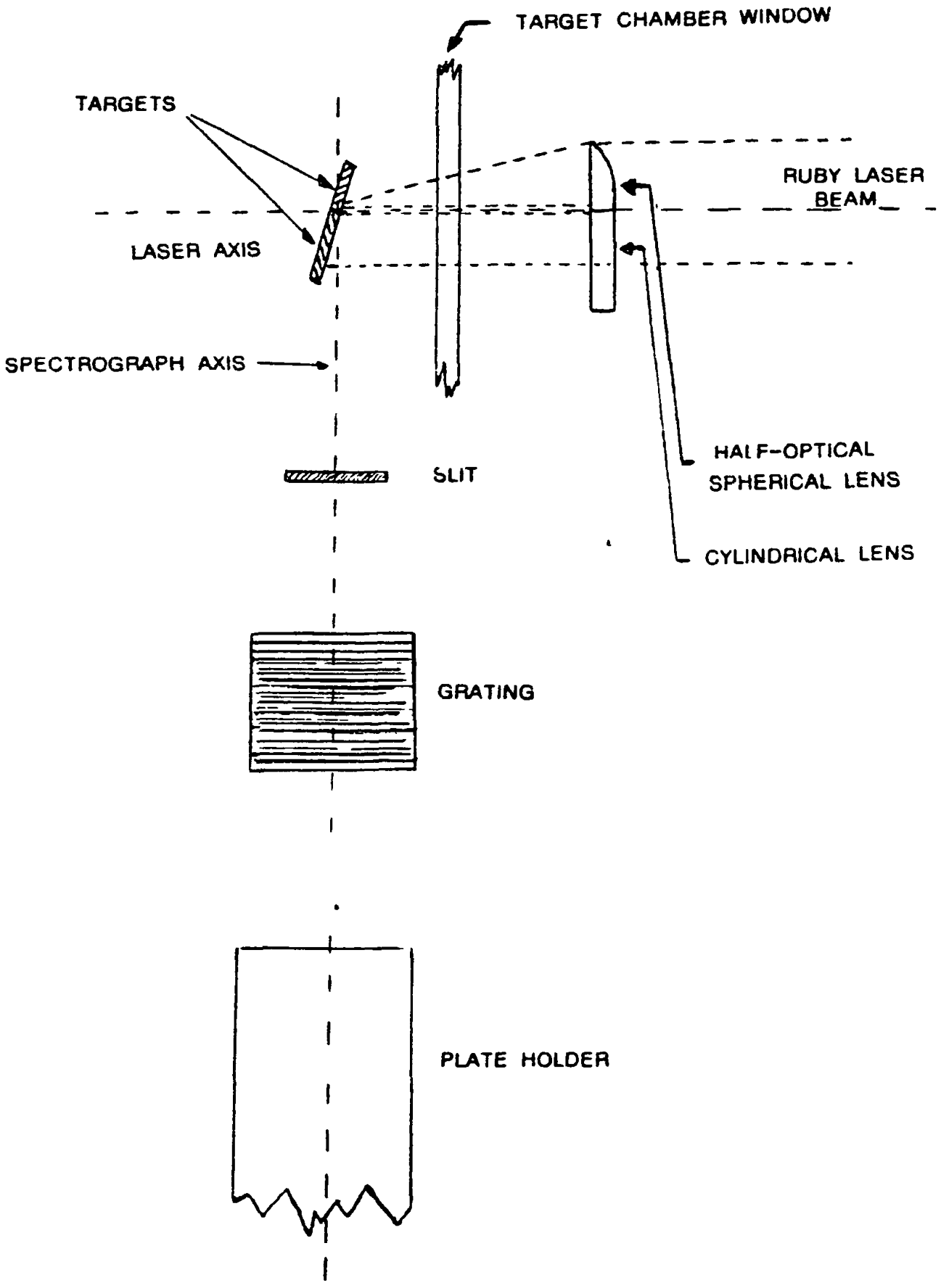

Fig (2 5) Shows the layout of the optical system used to study photoabsorption in ionized species produced in a laser produced line plasma using a point laser produced plasma as the continuum source

A number of important motions of the lenses are possible, these are required for accurate alignment of the source and absorbing plasmas with the entrance slit of the spectrograph Each lens may be independently moved backwards and forward along the laser axis this is particularly useful when an isonuclear series is to be studied since successive de-focusing of the absorbing plasma reduces the laser irradiance at the target surface and means that lower or higher ion stages can be selected This essentially gives a coarsely tunable source of ions simply be moving a lens one way or another (See fig(2 5))

Accurate (< 0 2mm) lateral and vertical motions of both lenses are also possible, however with the present system these motions do not exist independently for each lens The lateral motion of both lenses (that is motion parallel to the spectrograph optical axis) allows different portions of the laser output to be directed to each target Although it was usual to split the laser beam roughly 50-50 to each target it was found that even if as little as 30% of the beam was directed to the continuum producing target that absorption could still be seen in lower stages of ionisation For example an absorption spectrum of Mg^{2+} could be obtained by splitting the laser beam such that the continuum producing target received only 30% of the beam For higher ion stages, for example the absorption spectra of SiV reported in chapter three 50% of the beam was directed to each target

The large number of shots required to obtain an absorption spectrum (typically 300 - 400) require that the targets be constantly moved, in this case every 5-10 shots It is also required that the target be held rigidly at an angle of between approximately 2^0 and 5^0 to the spectrograph axis during the experiment These two factors alone impose restrictions on the focusing of both lenses onto the targets as well as on the alignment of the plasmas with the

spectrograph slit The alignment procedure whereby both plasmas were aligned accurately with each other and with the spectrograph slit involved carrying out photographic alignment tests These alignment tests are carried out after coarse alignment (by which is meant alignment by eye of the two HeNe laser beams positioned along the spectrograph axis and the ruby laser axis) of the plasma with the spectrograph entrance slit A target such as boron has many well known lines such as those in hydrogen and helium-like boron which will only be observed if the core of the plasma is directly in line with the entrance slit of the spectrograph So by moving the lenses in front of the slit over a predetermined range (typically 2mm) and at regular intervals within this range exposing a section of a photographic plate the optimum height of the plasma in front of the spectrograph entrance slit was easily found The sectioning of the plate was accomplished by the use of a baffle this baffle is located between the plateholder and the grating and consists of a brass plate with a rectangular section removed from the center, the baffle can be traversed at right angles to the spectrograph axis, and can be set to any width by using layers of insulating tape in such a way that a great many narrow stripes of the plate can be exposed in sequence The baffle was also used to overlap absorption spectra with a reference In another type of alignment test two targets one a high z metal the other a sample of magnesium were used and again a vertical range was chosen and after development of the plate the portion of maximum absorption was taken as optimum It should be noted here that these tests are only feasible due to the fast (< 20 minutes) "turn around time" of the system that is its fast pumping time and also because of the high (30 shots per minute) rep rate of the laser It is hoped in the future to be able to use the monochrometer attachment together with a photoelectric detection system (currently being developed in this laboratory by Mythen) to facilitate alignment

Focusing of both lenses was achieved in quite a simple way by observing scattered light from the alignment laser located at the rear of the target chamber with a small telescope focused at infinity This is not the best way to optimise the focusing of such a lens the correct focusing technique for such a system has been described by Kennedy (1977) However the technique was justified when one considers that the targets were constantly being moved by hand during the experiment and so very accurate focusing could not be maintained over the course of a single experiment (experiments consisted of on average, 300 shots) and so the above method which would appear to be accurate to about ±0 20mm was found over the course of this work to be adequate

2 6 TARGET CONSTRUCTION.

A relatively simple method of target construction was used. it involved the use of sheet materials of approximately 1mm thick This type of material is readily available in spectroscopically pure form Two such pieces of material are chosen. one is used as the continuum producing target while the other is used as the source of absorbing ions Both materials are placed flat on another piece of sheet material in this case used printed circuit board was found to have the right properties (that is the used PCB was found to be easy to cut to the required shape and was also found to bond well to the target materials. it was also freely available) The targets were then bonded to the piece of board using an epoxy resin in this case ARALDITE which is easily mixed and has a hardening time of about 5 minutes depending on the mix The edges of the targets were then surrounded with resin in this way they were held rigidly to the surface of the board After a sufficient drying time the targets could be worked with a smooth file to ensure that both target surfaces are aligned with respect to each other The targets thus made were then connected to the target rod The only problems associated with this technique are those encountered when using reactive materials such as Na and K whare the oxidation time is short when compared with the drying time of the resin

REFERENCES

Beutler HG J Opt Soc Am 35 311 (1945)

Burton WM Hatter AT, and Ridgley A App Opt 12 1851 (1973)

Hoag AA and Miller WC App Opt 8 12 (1969)

Kelly RL and Palumbo LJ NRL Report Number 7599 (1973)

Kennedy ET Ph D thesis 1977 University College Dublin Unpublished

Mack JE Stehn JR and Edlen B J Opt Soc Am 22 245 (1932)

Mythen C M Sc Thesis To be completed

Namioka T J Opt Soc Am 51 4 (1961),

O'Sullivan G Ph D thesis 1980 University College Dublin Unpublished

Rung CR, and Mannkopf R Z Physik 45 13 (1927)

Samson JAR "Techniques of vacuum ultraviolet spectroscopy " 1967 Wiley and sons inc

GENERAL REFERENCES FOR CHAPTER 2

Driscol WG and Vaughn W Ed's "O S A Handbook of optics " McGraw Hill Book Company (1978)

Ross D "Lasers light amplifiers and oscillators " Acedemic Press (1969)

CHAPTER THREE
EXPERIMENTAL RESULTS

3 1 INTRODUCTION.

Measurements and calculations for absorption spectra of various laser produced plasmas are reported here. the emphasis in this work has been placed on the study of both the neon and xenon-like isoelectronic sequences. although absorption in other ion stages (outside of these sequences) has also been observed Many of the lines observed in absorption were known from emission spectra previous to this work However many new lines particularly in the absorption spectra of Al III and Si IV have been recorded and are reported here for the first time Extensive calculations have been carried out to determine the nature of these unknown lines Absorption along the neon-like sequence has been extended to the fifth member (Si V) and results particularly for Al IV and Si V are presented here for the first time Also reported here are tentative results obtained from absorption studies of ions of the elements lanthanum and cerium particularly La IV and Ce V both of which are members of the xenon-like isoelectronic sequence

The principal series $2p^6\ ^1S_0 - 2p^5ns$ nd for each of the third fourth and fifth members of the neon-like sequence have been observed. the wavelengths of each of these lines have been measured and are compared with known values Also observed and measured for the above members of the neon-like sequence were the inner shell $2s^22p^6\ ^1S_0 \rightarrow 2s2p^6np\,^1P_1$ autoionizing transitions

Wavelengths for these asymmetric features have also been measured and are compared with previous experimental measurements where available. and with theoretical calculations

Lines due to known transitions in the higher ionization stage of magsesium (Mg IV) have also been identified, and in the spectra of aluminium and silicon about 100 unknown absorption lines have been measured Many of these lines are only observed in the absorption spectra of these elements and are absent from emission spectra obtained by focusing the laser output to form a single point plasma The absence of these (as yet unidentified) lines from emission spectra of aluminium and silicon would seem to suggest that these transitions are the result of inner-shell or two-electron excitations involving the 2s and 2p subshells Transitions from excited states may also be involved It is also possible that these unidentified absorption features may occur over a number of different ion stages (III - VI) Calculations have been carried out in an attempt to assign these transitions

Also presented in this chapter for the first time is the vacuum ultraviolet absorption spectrum of a laser produced lanthanum plasma obtained between 80 and 160Å several discrete absorption features have been observed in this region Of particular interest are those lines in the 85 - 120Å region which are thought to arise due to the collapse of the 4f wavefunction in La IV These features seem analogous to the lines which arise from the redistribution of oscillator strength which have been reported for Ba III by Lucatorto McIlrath Sugar and Younger (1981), the La IV spectrum is discussed in terms of that analysis

The overall objective in this chapter is to present a series of absorption spectra of ionized species (produced in laser plasmas) which have been obtained over the course of this work The large number of transitions seen in absorption together with the number of ion stages over which these transitions have been

observed clearly demonstrate the usefulness of the two laser produced plasma technique and show it to be a potentially powerful tool for the experimental investigation of atomic structure, particularly in relation to inner-shell and autoionizmg levels

3 2 THE NEON-LIKE ISOELECTRONIC SEQUENCE PREVIOUS WORK

3 2 A) Ne I.

The first member of the neon-like isoelectronic sequence is neutral neon Ne I which has the ground state configuration $1s^2 2s^2 2p^6\ ^1S_0$ The VUV absorption spectrum of Ne I was first studied by Codling, Madden and Ederer (1967) using as a light source the 180 Mev electron synchrotron at the National Bureau of Standards in Washington USA They observed the principal series of discrete structures which arise due to the excitation of a single 2p electron from the ground state $2s^2 2p^6\ ^1S_0$ to excited states of the form $2s^2 2p^5 ns$ nd converging on the $^2P_{1/2\ 3/2}$ limits Also observed were a very prominant Rydberg series of autoionizing resonances due to the promotion of a single inner-shell 2s electron to levels with energies greater than the $^2P_{1/2}$ ionization energy a number of series due to the simultaneous excitation of two of the 2p electrons in transitions of the type $2p^6 - 2p^4 m\ell, m'\ell'$ were also recorded

3 2 B) Na II

The VUV photoabsorption spectrum of the second member of the neon-like sequence Na II was studied by Lucatorto and McIlrath (1976) They used the tunable laser technique, pioneered by them, which has already been described in chapter one (see page 30) They obtained the vacuum ultraviolet absorption spectrum of Na II in the wavelength region 420-150Å and reported the observation of the $Na^+ 2p^6\ ^1S_0 - 2p^5 ns$ nd series together with the lowest-lying autoionization resonances involving the excitation of a single 2s subshell electron $2s^2 2p^6\ ^1S_0 - 2s2p^6\ ^1P_1$ Six members of this series were measured Also measured was the near-threshold photoionization crossection

$\sigma(Na^{+} \rightarrow Na^{++})$, which was derived from measurements made on photographic plates calibrated with the helium $1s^2\ ^1S_0 - 2snp\ ^1P_1$ autoionizing resonances

The objective of the tunable laser experiments of Lucatorto and McIlrath was to observe absorption from excited states of neutral sodium by using the laser to create a column of excited sodium atoms However although photoabsorption of neutral sodium was observed in the absence of the laser (i e absorption of the sodium vapor contained in the heat pipe) no evidence of transitions from excited states was reported

3.2.C) Mg III

The vacuum ultraviolet absorption spectra of neutral and ionized magnesium (Mg I Mg II and Mg III) were produced by Esteva and Mehlman (1974) using a two-plasma technique involving two low inductance vacuum sparks, (see chapter one page 22) More recently Kastner, Crooker Behring and Cohen (1977) have obtained the absorption spectrum of Mg III (again using a low inductance vacuum spark as the ion source) in a magnesium plasma

Esteva and Mehlman (1974) identified a total of 68 resonances from Mg I, II and III Of these 38 lines of singly ionized magnesium were unclassified They observed the absorption spectrum of Mg III which in the wavelength region 240 - 150Å consists of the normal series transitions involving the excitation of a single 2p electron These lines were previously observed in emission by Soderqvist (1934) Also recorded by Esteva and Mehlman were a Rydberg series of autoionizing resonances due to the excitation of an inner shell 2s electron The wavelengths of six members of this series were measured

3 2 D) Al IV

The next member of the neon-like isoelectronic sequence is Al IV Some features in the absorption spectrum of this ion were studied by Carillon Jamelot, Sureau and Jaegle (1972) using the technique of two laser produced plasmas one acting as the continuum source and the other as the ion source (see chapter one page 25) Kastner et al (1977) studied the absorption of an aluminium plasma in the vacuum ultraviolet using a single low inductance vacuum spark and have observed the $2p^6 - 2p^5ns$ nd series along with several members of the inner shell autoionizing transitions $2s^22p^6\ ^1S_0 - 2s2p^6\ ^1\ ^3P_1$ However with both of these techniques a true absorption spectrum of the aluminium plasma was not obtained In the case of the technique used by Carillon et al, this was due to the fact that the target used by them to produce the continuum radiation was the same as the ion producing target and the emission spectrum of an aluminium laser pruduced plasma is in this wavelength region (160 - 70Å) dominated by intense line emissions which has the effect of partially obscuring absorption features which may exist in the underlying recombination continuum (In the case of the theta-pinch technique used by Kastner et al a similar effect occurs i e the absorption spectrum is obscured by emission features) Jamelot Sureau and Jaegle (1972) identified with density traces of photographic recordings new lines in the $2p^6\ ^1S_0 - 2p^5nd$ series in A IV in addition to those identified by Soderqvist (1934) who assigned the series to n=5 As well as these identifications Carillon Jamelot Sureau and Jaegle (1972) reported the identification of two members of the $2s^22p^6\ ^1S_0 - 2s2p^6np\ ^1P_1$ and three members of the $^3P_1$ series However Kastner etal (1977) dispute the assignment by Carillon et al (1972) of the $^3P_1$ series and have identified this series of strong absorption features as the $^1S_0 \rightarrow {}^1P_1$ series Both Kastner et al (1977) and Carillon et al (1972) have reported

the observation of the intercombination transitions $^1S_0 \rightarrow {}^3P_1$ Kastner et al describe these features (shown below in fig(3 1 b)) as appearing as narrower profiles superimposed on the longer wavelength side of the main $^1S_0 \rightarrow {}^1P_1$ profiles

The difficulty of identifying absorption features from a spectrum dominated by strong emission lines can be judged by reference to the density trace (fig (3 1 a)), recorded by Jamelot et al (1975) and also from the subsequent controversy which surrounded the anouncement of a stimulated emission reported by this group (Jagele etal (1971) and Jaegle etal (1974)) One of the problems with an intense line spectrum is that any intensity anomalies which may arise in density traces of such spectra are clearly open to interpretation Both fig (3 1 a) and fig (3 1 b) (which was recorded by Kastner et al (1977)) show such an intense emission spectrum for aluminium over the 100 - 70Å wavelength region

3 2 E) Si V

The fifth member of the neon-like sequence is four times ionized silicon (Si V) the VUV absorption spectrum of this member is reported here for the first time The main ns and nd series have been observed in emission (Soderqvist (1934) Ferner (1941)) and more recently in absorption (Kastner et al (1977)) previous to this work However no observation of autoionizing structures above the $^2P_{1/2}$ limit have as yet been reported for the Si V ion

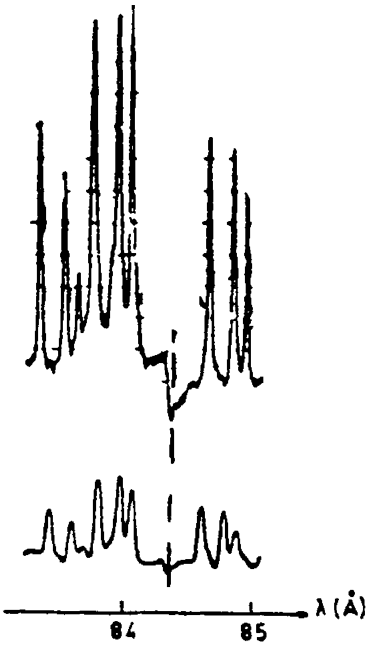

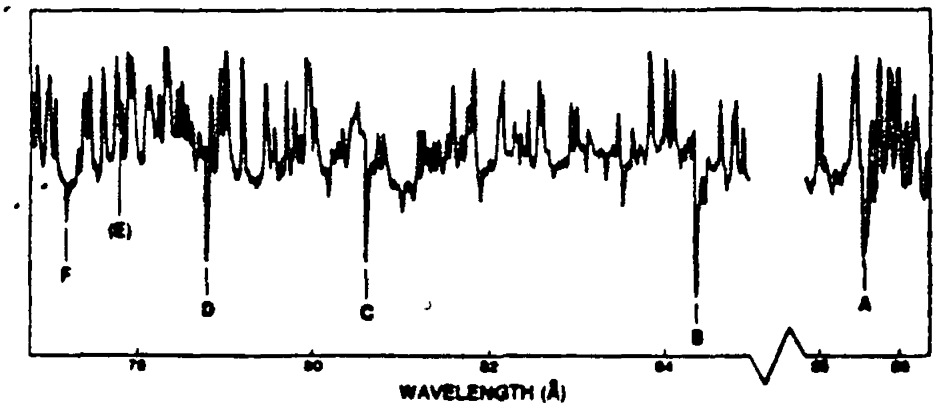

Fig (3 1 a b) Shows two density traces taken in the same wavelength region both are of aluminium plasmas Fig (3 1 a) which is taken from Jamelot et al (1972) shows the region of the spectrum around the second member of the series of autoionizing resonances $2s^2 2p^6\ ^1S_0 - 2s2p^6np\ ^1P_1$ Fig (3 1 b) is taken from Kastner et al (1977) and is a trace of the wavelength region 96 - 75Å and shows the members of the series to n=8 In both fig (3 1 a) and fig (3 1 b) the dominant features of the region are in fact the strong emission lines which make it difficult to obtain unambiguous information about the absorption features Fig (3 1 b) also shows the $^3P_1$ series which according to Kastner et al are observed as weak absorption features to the longer wavelength side of the $^1P_1$ profiles

3 3 THE NEON LIKE SEQUENCE PRESENT WORK

An overview of the present work on photoabsorption along the beginning of the neon-like isoelectronic sequence is given in table (3 1) and fig (3 2) Table (3 1) contains the wavelengths of the $2s^22p^6\ ^1S_0 - 2s2p^6np^1P_1$ autoionizing resonances for the second third fourth and fifth members of the sequence (Na II - Si V) Also included in table (3 1) for comparision are theoretical and experimental values of the same features obtained by other workers previous to this work Fig (3 2) shows the absorption spectra of Mg III, Al IV and Si V

3 3 A) Mg III

The VUV absorption spectrum of Mg ions obtained during the course of this work is shown in fig (3 2) and in more detail in fig (3 3) The spectrum is different from that obtained by Esteva and Mehlman (1974) in that we have observed lines from stages III, IV and V but not from I or II This is to be expected given the conditions of the experiment, I e the fact that the continuum producing portion of the backlighting plasma is located at the hottest region (about 0 5mm from the surface) of the continuum producing target This means that only the hottest region of the fore-plasma will be exposed to the continuum produced in the backlighting plasma, and it would appear from the magnesium spectra reported in this work that only ions of stage higher than II are produced here despite the fact that the cylindrical lens producing the fore-plasma was, in the case of magnesium focused either in front of or behind the target by up to 1 5 cm The fact that no time delay exists between the two plasmas in the experiment is also a factor Focusing of the laser directly onto the magnesium target gives essentially the same type of spectrum

as de-focusing does But when the ion producing portion of the beam was de-focused it was found that the features due to absorption of Mg III ions were enhanced This enhancement can be attributed to the fact that the de-focused plasma contains a greater density of Mg III ions

Fig(3 3 a) shows the principal series of the Mg III ion due to the excitation of a single 2p electron The lines due to these $2s^22p^6\ ^1S_0 - 2s2p^5nsnd$ transitions are strong and in the case of the nd series are seen also to be very broad indicating that the fore plasma contained a large number of Mg III ions in the ground state these lines are listed in table (3 2) together with literature values taken from Kelly and Palumbo (1973) Also in fig (3 3 a) are lines due to transitions in the Mg IV ion of the type $2s^22p^5\ ^2p_{1/2} - 2s^22P^4ns$, which will be discussed in section 3 4 Figure (3 3) shows the spectacular onset of continuum absorption after the $^2P_{1/2\ 3/2}$ limits Fig (3 3 b) shows the absorption of magnesium in the 200-150A wavelength regions Seen here are further groups of lines due to Mg IV transitions of the type $2s^22P^5\ ^2P_{1/2}$ - $2s^22p^4nsnd$ also to be discussed in section 3 4 To shorter wavelengths are observed the Rydberg series of asymmetric structures assigned to the transitions $2s^22p^6\ ^1S_0 - 2s2p^6np\ ^1P_1$ (which are listed in table (3 1)) In the above case six members of this series were observed Fig(3 3 c) is an enlargement of the region containing the inner shell structures showing clearly their asymmetric nature

3 3 B) Al IV

The features observed in the absorption of an aluminium plasma are now discussed This is the first absorption spectrum of aluminium ions to show clearly the discrete ns nd series together with the strong autoionizing resonances above the $^2P_{1/2}$ limit As shown in fig (3 2) the structures observed

are essentially the same as the isoelectronic structures observed in the spectrum of Mg III also shown in fig (3 2) The dominant absorption is again as in the case of Mg III due to the principal $2s^22p^6\ ^1S_0 - 2s^22p^5nsnd$ series with some less intense absorption features possibly being due to the higher stage Al V or the lower stage Al III ion

It is also clear from Fig (3 2) that the onset of the photoionization continuum is not as dramatic as in the case of magnesium This may be expained by the fact that it is more difficult to generate large numbers of Al IV ions than Mg III ions As with magnesium the Rydberg series of asymmetric resonances $2s^22p^6\ ^1S_0 - 2s2p^6np^1P_1$ can be clearly seen in the photoionization continuum Also noticable in fig(3 2) is the energy gap between the $2p^6\ ^2P_{1/2\ 3/2}$ limits and the first member of the autoionizing series in Al IV which is not as great as that of Mg III It can be seen that there is no absorption observed between the limits and the first member as there is in the case of the magnesium spectrum. niether is there any absorption observed to wavelengths shorter than the first ($2p^63p^1P_1$) member This spectrum was obtained using the method described in chapter two with a halfnium target providing the continuum radiation

Measured values of the $2s^22p^6\ ^1S_0 - 2s2p^5ns,nd$ lines in Al IV are are presented in table (3 2) together with literature values (taken from Kelly and Palumbo (1973)) The list of measured wavelengths of the autoionizing features $2s^22p^6\ ^1S_0 - 2s2p^6\ ^1P_1$ observed in the photoionization continuum of Al IV between 100 and 70Å are listed in table (3 1) along with the values obtained by Carillon et al (1972) and more recently those of Kastner et al (1977) together with calculated values obtained in the course of this work As was mentioned in section 3 2 above both Carillon et al (1972) and Kastner et al (1977) reported the observation of the $2s^22p^6\ ^1S_0 - 2s2p^6np^3P_1$ auto-

ionizing structures in absorption spectra of Al IV These features can be seen in the density trace of Al IV recorded by Kastner et al and shown above in fig(3 1 b) They appear as prominant absorption dips to the longer wavelength side of the $^1S_0 \rightarrow {}^1P_1$ profiles It must be noted here that the present work which has revealed the first unambiguous absorption spectrum of the Al IV ion in this wavelength region (70 – 100Å) has not revealed the existence of the $^1S_0 \rightarrow {}^3P_1$ series An enlarged view of the wavelength region containing the $^1S_0 \rightarrow {}^1P_1$ resonances is shown in fig(3 4 a)

3.3 C) Si V

The VUV photoabsorption spectrum of a silicon plasma is also shown in fig (3 2) The spectrum is isoelectronic to the magnesium and aluminium spectra discussed earlier The principal series of the neon-like Si V ion together with the first member of the $2s^22p^6\ {}^1S_0 - 2s2p^6np\,{}^1P_1$ autoionizing series are shown The spectrum also shows many other absorption lines some of which are equal in (and in some cases of greater) intensity than those assigned to the Si V ion These structures are thought to be due to absorption in the lower stage Si IV ion The reason for this tentative assignment is as follows The absorption spectrum of Si V was, by far, the most difficult of the spectra to obtain this is because in producing Si V we are at the limit of the laser energy available for the production of ions Thus it is assumed that instead of producing a plasma in which the dominant ion population is Si V we are in fact producing a plasma which contains significant populations of both Si V and the lower stage Si IV ion The spectrum of Si V shown in fig(3 2) was recorded using a two half-optical spherical lens configuration the use of a cylindrical lens to create the fore plasma results in a spectrum in which the Si V features

are extremely weak A similar effect occurs in the case of a magnesium plasma in which populations of both Mg III and Mg IV are found to be present despite de-focusing of the lens used to create the fore plasma

Kastner et al (1977) reported the observation of inner shell autoionizing levels in the ions along the beginning of the neon-like isoelectronic sequence They state, with reference to silicon, that although the neon-like Si V ions were present in the plasma under investigation, (evident from the observed Si V emission lines) no evidence of the $2s^2 2p^6\ {}^1S_0 - 2s2p^6np\ {}^1P_1$ series was found The authors suggested that the spark used does not always take place in such a way as to produce the spatial plasma configuration needed to observe absorption lines and suggest further that observation of Si V absorption would require a hot central continuum emitting region surrounded by a cooler region containing the Si V ions

The present series of experiments enabled the observation of the first three members of the autoionizing $2s^2 2p^6\ {}^1S_0 - 2s2p^6np\ {}^1P_1$ series in the neon-like Si V ion to be made the wavelength of the 3p 4p and 5p members are given in table (3 1) The first member is shown in fig(3 4 b) and is clearly an asymmetric structure

The spectra shown in fig(3 5 a-d) were recorded by focusing the entire laser output onto the surface of a plane silicon target with a single spherical lens and sucessively de-focusing the laser beam by moving the lens with respect to the target This series of spectra demonstrate two important features of this variation in the absorption technique Firstly the fall off in the number of emission lines from higher ion stages in the plasma is clearly shown The fall off in emission lines with progressive de-focusing especially at shorter wave-

lengths enables the underlying recombination continuum to be observed which although weak is clearly visible Secondly because of de-focusing the actual size of the plasma increases as the laser beam is progressively de-focused the diameter of the plasma resulting from de-focusing of the laser beam between 2 5 and 7 5mm varies between 1 and 3mm This plasma will not be either as dense nor will it contain significant populations of highly ionized atoms however it does provide a significant path length along which transitions from lower ion stages in the plasma absorb the recombination continuum The absorption of the $2s^2 2p^6 - 2s^2 2p^5 nd$ series is observed in the more de-focused plasma also visible in the more de-focused plasma Fig(3 5d) is the almost complete absorption of the n=3 members of the $2p^6 - 2p^5 ns$ series Three members of the inner shell autoionizing series $2s^2 2p^6\ {}^1S_0 - 2s2p^6 np\ {}^1P_1$ are also clearly visible and are indicated in the central spectrum of fig (3 5) The n=3 first member of this series can be seen clearly in fig (3 5 a) and as can be seen the structure appears asymmetric However in fig's (3 5 b and c) the asymmetric shape of this feature seems to receed and be replaced by what appears to be the emergence of a second absorption line to the short wavelength side of the n=3 member This may also be interpreted as being a change in the shape of the profile of the n=3 member which seems to change significantly from fig (3 5 a) to fig (3 5 d) however the exact nature of the effect giving rise to this apparent profile change cannot be confirmed without a series of density traces from a number of such plates taken under varying conditions It is interesting to note however that the wavelength of the first ($2s2p^6 3p$) member of this autoionizing series has been measured during the course of this work at 75 10Å, the $^2P_{3/2\ 1/2}$ limits are given (Martin and Zalubas (1983)) as 74 35Å and 74 07Å respectively Calculated values of these limits (also this work) are 74 15Å and 74 04Å respectively while the calculated wavelength of this first member is 74 47Å

Clearly the feature lies to the long wavelength side of the $^2P_{1/2}$ limit i e it falls in energy terms below the ionization limit If this is the case then the feature should not be autoionizing However the results of absorption experiments (fig 3 4 b)) show the feature to be asymmetric thus strongly suggesting that it has an autoionizing character One very tentative suggestion to explain this apparent paradox is that plasma broadening effects lower the effective ionization limit and so the level which falls below E_∞ for the isolated atom in fact falls above E_∞ for the plasma case This might also serve to explain why the profile shape for this feature seems to vary with plasma conditions

Measured values of the $2p^5$ ns, nd series observed in Si V are given in table (3 2) together with values taken from Kelly and Palumbo (1973)

TABLE (3 1)

Wavelengths of the autoionizing features

$$2s^2\ 2p^6\ {}^1S_0 \text{ —— } 2s2p^6\ np\ {}^1P_1$$

observed in the second third fourth and fifth members of the neon like isoelectronic sequence
All wavelengths are given in angstroms

	Na II			Mg III					Al IV					Si V	
	λ_{LM}	λ^*_{LM}	λ^*_{TW}	λ_{TW}	λ_{EM}	λ^*_{TW}	λ^*_{EM}	λ_K	λ_{TW}	λ_C	λ_K	λ^*_{TW}	λ^*_C	λ_{TW}	λ^*_{TW}
n = 3	177 24	176 90	174 61	126 48	126 50	125 65	125 19	126 49	95 35	94 48	95 56	94 73	91 93	75 10	74 47
n = 4	164 92	164 90	162 80	114 30	114 32	113 44	113 36	114 34	84 27	84 14	84 38	83 82	82 97	65 10	64 71
n = 5	160 66		158 68	110 13	110 16	109 31	109 27	110 12	80 62		80 58	80 09	79 87	61 67	61 43
n = 6	158 57			108 02	108 08	107 31	107 34				78 79	78 33			
n = 7	157 55		155 66		108 92		106 26	107 05			77 79				
n = 8	156 88				106 30		105 60				77 18				
$^2S_{1/2}$ limit					104 50		103 61	104 39			75 38	74 97			56 86

λ^* are calculated values
λ_K are the results of Kastner et al (1977)
λ_{LM} are the results of Lucatorto and Mcilrath (1976)
λ_{EM} are the results of Esteva and Mehlman (1974)
λ_C are the results of Carillon et al (1972)
λ_{TW} are results obtained during this work

TABLE 3 2

Wavelengths of the principal $2s^2 2p^6\ {}^1S_0 - 2s^2 2p^5 ns, nd$ series measured for the third fourth and fifth members of the neon-like isoelectronic sequence (Mg III Al III and Si V) Wavelengths are considered to be accurate to about ±0 03A and were measured from a number of plates All wavelengths are given in angstroms

Mg III			Al IV			Si V		
λ_{TW}	λ_{KP}		λ_{TW}	λ_{KP}		λ_{TW}	λ_{KP}	
188 53	188 528	3d	161 68	161 686	3s	118 95	118 968	3s
187 18	187 194	3d	160 06	160 073	3s	117 83	117 860	3s
186 47	186 510	3d	131 64	131 652	3d	97 13	97 143	3d
182 97	182 973	4s		129 729	3d	96 08	96 439	3d
182 25	182 240	4s	124 52	124 543	4s	90 83	90 852	4s
171 37	171 395	4d	124 03	124 034	4s	90 08	90 453	4s
170 80	170 802	4d	116 93	116 921	4d	85 51	85 579	4d
169 78	169 740	5s	116 48	116 464	4d	85 14	85 175	4d
169 12	169 150	5s	114 74	114 737	5s			5s
164 93	164 954	5d	114 33	114 313	5s			5s
164 37	164 384	5d	111 59	111 589	5d	80 93	81 113	5d
163 54	163 586	6s	111 20	111 196	5d	80 37	80 807	5d
161 61		6d	110 59		6s			6s
160 78		7s	110 13		6s			6s
160 24		7s	108 87	108 907	6d	78 94	78 903	6d
159 80	159 755	7d	108 506	108 535	6d	78 65	78 611	6d
					7s			7s
					7s			7s
			107 31	107 370	7d			7d
			106 88	106 990	7d			7d

gp are values taken from Kelly and Palumbo (1973).
w are values measured over the course of this work.

Fig (3 2) Shows absorption in the third fourth and fifth members of the neon-like sequence The principal ns nd series are seen together with the inner shell autoionizing levels The magnesium and aluminium spectra were both obtained using a hafnium target to provide the backlighting source in both cases a cylindrical lens was used to create the fore plasma The silicon spectrum was obtained using two half-optical spherical lenses and a tungsten plasma was used to backlight the fore plasma

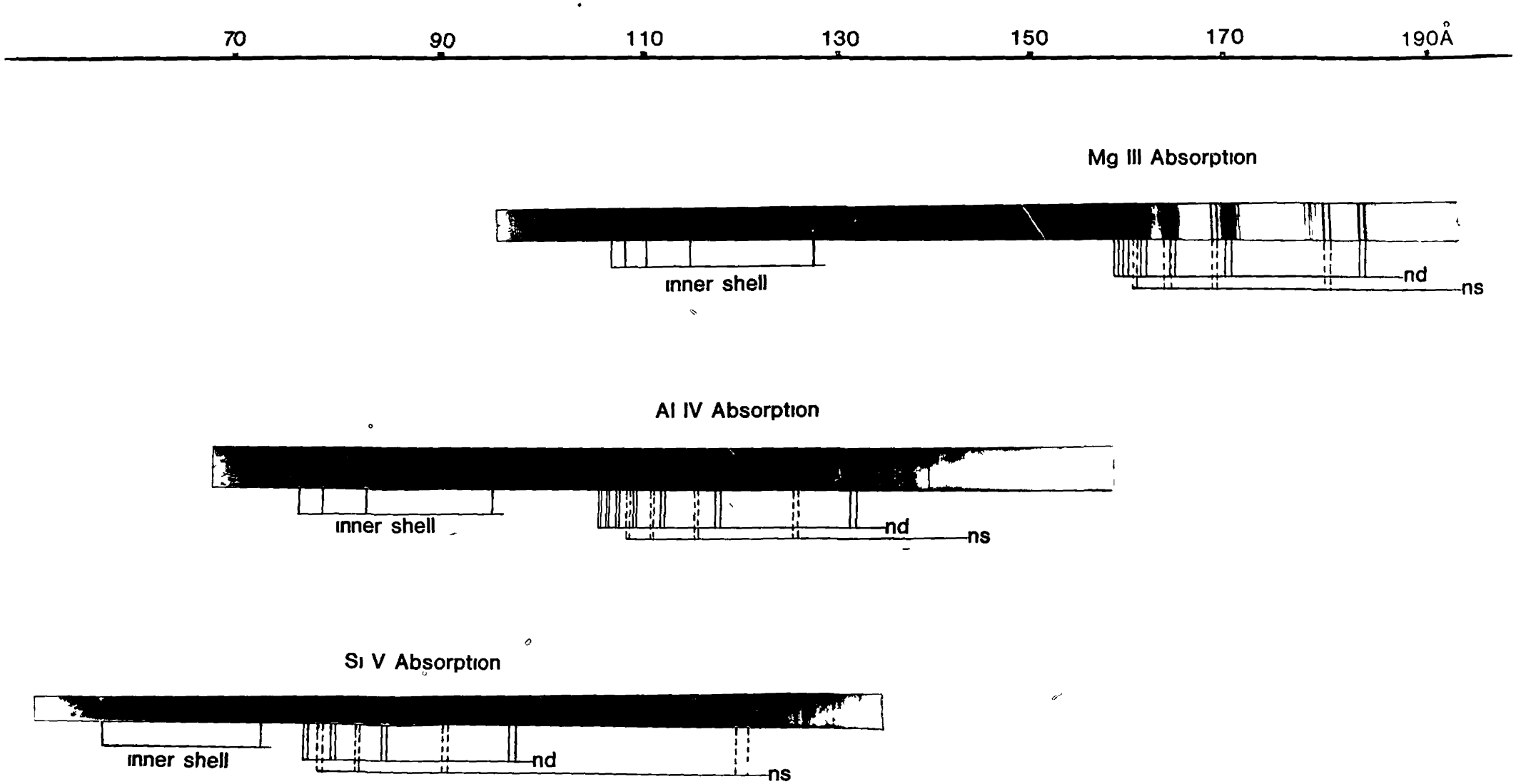
70
90
110
130
150
170
190Å
Mg III Absorption
inner shell
nd
ns
Al IV Absorption
inner shell
nd
ns
Si V Absorption
inner shell
nd
ns

Fig (3 3 a b c) Shows the absorption spectrum of a magnesium plasma in the wavelength region 190 – 90A and shows absorption in Mg III and Mg IV (see text for details)

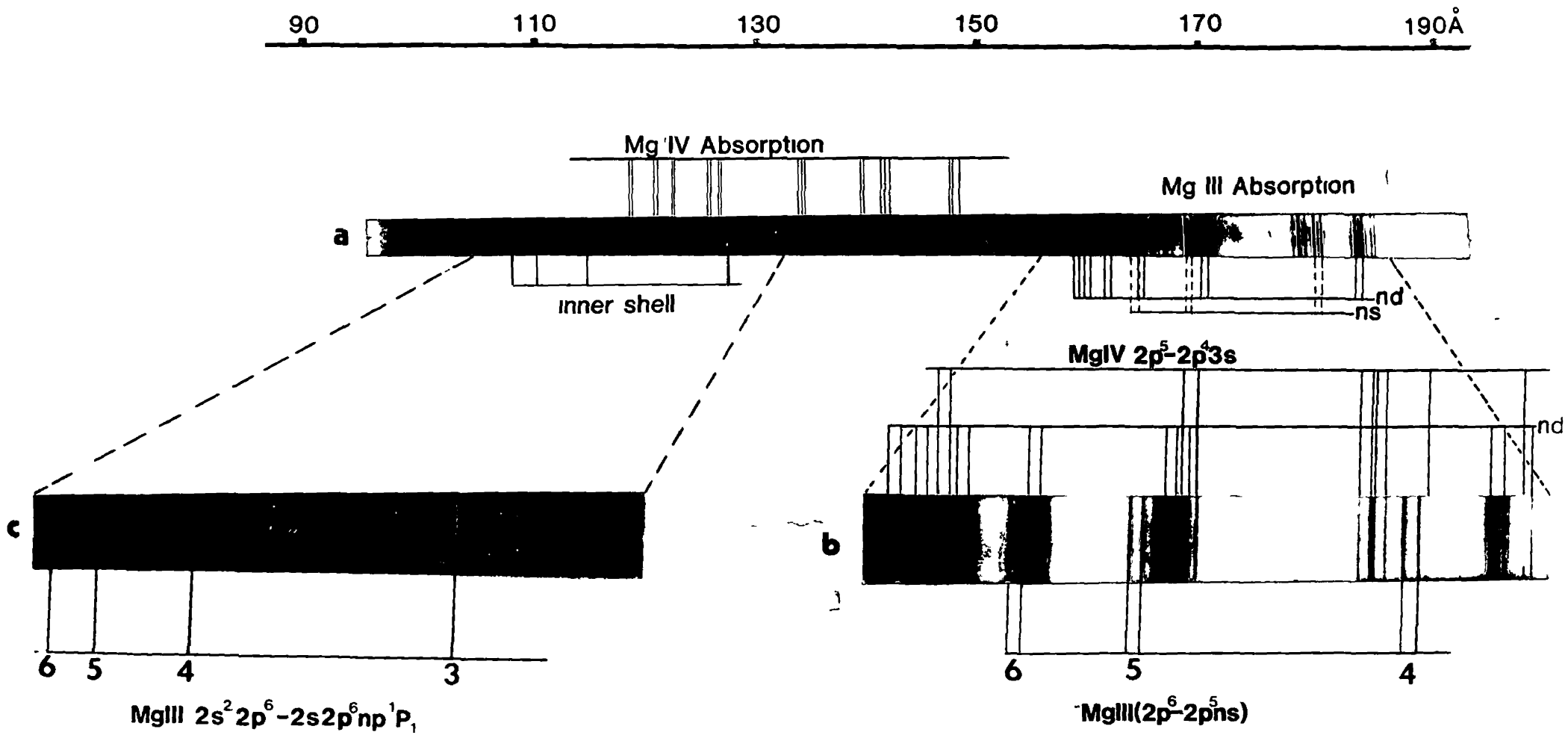
90
110
130
150
170
190Å
Mg IV Absorption
Mg III Absorption
a
inner shell
ns
nd
MgIV 2p5-2p43s
nd
c
b
6
5
4
3
6
5
4
MgIII 2s22p6-2s2p6np1P1
MgIII(2p6-2p5ns)

Fig (3 4 a b) Shows enlargements of the wavelength regions containing the autoionizing series in both Al IV and Si V observed in the absorption spectra of laser produced plasmas in the course of this work

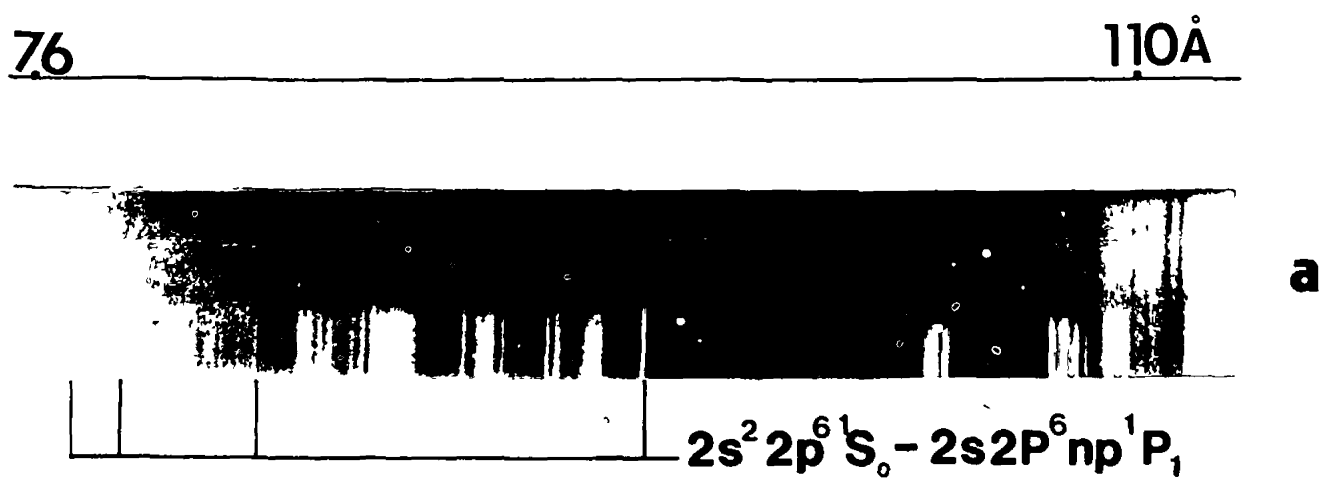

Al IV Autoionizing series

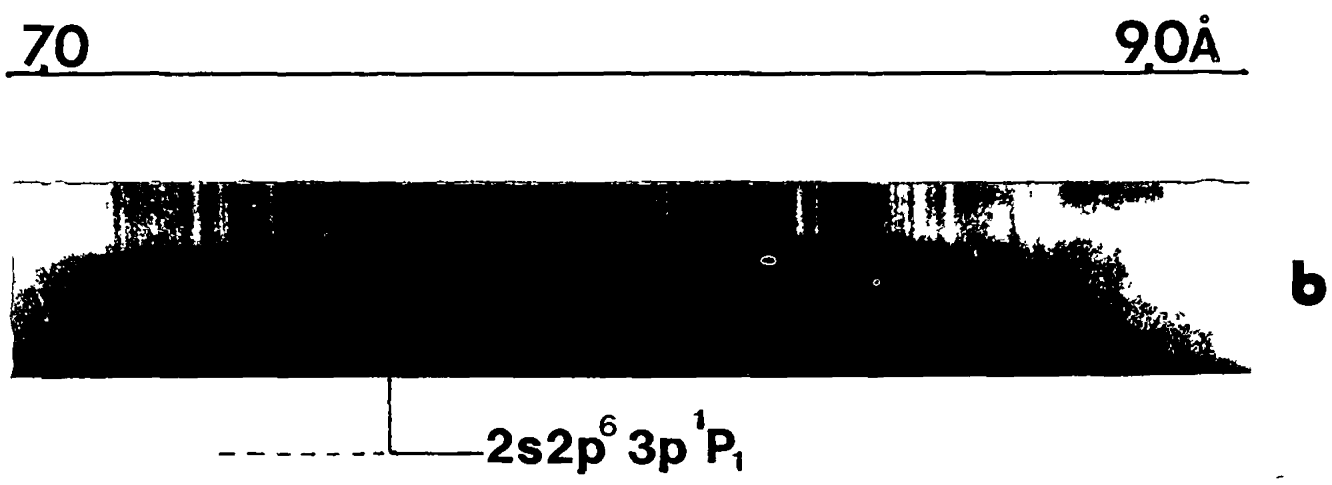

Si V Autoionizing series

Fig (3 5 a-d) A series of silicon spectra in which the plasma conditions were varied i e the laser producing the plasma was progressivly de-focused from 0 - 7 5mm (See text for details)

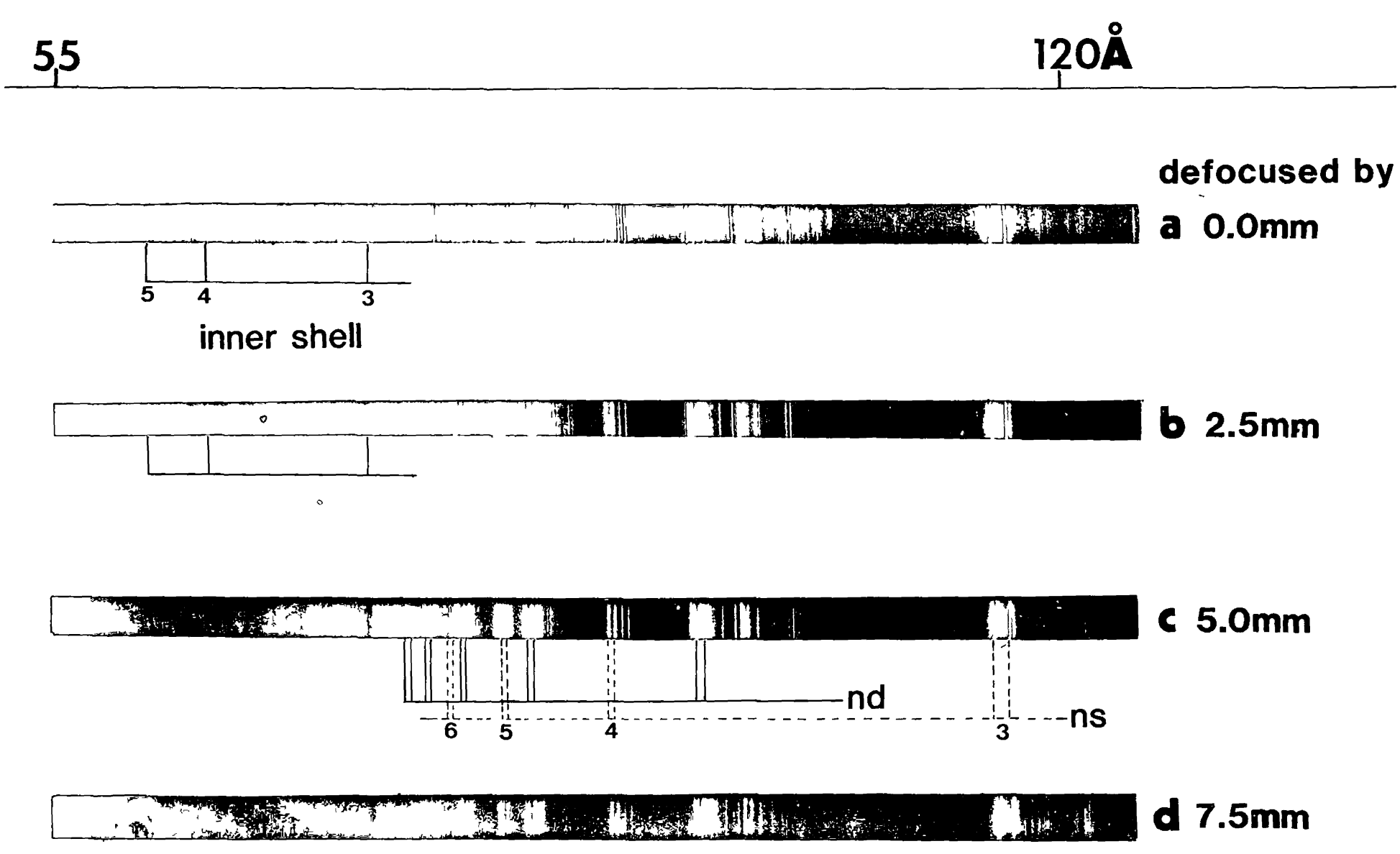
55
120Å
defocused by
a 0.0mm
5
4
3
inner shell
b 2.5mm
c 5.0mm
nd
ns
6
5
4
3
d 7.5mm

3 4 ABSORPTION IN MAGNESIUM IONS Mg IV

The measured wavelengths of lines due to transitions in Mg IV observed in the wavelength region (200–100Å) are given in Table (3 3) the measured wavelengths of the $2p^4ns, nd$ series in Mg IV are given together with values of these lines taken from Kelly and Palumbo (1973) These features are shown above in fig (3 3) and are strong indicating that a large number of these ions were present in the fore plasma Between 130 and 110Å there are groups of weaker absorption lines, most of which are unresolved Kelly and Palumbo (1973) list many lines of the type $2p^4nd$ in this wavelength region in the Mg IV ion It is therefore reasonable to assume that the wavelengths listed as unknown in table 3 3 are due to this type of transition

TABLE 3 3

Known lines observed in absorption in the spectrum of Mg IV

All wavelengths are given in angstroms

lines have been measured from a number of plates

λ_{TW}	λ_{KP}	classification
188 15	188 146	$2s2p^6\ {}^2S_{1/2}$ — $2p^6 3s\ {}^2P_{3/2}$
183 35	183 442	$2p^5\ {}^2P_{3/2}$ — $2p^4 3s\ {}^4P_{3/2}$
181 38	181 345	${}^2P_{1/2}$ — ${}^2P_{3/2}$
180 80	180 797	${}^2P_{1/2}$ — ${}^2P_{1/2}$
180 65	180 818	${}^2P_{3/2}$ — ${}^2P_{3/2}$
180 06	180 071	${}^2P_{3/2}$ — ${}^2P_{1/2}$
172 36	172 311	${}^2P_{1/2}$ — ${}^2D_{3/2}$
171 59	171 657	${}^2P_{3/2}$ — ${}^2D_{5/2}$
160 77	160 8088	${}^2P_{1/2}$ — ${}^2S_{1/2}$
160 24	160 2358	${}^2P_{3/2}$ — ${}^2S_{1/2}$
147 58	147 535	$2p^5\ {}^2P_{1/2}$ — $2p^4 3d\ {}^2D_{3/2}$
146 94	146 954	${}^2P_{3/2}$ — ${}^2D_{5/2}$
146 52	146 526	${}^2P_{3/2}$ — ${}^2P_{3/2}$
140 83	140 815	${}^2P_{1/2}$ — ${}^2S_{1/2}$
140 52	140 525	${}^2P_{3/2}$ — ${}^2P_{3/2}$
140 17	140 176	${}^2P_{3/2}$ — ${}^2D_{3/2}$
138 70	138 6884	$2p^5\ {}^2P_{1/2}$ — $2p^4 4s\ {}^2P_{3/2}$
138 32	138 395	${}^2P_{1/2}$ — ${}^2P_{1/2}$
138 06	137 970	${}^2P_{3/2}$ — ${}^2P_{1/2}$
133 21	133 1966	${}^2P_{1/2}$ — $3d\ {}^2D_{3/2}$
132 83	132 800	${}^2P_{3/2}$ — ${}^2D_{3/2}$
132 58	130 625	${}^2P_{1/2}$ — $4d\ {}^4P_{3/2}$
132 55	132 510	${}^2P_{1/2}$ — $4s\ {}^2D_{3/2}$
125 96	125 810	${}^2P_{1/2}$ — ${}^2S_{1/2}$
125 54	125 495	${}^2P_{3/2}$ — ${}^2S_{1/2}$

the wavelengths listed below were measured at the centers of broad features assumed to be closely spaced lines due to transitions similar to those listed above

λ	classification
124 90	not known
124 30	
123 20	
120 09	
111 83	

3 5 THE SODIUM ISOELECTRONIC SEQUENCE

3 5 A) Al III.

Ions from the sodium isoelectronic sequence have also been studied in absorption in the course of this work The spectrum which is shown in fig (3 6 b) shows many differences when compared with the spectrum of fig (3 6 a) Both spectra were recorded using the same technique with a hafnium plasma providing the backlighting source In the case of the spectrum shown in fig (3 4 a) however the portion of the laser beam used to create the fore-plasma was tightly focused onto the aluminium target The spectrum shown in fig (3 4 b) was obtained under similar conditions but for this spectrum the fore-plasma was created with a de-focused laser beam i e the portion of the laser beam used to create the ions was focused in front of the aluminium target The differences in the two spectra are very distinct Spectrum (b) shows many more absorption lines than spectrum (a) These spectra also show when compared with the overlaping emission reference (fig(3 6 b) also aluminium) that the majority of the absorption lines observed in spectrum (b) do not appear as emission features in the emission spectrum This fact would seem to indicate that the transitions giving rise to these absorption features may in fact be due to inner shell excitations or to levels involving the simultaneous excitation of two electrons These transitions may also occur over a number of different ion stages although the following argument would seem strongly to favor the lower ion stage Al III

If we refer back to the magnesium spectra shown in fig's 3 2 and 3 3 it can be seen that these spectra consist of strong absorption features due to the Mg III ion and also equally strong absorption in the Mg IV ion The spectrum of Si V

also shown in fig(3 2) is also a mixture of more than one ion stage the other stages probably being III and IV The absorption spectrum of an aluminium plasma shown in fig(3 2) however, only shows strong absorption in the Al IV stage with only very weak contributions from other ion stages Thus we may conclude that under the plasma conditions obtaining in the experiments reported here it is possible to observe absorption in ion stages III IV and V only Contributions from stages II and VI may occur but are so weak as to be unobserved So for the spectrum shown in fig(3 6 b) which was observed in a defocused line plasma and contains the principal series of Al IV along with many other strong absorption lines) it may be assumed most of the absorption must arise from the lower stage Al III ion However despite this qualitative assessment extensive calculations have been carried out to establish the exact nature of these features these calculations are discussed below

Calculations were carried out over a number of ion stages (III–VI) in order to assign the unknown lines to transitions The possibility that these lines might be due to transitions involving single valence electron excited states of any or all of the ion stages (Al II–Al VII) was ruled out after all possible wavelengths resulting from such transitions were calculated according to the selection rule $\Delta J=0\pm1$ for all known levels of the aluminium atom and its positive ions up to Al VI The levels and corresponding quantum numbers were taken from Martin and Zalubas (1979) The computer program used to compute the wavelengths of the excited states is given, along with sample input and output in appendix two

Two electron excitations have been largly ignored in this work All of the two-electron transitions calculated here fall out side of the wavelength range 170–120Å There is also the difficulty of calculating this type transition with the

Dirac Fock package of Grant et al (1980) (which was used for all of the calculations reported in this work) in that two-electron exctiations usually result in configurations with three or more open shells for non-relativistic configurations the program sets a limit of three on the number of open shells allowed For configurations involving more than this number of open shells the Dirac Fock program will not perform the calculation unless the problem is defined in terms of relativistic cofigurations In the work reported here only the non-relativistic mode was used It has been the experience of this work that most of the two-electron transitions atempted could not be calculated with the Dirac Fock program

Since as mentioned above the lines appear in absorption only it must be concluded that these lines are in fact due to inner shell transitions involving either a single 2s or 2p electron Calculations on transitions of this type were carried out and by a process of elimination it was found that the Al III ion was the only ion stage in which such transitions fall into the correct wavelength region The type of transitions considered most likely to be responsible for the observed structures are given below

(1) $2s^2 2p^6 3s\ {}^2S_{1/2} - 2s^2 2p^5 3s^2\ {}^2P_{1/2,3/2}$

(2) $2s^2 2p^6 3s\ {}^2S_{1/2} - 2s^2 2p^5 3s\ ns$

(3) $2s^2 2p^6 3s\ {}^2S_{1/2} - 2s^2 2p^5 3s\ nd$

Similar levels in the sodium like Mg II ion were observed by Esteva and Mehlman (1974) and so before proceeding further with the discussion of the Al III and Si IV lines observed during the course of this work a discussion of the Mg II lines will be given Many of the Mg II lines were recalculated during this work in order to provide an isoelectronic comparison with the calculations

carried out for the Al III and Si IV ions

The Mg II levels reported by Esteva and Mehlman are due to one-electron excitation configurations of the type $2p^5 3snl$ with l = 0 or 2 The upper level classification becomes difficult here because of the three open shells, and in fact single configuration calculations with the Dirac Fock package of Grant et al (1980) fail completely for many of the Mg II levels observed by Esteva and Mehlman because of the strong configuration interaction involved Presented in table 3 6 are a few of the Mg II levels observed by Esteva and Mehlman together with their calculated values The calculations carried out by Esteva and Mehlman involved computation of core parameters under LS coupling first and then computations taking the running electron into account

The calculations carried out as part of this work for Mg II and the isoelectronic Al III involved simply the computation of specific configurations with total angular momentum quantum number J=1/2 or 3/2 (Calculations involving configuration interactions for these levels have not at this stage been undertaken) These calculations are intended to represent only a tentative analysis of the absorption structures observed in the spectrum of Al III The results of the calculations are listed in table 3 4 for Mg II and in table 3 5 for Al III Also listed in table 3 5 are experimental values for absorption lines observed in the spectrum of an aluminium plasma in the course of this work and which correspond to the wavelength range of the calculated Al III lines Relative intensities of these lines are also given Some of the experimental wavelengths listed in table 3 5 are listed more than once, this is because these particular values were found to fit into more than one range of calculated wavelengths (see table 3 5)

TABLE 3 4

Contains some of the Mg II autoionizing levels with the experimental and calculated values of Esteva and Mehlman (1974) Also listed are calculations carried out for these Mg II levels in the course of this work Intensities have been measured from the density trace of Esteva and Mehlman, taking their strongest line to be 10 0

λ^{*}_{TW}	λ_{EM}	Intensity	λ^{*}_{EM}	Classification
249 53	248 47	9 5	255 06	$2p^6 3s\ ^2S_{1/2}$ — $2p^5 3s^2\ ^2P_{3/2}$
248 10	247 14	8 0	253 64	$2p^6 3s\ ^2S_{1/2}$ — $2p^5 3s^2\ ^2P_{1/2}$
204 10	203 42	10 0	205 03	$2p^6 3s\ ^2S_{1/2}$ — $2p^5 3s3d(J=3/2)$
203 88	202 27	10 0	200 90	$2p^6 3s\ ^2S_{1/2}$ — $2p^5 3s3d(J=1/2)$
198 21	193 64	3 0	197 93	
198 16				
197 77	193 31	4 0	197 39	
197 70				
197 41	193 09	4 0	197 08	$2p^5 3s4d$ [J = 1/2 3/2]
197 15				
197 14	192 55	6 0	196 40	
196 84				
195 66	192 40	6 0	196 16	
195 63				
195 32	191 56	6 0	196 08	$2p^5 3s\ 4d$ [J = 1/2 3/2]
	191 30	6 0	194 34	
193 88	189 37	4 0	193 56	
193 85				
193 81				
193 59				
193 29				$2p^5 3s\ 5d$ [J=1/2 3/2]
193 21				
193 20				
192 81				
191 56	188 91	5 0	192 62	
191 66	188 84	4 0	190 69	
191 64				
191 50				
191 43				
191 11				$2p^5 3s\ 6d$ [J=1/2 3/2]
191 10				
191 09				
190 71				
189 44				
189 38	186 47	3 0	190 21	
190 38	185 98	2 0	189 96	
190 36				
190 27				
189 86				
189 84				$2p^5 3s\ 7d$ [J = 1/2 3/2]
189 47				
188 20				
188 18	185 59	2 0	189 47	
	184 05	2 0	187 87	

EM are the results of Esteva and Mehlman (1974)
TW are results obtained as part of this work
* are theoretical results

TABLE 3 5

Contains the list of absorption lines observed in the spectrum of a de-focused aluminium line plasma and are thought to be due to levels in the Al III ion Each of the experimental values has a number of calculated values The classification is given simply as the configuration and the total angular momentum qunatum number J used in the calculation of the level

Classification	λ^{a}_{TW}	λ_{TW}	Intensity
$2p^5 3s^2$ [J=3/2]	170 00		
$2p^5 3s^2$ [J=1/2]	168 99		
	141 60		
	141 49		
	140 89		
	140 55	139 68	2 0
		139 51	2 0
	140 46	138 72	5 0(b)
		138 48	5 0
$2p^5 3s3d$ [J = 3/2 1/2]	139 81	138 19	2 0
		137 98	5 0
	139 43	137 73	8 0
	139 37	137 32	6 0
	138 46	136 45	1 0
	138 20		
	137 33		
	130 59	131 60	2 0
		128 53	2 5
	130 14	128 45	2 5
		128 29	2 5
$2p^5 3s4d$ [J = 3/2 1/2]	129 79	128 21	2 5
		127 37	6 5
	128 98	126 76	1 0
		126 13	1 0(b)
	126 37		
	126 36		
	126 34		
	126 17		
		126 76	1 0
	126 12		
		126 13	1 0(b)
	125 93		
$2p^5 3s5d$ [J = 3/2 1/2]		124 51	1 5
	125 81		
		124 02	1 0
	125 64		
	124 98		
	124 97		
	124 90		
	124 24		
	124 13		
		124 51	1 5
	123 90	124 02	1 0
$2p^5 3s6d$ [J = 3/2 1/2]	123 87		
		123 41	3 0
	123 62	122 49	1 0
	122 95		
	122 91		
	123 02		
	122 96		
		123 41	3 0
	122 71		
$2p^5 3s7d$ [J = 3/2 1/2]	122 69	122 49	1 0
	122 44		
		121 90	1 0
	121 77		
	121 75		

TW are results obtained as part of this work
[a] are theoretical results

Intensities are relative to the 160 07SA line in Al IV which was the strongest line observed on the plate and has been given an estimated intensity of 10 0

There are also other lines from the spectrum of the aluminium plasma which do not fit into the range of lines tentatively identified in the work described above Some of these lines may belong to configurations of the type $2p^6 3s - 2p^5 3sns$ which cannot be calculated using the Dirac Fock package of Grant et al (1980) it is also possible that these lines are the result of configuration interactions between the levels listed in table 3 6 or that they arise from higher or lower ion stages than Al III These lines are listed below in table 3 7 along with unidentified absorption lines observed in the spectrum of a silicon plasma

3 5.B) Si IV

The absorption spectrum of a silicon plasma presented in fig(3 7) shows absorption lines from the Si V ion and also other intense absorption features thought to be due to the lower ion stages Si IV and Si III These lines are visible in the wavelength region 120 - 85Å and are thought to be mainly due to the Si IV ion and are therefore analogous to the lines which have already been discussed above for the case of the aluminium spectrum and have been tentativly asigined to transitions in the Al III ion These lines are also listed below in Table (3 7) as being un-identified No analysis of these levels has as yet been undertaken However, it may be assumed that if these unidentified lines belong to the Si IV ion then such an analysis would follow along the lines of the Al III case

TABLE 3 6

Wavelengths of unknown lines measured in the specta of both aluminium and silicon plasmas and thought to be from Al III and Si IV respectivly Wavelengths were measured from a number of plates Estimated intensities are given for the Al III lines only and are (as in table 3 6) relative to the 160 073A line in Al IV which is taken as 10 0 (b) indecates a broad line

Al III	Intensity	Si IV
150 78	2 0(b)	
		110 37
149 99	2 5(b)	
		107 05
146 85	3 0	
		106 78
146 04	2 0	
		106 34
145 70	2 0	
		105 62
144 00	4 0	
		105 18
143 79	4 0	
		104 52
136 25	1 0	
		102 43
136 08	1 0	
		102 10
136 00	1 0	
		101 62
135 67	1 0	
		100 50
135 51	3 0	
		99 64
135 35	1 0	
		99 20
135 18	1 0	
		98 72
134 77	1 0	
		97 50
134 45	3 0(b)	
		97 08
134 04	1 0	
		96 40
133 87	1 0	
		92 35
133 71	1 0	
		91 93
133 14	1 0	
		91.67
132 82	1 0	

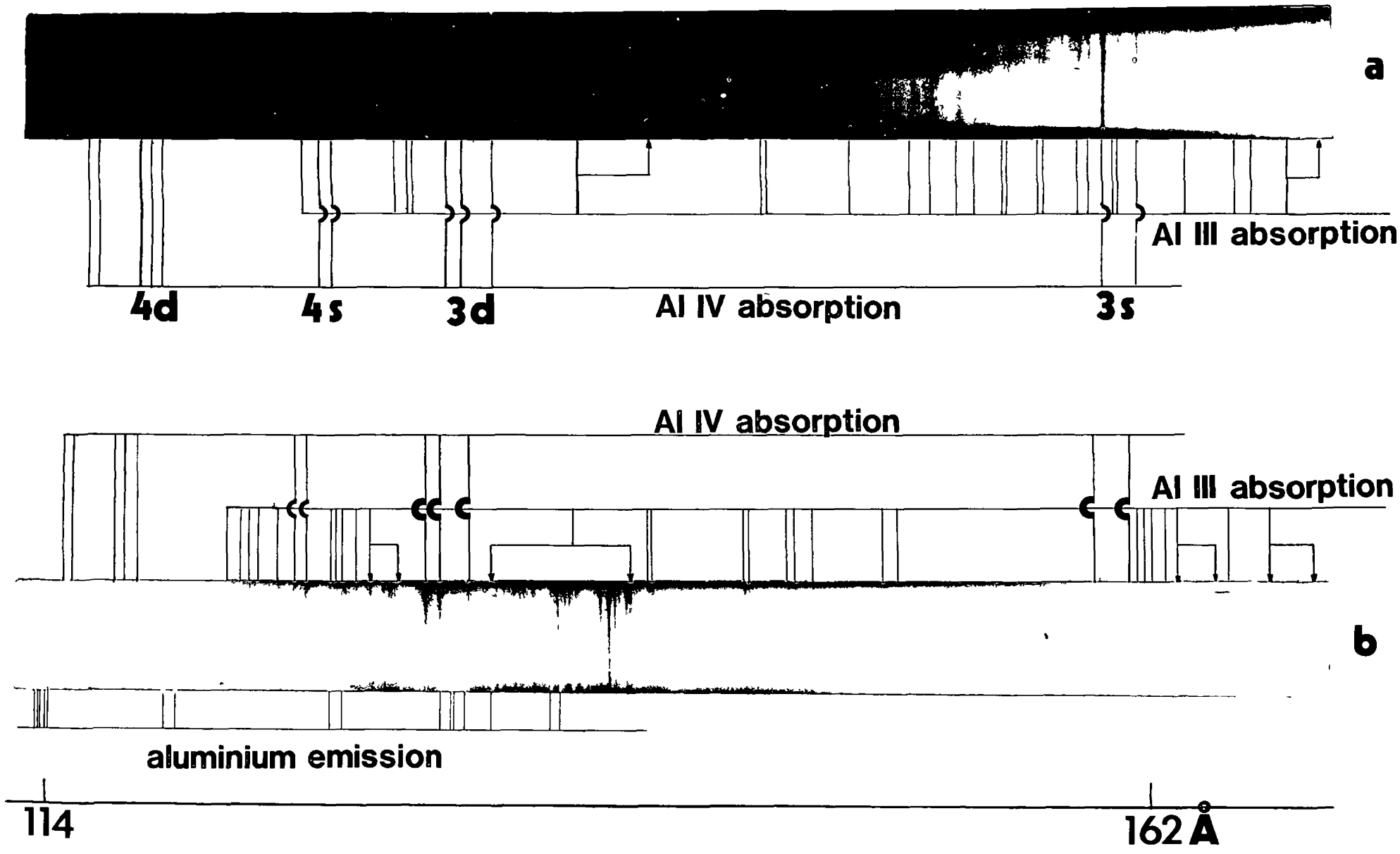
a
Al III absorption
4d
4s
3d
Al IV absorption
3s
Al IV absorption
Al III absorption
b
aluminium emission
114
162 Å

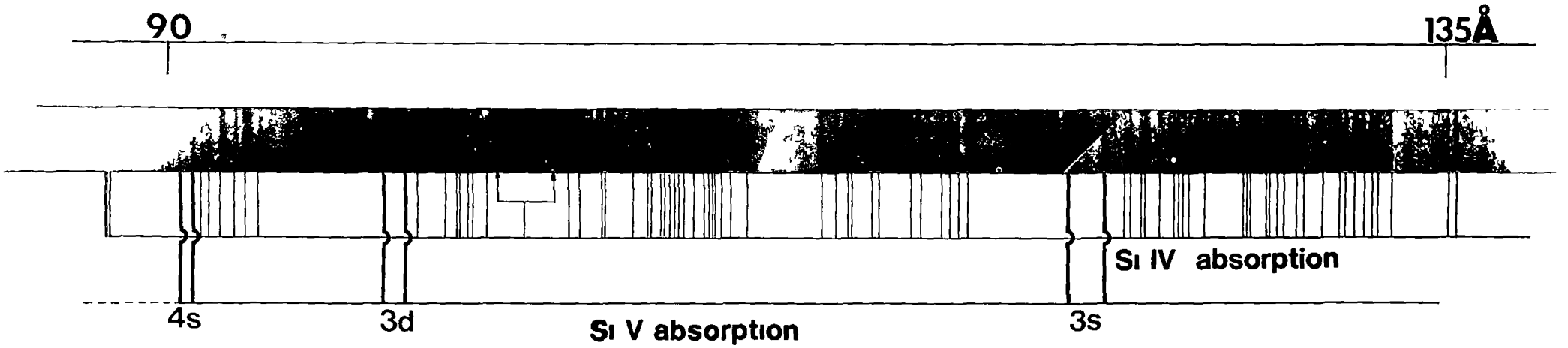
90
135Å
Si IV absorption
4s
3d
Si V absorption
3s

3 6 THE XENON ISOELECTRONIC SEQUENCE

The xenon isoelectronic sequence is of considerable theoretical interest at this time The fourth and fifth members of this sequence La IV and Ce V have been studied in absorption in the course of this work, the same technique being used as with the neon-like and other ions reported above

The xenon sequence has been the subject of intense theoretical study since the experimental observation by Lucatorto McIlrath Sugar and Younger (1981) of discrete structure in the 4d photoabsorption spectrum of Ba III The VUV photo absorption spectra of the 4d subshell in the isonuclear sequence consisting of Ba I Ba II and Ba III observed by Lucatorto et al (1981) is shown in fig (3 8) Of particular interest in the sequence is the Ba III spectrum which exhibits several sharp resonances each containing appreciable oscillator strength below the ionization threshold This situation is to be contrasted with neutral barium for which only a broad resonance above threshold is observed

Barium with Z=56 is at the edge of 4f collapse, neutral ground state atoms with $Z < 56$ have 4f orbitals which are hydrogenic and have $r_{av} \simeq 17a_0$ while elements with $Z > 57$ have a collapsed 4f orbital with $r_{av} \simeq 1a_0$ The nature of the 4d photoabsorption is therefore expected to depend critically on whether or not the 4f orbital can be considered collapsed or not

Several atempts have been made to analyse this "redistribution of oscillator strength" since its experimental observation, some of this work is briefly discussed below

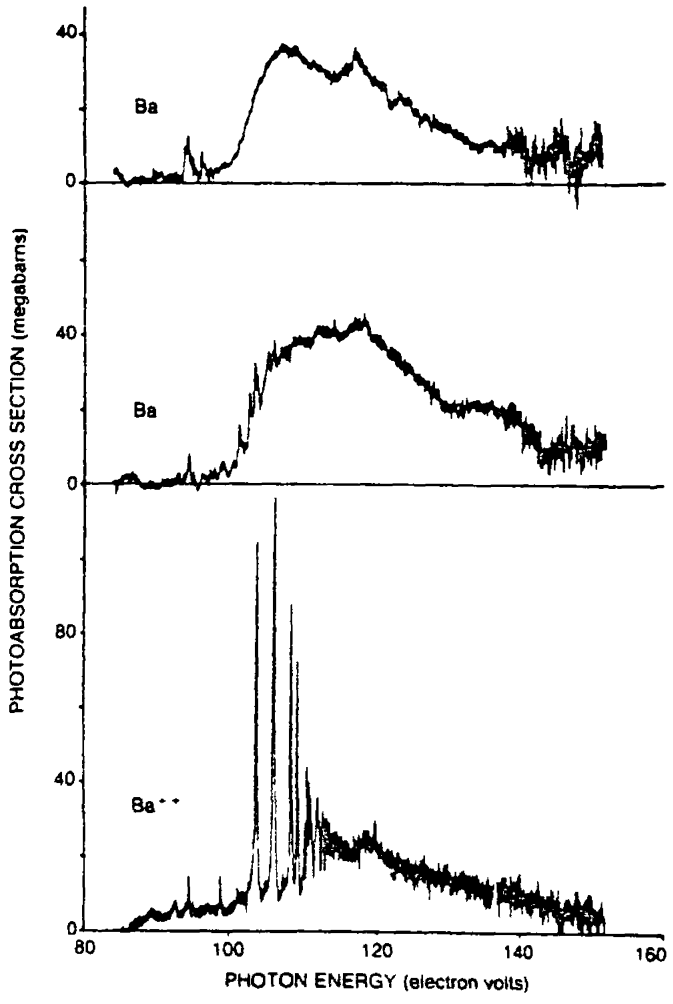

Fig (3 8) Shows the photoabsorption spectrum of the isonuclear sequence Ba I Ba II and Ba III in the 80 to 160eV energy range Plotted are cross sections for the photoexcitation of a 4d electron along the isonuclear sequence The striking difference in the Ba III spectrum indicates a partial contraction of the 4f orbital in the absence of barium's two outer electrons (after Lucatorto et al (1981))

Connerade and Mansfield (1982) discussed the 4d photoabsorption spectrum of Ba III in terms of a term-dependent hybridization of the 5f wave functions in Ba I and Ba III They state that unlike in neutral barium the 4d→5f transition cannot be neglected in the discussion of the 4d spectrum of Ba III They point out that 4d→nf(n≥5) transitions (rather than 4d→np) must be responsible for the prominent discrete structure below the 4d threshold of Ba III Kelly Carter and Norum (1982) calculated the photoionization of the 4d subshells of Ba I

and Ba III using a Hartree-Fock approximation with and without the inclusion of relaxation effects They conclude that Hartree-Fock calculations can give reasonable photoionization results for a complicated system such as the $4d^{10}$ subshell of barium they also suggest that relaxation effects can in cases such as neutral barium be very important in cross section calculations Nuroh Stott and Zaremba (1982) performed calculations for the photoabsorption spectra of Ba I II and III near the 4d ionization threshold using the time-dependent local density approximation, these calculations have provided results which are in quantitive agreement with the experimental data of Lucatorto et al (1981) The results also suggest that the sharp resonant structures below threshold in Ba III are due to transitions to hybridized f states which are strongly modified by electron-electron interactions, which is consistant with the term-dependent Hartree Fock calculations (Connerade and Mansfield (1982)), but goes beyond these calculations in predicting the detailed spectral distribution Kucas Karosene and Karazija (1983) used a Hartree Fock model to study the 4d-photoabsorption spectrum of Ba III and have shown that the strong absorption lines in the spectrum of Ba III correspond to excitations of a 4d electron in the Rydberg nf series Cheng and Froese Fischer (1983) considered the collapse of the 4f orbital for xenon like ions in the region of the $4d \rightarrow nf$ ϵf excitations also using a term-dependent Hartree Fock technique They have found the 4f orbital to be strongly term-dependent and have concluded that the appearence of intense absorption lines in the observed spectrum of Ba III is due to the partial collapse of the 4f orbital in the $4d \rightarrow f\,^1P$ channel They have also extended their calculations to include other ions of the xenon isoelectronic sequence and have generated the theoretical absorption spectra for the xenon like isoelectronic sequence from Xe I to Nd VII These spectra are shown in fig (3.9) below and show that after the 4f orbital is compleiely collapsed for high degrees of ionization along the

isoelectronic sequence the bulk of the absorption oscillator strength is concentrated at the $4d^9 4f\,^1P$ level so that the only strong line in the spectrum is again the $4d \rightarrow 4f\,^1P$ transition Cheng and Johnson (1983) used the relativistic random phase approixmation to study photoionization of the inner 4d shells of Xe I Cs II Ba III and La IV they calculated total cross sections partial cross sections branching ratios and angular-distribution asymmetry parameters and have studied their systematic trends along the isoelectronic sequence

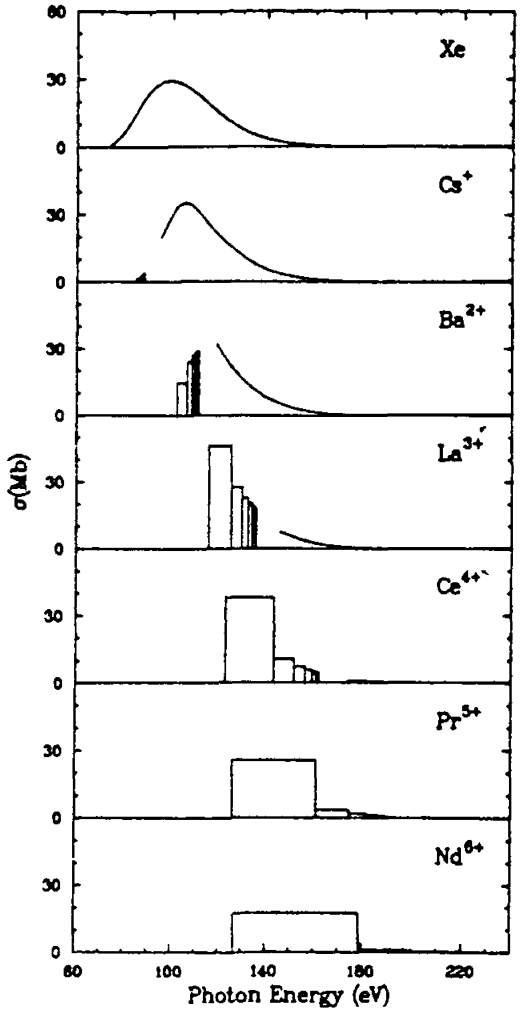

Fig (3 9) Shows theoretical absorption spectra for the first seven members of the xenon-like isoelectronic sequence The rectangles represent the effective ocillator strength distrobutions of Cheng and Froese Fischer (1983) for the $4d \rightarrow nf\,^1P$ transitions (n=4-9) The continuum cross sections are random phase approximation results of Cheng and Johnson (1983) (after Cheng and Forese Fischer (1983))

They obtained important dynamic effects of electron correlation from an eigen channel analysis involving the eigen quantum defects the eigen dipole amplitudes and the transformation U matrices They have also found that there are shape resonances in the effective potential for f electrons and that the collapse of the 4f orbital along the isoelectronic sequence is clearly related to changes in f orbitals in passing through these resonances The most recent theoretical work on Ba III is that of Clark (1984) in which he shows that the role of true collective effects in the 4d photoabsorption spectrum of Ba III are minor His analysis shows that the most significant departures from independent particle behaviour are in fact due to correlations involving the 5p not the 4d shell their importance is magnified by the delicate balance of opposing single-particle forces His reevaluation of ionization limits has revealed the presence of Beutler-Fano structures in the experimental data of Lucatorto et al (1981)

The analysis of this type of spectrum is quite involved as has been shown above The next section however deals with the recent observation in this laboratory of what appear to be similar structures in the spectra of La IV and Ce V

3 6 A La IV AND Ce V

The absorption spectrum of lanthanum is shown in fig(3 10) and shows the absorption spectrum of a lanthanum plasma recorded between 160 and 80A also shown in fig(3 10) is the discrete structure observed between 110 and 90A which is entirly analogous to the features observed by Lucatorto et al (1981) in the VUV absorption spectrum of a column of Ba III ions

The spectrum of a cerium plasma has also been investigated in the same wavelength region as part of this work This spectrum is however exremely weak and despite numerous atempts at improvement the spectrum still remains to be recorded with the same strength as the lanthanum spectrum and is therefore not reproduced photographically here The 4d photoabsorption spectrum of Ce V (which is not reproduced here) also shows a degree of discrete structure in the 90Å region similar to that observed in Ba III and La IV

Table 3 7 a is a list of the absorption features measured in the spectrum of a lanthanum laser produced plasma between 160 and 120A while table 3 7 b lists the wavelengths of the discrete structure observed between 110 and 90A The relative intensities of these features are also given in table 3 7 The strongest lines in the region have been given an intensity of 10 The weaker features were measured from photograpic prints of this wavelength region As the summary of previous theoretical work on the isoelectronic Ba III features suggest the analysis of this type of structure presents a serious degree of difficulty For this reason no analysis of the La IV spectrum is presented here Consequently all of the structures observed in the La IV spectrum are classified in table 3 7 as unknown and the spectrum is therefore presented here simply as a qualitative observation

LaIV 4d photoabsorption

TABLE 3 7 A

Wavelengths of absorption structure observed in the spectrum of a lanthanum plasma in the wavelength range 160 to 120A Wavelengths were measured from a number of plates

λ_{exp}		classification
160 81		Unknown
159 43		
159 44		
150 24		
140 93		
140 92		
140 52		
137 19		
136 70		
136 08		
132 42		
129 75		
129 76		

TABLE 3 7 B

Wavelengths and relative intensities of absorption features observed in the spectrum of a lanthanum plasma in the wavelength range 110 to 90A Wavelengths of the strong features were measured from a number of plates

λ_{exp}		relative intensity	classification
104 33		3 0(b)	Unknown
99 06	*	10 0	
98 41		1 0	
97 85		2 0	
97 08	*	8 0	
96 21		3 0	
95 52	*	10 0	
95 14		2 0	
94 15		3 0	
93 43	*	8 0	
92 77	*	6 0	
92 19		2 0	
91 81	*	8 0	
91 59	*	6 0	
91 20		1 0	

REFERENCES

Carillon A Jaegle P and Dhez P Phys Rev Lett 25 3 (1970)

Carillon A Jamelot G Sureau A and Jaegle P Phys Lett 38 2 (1972)

Carillon A Jamelot G Jaegle P and Sureau A Proc of the 4th conference on vacuum ultraviolet radiation physics Hamburg Germany PP 50 - 52 (1974)

Cheng KT and Froese Fischer C Phys Rev A 28 5 (1983)

Cheng KT and Johnson WR Phys Rev A 28 5 (1983)

Clark CW J Opt Soc Am 1 4 (1984)

Codling K Madden RP and Ederer DL Phys Rev A 155 1 (1967)

Connerade JP and Mansfield MWD Phys Rev Lett 48 131 (1982)

Esteva JM and Mehlman G Astro Phys J 193 1 (1974)

Ferner E Ark Mat Astron Phys 28A PP 1 - 21 (1941)

Jaegle P Carillon A Dhez P Jamelot G Sureau A and Cukier M Phys Lett 36 3 (1971)

Jaegle P Jamelot G Carillon A Sureau A and Dhez P Phys Rev Lett 33 18 (1974)

Jamelot G Sureau A and Jaegle P Phys Lett 41A2 (1972)

Kastner SO Crooker AM Behring WE and Cohen L Phys Rev A 16 2 (1977)

Kelly HP Carter SL and Norum BE Phys Rev A 25 4 (1982)

Kelly HL and Palumbo LJ NHL Report Number 7599 (1973)

Kuckas Sov Phys Coll (USA) Vol 23 3 PP 23-31 (1983)

Lucatorto TB and McIlrath TJ Phys Rev Lett 37 7 (1976)

Lucatorto TB McIlrath TJ Sugar J and Younger SM Phys Rev Lett 47 16 (1981)

Nuroh K Stolt MJ and Zaramba E Phys Rev Lett 49 862 (1982)

Soderqvist J Nova Acta Ragiae Soc Sci Ups Ser IV 9 PP 1 - 103 (1934)

APPENDIX I LUMINESCENCE IN SOLIDS

APP 1 1 INTRODUCTION

The work reported in the preceding four chapters of this thesis has dealt with the application of laser produced continua to the study of photoabsorption of ionized species also laser produced This application of the laser produced continuum source serves to demonstrate its usefulness in the VUV region The uses of such a versatile source of VUV continuum radiation are not limited to the study of atomic structure, as was pointed out in chapter one The ease of production intensity, spectral purity and spectral coverage of the laser produced continua make them ideal for other applications for example laser produced continua are suited for use as radiometric standards and in particular as transfer standards (Kuhne (1980) and Carroll Kennedy and O'Sullivan (1980))

The reproducibility of laser produced continua (also discussed in chapter one) makes them suitable for relative intensity measurements Laser produced continua are also usefull for transmission / refelection measurements in the vacuum ultraviolet/soft x-ray region

It is proposed to discuss in this appendix one further application of laser produced continua This application concerns the use of laser generated VUV continuum radiation to carry out studies into the luminescence efficiency of amorphous solids (glasses) as a function of irradiation wavelength It should be pointed out here before further discussion that the work described in this appendix is at present being undertaken in this laboratory but has not yet reached completion Therefore this appendix must be seen as a progress

report on the application of laser produced continua to the study of luminescence in solids The work in progress involves the measurement of relative luminescent decay times and spectral emission as a function of base glass composition and activator type The long term object of this project is to develop new detector materials for use throughout the vacuum ultraviolet (3 - 200nm)

APP1 2 DETECTOR MATERIALS FOR THE VUV

The various modes of interaction between radiation and neutral matter provide the underlying principles of all detectors For vacuum ultraviolet radiation these interactions involve the photoionization of gases, the ejection of photoelectrons from solids chemical changes photo-conductivity fluoresence or thermal effects The range of detectors for the VUV is extensive among the most widely used are photographic emulsions (which were used for the work reported in the preceeding sections of this thesis) photoelectric detection and the use of fluorescent materials A full discussion of the various detector materials used in the vacuum ultraviolet region has been given by Samson (1967) Discussions in this appendix will be confined to fluorescent materials only

APP1 3 FLUORESCENT MATERIALS

Since the construction of the first photomultiplier in 1936 fluorescent materials have been used to detect γ-rays and nuclear particles The first use of fluorescent materials for the detection of ultraviolet radiation was made by Parkinson and Williams (1949) who used a manganese activated willemite phospher which responded down to 1450Å Johnson Watanabe and Tousey

(1951) studied several fluorescent materials in the 850 - 2000Å wavelength range Included in this group of materials was the phospher sodium salicylate ($NaC_7H_5O_3$) which was found to have the highest efficiency over the entire wavelength range studied they found it easy to prepare and not to be affected by a vacuum These properties have made sodium salicylate the most commonly used fluorescent detector in the VUV The first measurement of the relative fluorescent yield of sodium salicylate was carried out by Dajardin and Schweegler (1934) who reported a constant efficiency between 2200 and 3400A these results have also been confirmed (Slavin, Mooney and Palumbo (1961)) for wavelengths shorter than 2200Å However other measurements (Samson (1964) and Knopp and Smith (1964)) reveal that there appears to be an aging effect which reduces the fluorescence efficiency at shorter wavelengths they suggest (contrary to the results of Johnson et al (1951)) that this is possibly due to the vacuum environment in which the detector in used

The fluorescent emission spectrum of sodium salicylate was first measured by Thurnau (1956) who also found the spectrum to be independent of the exciting wavelength for the wavelength region 275 - 2537Å The fluorescent emission spectrum of sodium salicylate has also been measured in the course of this work and is shown in fig (APP1 3) The maximum intensity of fluorescence is located at 4200Å The fluorescent decay time of sodium salicylate seems to be in the region between 7 and 12nsec, early measurements made by Nygaard and Sigmond (1961) gave a value of 12nsec, however Nygaard (1965) quotes a decay time of 7nsec Other measurements by Herb and Sciver (1965) give a value of between 8 5 and 10nsec

Plastic scintillators form an important group of fluorescent materials for use in

the VUV region Although the fluorescent efficieny of plastic scintillators is much less than that of sodium salicylate and is not even approximately constant with wavelength these scintillators are used in the VUV from 100 - 2000Å Several of these scintillators are commerically available, the most common of which is the NE102 scintillator (Nuclear Enterprises Ltd) the fluorescent wavelength at maximum emission is 4200A and the fluorescent decay time is of the order of 2 2nsec

Glass scintillators have not as yet been developed for use as VUV detectors but they do offer advantages over both plastic scintillators and sodium salicylate in that glass is a much more robust material and is ideal for use under vacuum conditions Work in this area at present under way in this laboratory is described in what follows The work is concerned with the evaluation of neutron scintillating glasses as VUV detectors The glasses which are presently under investigation were originally developed by Spowart (1969) for the detection of thermal neutrons A review of neutron scintillating glasses has been given by Spowart (1976) in which the physics of the various glass types is described The glasses are critically doped with rare earth impurity activators either cerium in the form of Ce^{3+} or terbium in the form of Tb^{3+} (Spowart (1979 a b)) The glasses also contain lithium which is used to detect the neutrons through the $^{6}Li(n\alpha)$ reaction When a thermal neutron is incident on a sample of glass containing ^{6}Li the neutrons react at the ^{6}Li site in the glass via the $^{6}Li_{3}(n\alpha)$ reaction two charged particles the α particle and the triton are released as a result of the interaction The Q-value for the reaction is of the order of 4 76MeV and the angle between the emergent particles is 180^{0} The triton carries away 2 72MeV of the energy and the α particle the remaining 2 04MeV The range of the α particle in glass is much shorter than the triton due to its greater charge and mass Both of these particles on passing through

the glass host create a series of electron hole pairs which drift through the solid and eventually recombine at the Ce^{3+} or Tb^{3+} activator sites The atomic physics of the Ce^{3+} activator is discussed below The cerium is present in the glass host as Ce^{3+} having lost three electrons ($5d^1$ $6s^2$) A Ce^{3+} concentration of >99% is deliberately arranged during the manafacture of the glass as Ce^{4+} is unwanted due to its strong absorption band which overlaps the Ce^{3+} emission In general the luminescence of rare earth impurities in glass hosts is characterised by sharp emission bands because the transitions occur among inner well shielded 4f electrons Electrons in this deep 4f shell are screened from the environment by outer electrons Cerium differs from the other rare earth activators, in that being at the beginning of the lanthanide series it has only one 4f electron This single 4f electron can give rise to two energy levels in one the orbital and spin moments of the electron are parallel ($^2F_{7/2}$) and in the other state both moments are anti-parallel ($^2F_{5/2}$) The excitation process is thus $4f^n \rightarrow 4f^{n-1}5d^1$ and the emission is from the 5d states The 5d orbit lies at the surface of the ion and is strongly influenced by the varying energy environment provided by the disorderd crystal field of the amorphous glass host As a consequence of this the 5d state is split into many components depending on the site symmetry of the cerium activator This leads to a broad emission band centered at 3500Å In the cerium doped glasses under investigation in this work the separation of the 4f - 5d band has been estimated (Spowart (1976)) at about $25X10^3 cm^{-1}$ Thus the 4f electron probably requires its energy in units of ≈ 2-3eV for transfer into the excited 5d state (Spowart (1976)) The average lifetime of the 5d state is short of the order of 10^{-7} to 10^{-8}sec since the 5d - 4f emitting process is an allowed electric dipole transition This results in decay times (Spowart (1976)) for the Ce^{3+} emission of about 0 14μsec

The cerium activators may be excited directly by completely by-passing the Li($n\alpha$) centers A photon of sufficient energy incident on the glass will excite the Ce^{3+} center and the resulting fluorescence may then be detected Thus the glasses described may be used as photon detectors The experimental method used to evaluate these glasses as VUV detectors, together with initial results of the work presently in progress are described in the next section

APP1 4 EXPERIMENTAL DETAILS.

The series of experiments which are at present being carried out in this laboratory to evaluate the scintillating glasses described above as detector materials for use in the VUV are discussed below

The laser produced continua from various high Z metal targets (discussed in chapters one and two) are used as the radiation source The experiments have been designed to measure the luminescent output of the various glass types under investigation by irradiating the glass samples with the laser produced continuum radiation The eventual aim of the experiments is to obtain luminescence efficiency measurements for the various glass types over the entire VUV wavelength region 2000-30Å To carry out the proposed experiments two vacuum ultraviolet instruments are used The first of these is a scanning normal incidence monochrometer which covers the wavelength range 5000-400Å the second instrument for use below about 500Å is the grazing incidence spectrograph equiped with the monochrometer attachment already discussed in chapter two

The experimental arrangement used to study the luminescent emission of the various glass types as a function of irradiating wavelength in the normal

incidence region is shown in fig (APP1 1 a) Samples of the various materials under investigation are placed in the sample holder (specially constructed for the purpose) shown in fig (APP1 1 b) The sample holder is located in one arm of the normal incidence monochrometer in place of the exit slit attachment such that the various samples can be located in turn approximately on the Rowland circle The sample holder is constructed from brass and can hold a total of twelve samples each sample is rotated in turn manually onto the Rowland circle so as to be irradiated by a monochromatic portion of the laser produced continua Also connected to the exit arm of the monochrometer is the sample chamber which is both light and vacuum tight A photomultiplier tube (EMI type 9813B) is attached to the sample chamber and is used to detect the luminescence Between the glass samples and the photomultiplier is placed a piece of plane glass which serves to filter out any of the VUV radiation which may emerge from the monochrometer during the experiment (for instance, if one of the samples being investigated was to fall from the sample holder) This filter also ensures that only the luminescence emission from the various samples is being detected by the PM tube

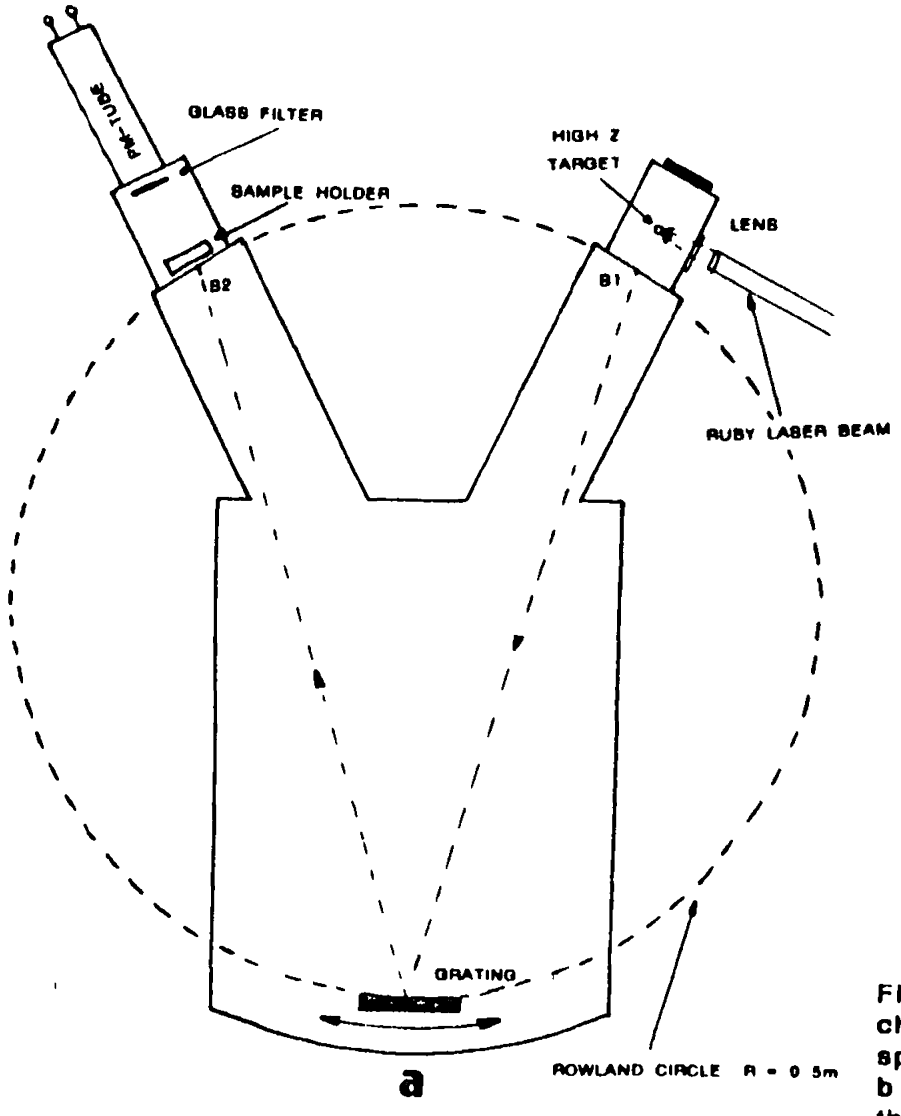

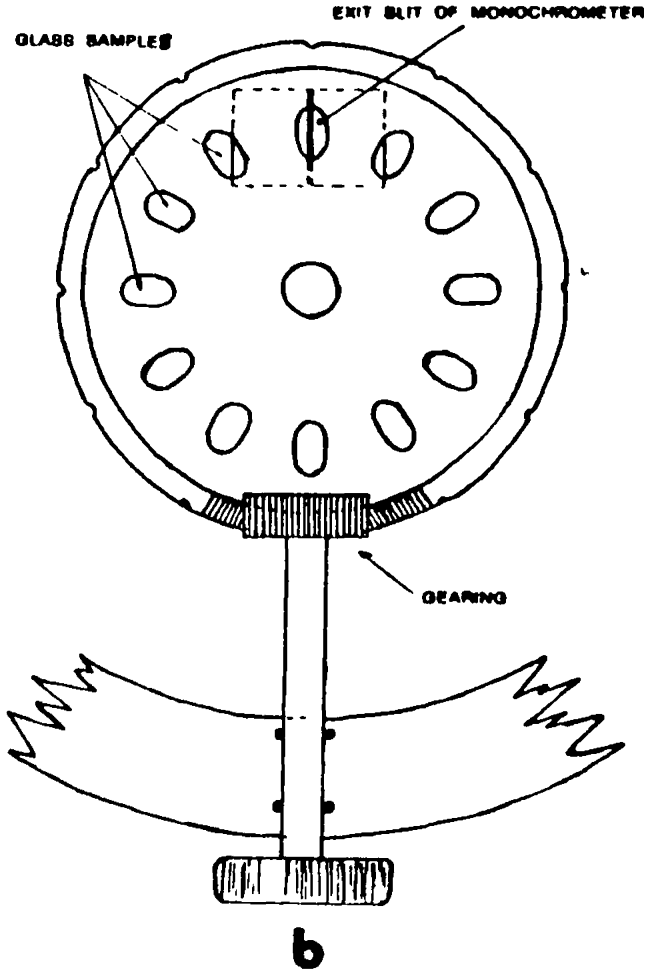

Fig (AP) 1 a b) a) Shows the arrangement of both the target chamber and sample chamber attached to the normal incidence spectrograph
b) Shows the construction of the brass sample holder used to hold the samples during the experiments

The time duration of the continuum emission from the laser produced plasmas used to excite luminescence in the glass samples is typically of the order of 30nsec (FWHM) and the luminescent decay times of the various samples (both glass and other scintillator types) lie in the range 10 - 0 1μsec Each of the light pulses when incident on the photocathode of the photomultiplier will result in a negative charge pulse as output The time duration of this charge pulse will depend on a number of factors (such as the decay time of the photomultiplier the particular output circuit being used and the input impedence of the instrument used to record the pulse) but will in general be of a similar time duration to the decay times of the samples The instrumentation requirements of the experiments described here are therefore dictated by the temporal properties of the output pulses discussed above The instrumentation used must also be compatible with the repetition rate of the laser used to produce the plasmas which in this case as was discussed in chapter two is low The requirement is therefore that of an instrument capable of taking the negative pulse of the photomultiplier as an input and giving as its output a voltage/number which is proportional to either the pusle height or the area under the pulse respectively

The instrument which has been acquired for this purpose is a digital storage oscilloscope (Philips PM 3311) which is capable of recording at intervals of 8nsec A full description of the instrument will be given by Mythen at a later date The oscilloscope records the photomultiplier output by sampling at intervals of 8nsec the samples are then used to reconstruct the pulse which may then be displayed on the oscilloscope screen The oscilloscope can store in memory a total of four complete pulses which may then be displayed simultaneously for comparison The oscilloscope is also interfaced with a

microcomputer which enables a large number of pulses to be stored permanently and analysed at a later date A chart recorder and/or a printer are also connected to the computer and are used as final output devices this arrangement is shown schematically in fig (APP1 2)

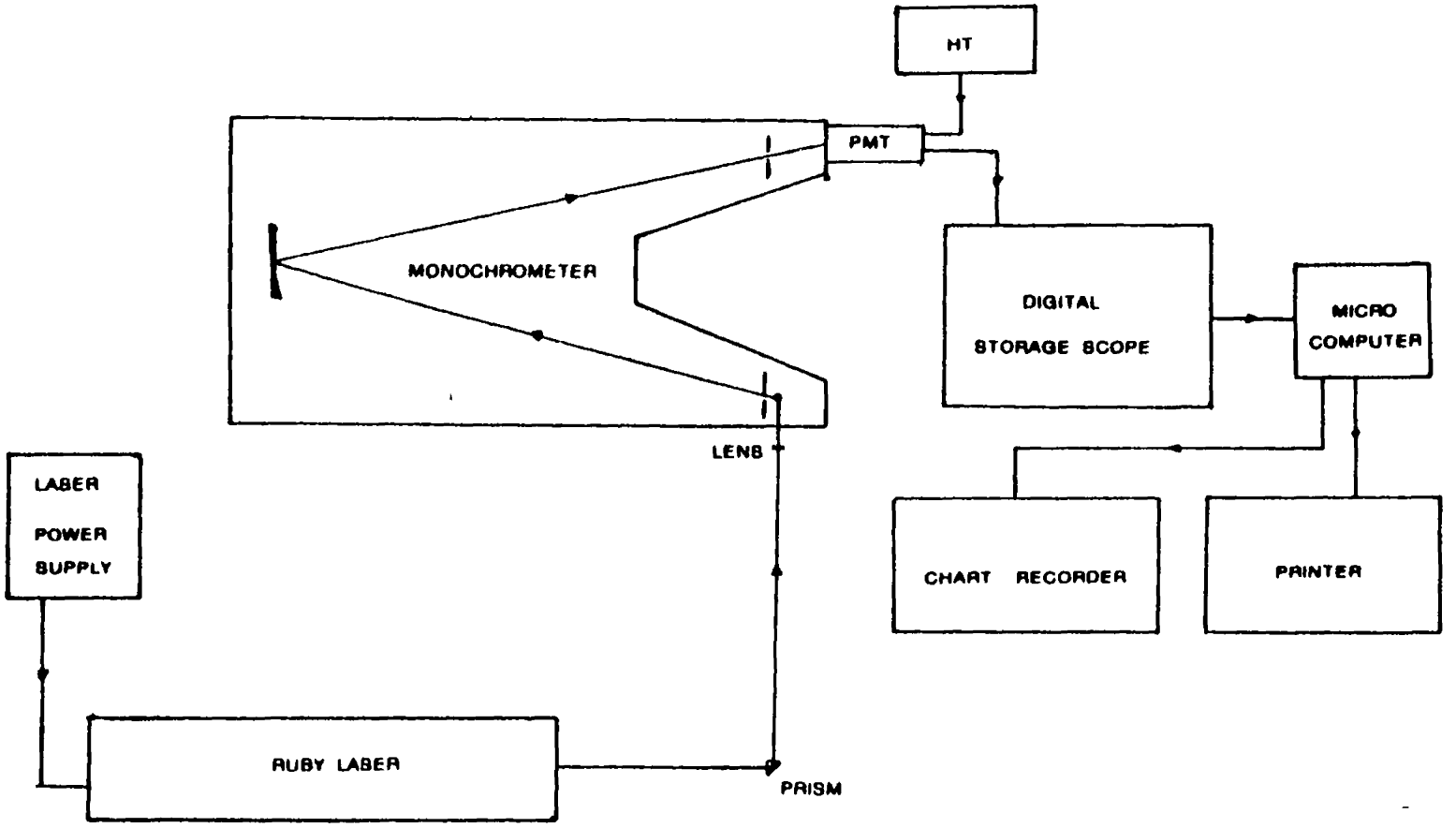

Fig (AP1 2) Shows a schematic view of the experimental arrangement used to aquire and process data used to evaluate the proformance of neutron scintillating glasses as VUV radiation detectors in the normal incidence region

To measure the luminescence output as a function of excitation wavelength in the normal incidence region the following procedure is followed The samples to be investigated are placed in the sample holder which would typically contain a number of the glass samples to be investigated and would also contain for comparison samples of sodium salicylate other commericialy available scintillators and a sample of non-scintillating ("ordinary") glass The monochrometer is then scanned in steps of 5 - 10Å over the wavelength range 2000 - 400Å At each wavelength interval each sample is rotated into position so as to be exposed to the laser produced continuum radiation Each sample is held in position for 10 laser shots and the pulses recorded by the storage scope are transfered to the computer where an average value is taken and stored along with the wavelength at which the measurement was taken This procedure is repeated for each sample in the holder and when the monochrometer has reached the end of the wavelength range a curve of wavelength against luminescent emission intensity for each of the twelve samples in the sample holder can be plotted and compared

For wavelengths shorter than 400Å the experiment is repeated using the monochrometer attachment of the two metre grazing incidence spectrograph (described in chapter two) The work described above has not as yet been completed and so results obtained by the method described above are not presented here However the luminescent emission spectra of some of the glass samples under investigation have been measured using an integrating sphere These results are shown in fig (APP1 3) along with the luminescent emission spectrum of sodium salicylate obtained in the same way It may be seen from fig (APP1 3) that the glass scintillators have a response which is similar to, but not as intense as that of sodium salicylate However glass

scintillators because of the nature of glass offer advantages over sodium salicylate and plastic scintillators in that they are robust and solid detectors Whereas sodium salicylate is only a coating of crystals on a piece of glass and is therefore subject to wear and also to adverse conditions (such as oil vapor) found in a typical vacuum environment (Samson (1964)) Plastic scintillators are also subject to mechanical wear but have the added problem that the fluorescent efficiency of plasitc scintillators is not even approximately constant with wavelength and is much less than sodium salicylate The glass detectors may also be removed from the spectrograph and cleaned whereas sodium salicylate must be replaced

When the experiments described above are complete it is hoped to have response curves for the various glass samples along with that of sodium salicylate and other commercially available plastic scintillators over the entire VUV wavelength range (30 - 2000Å) It is also hoped to obtain quantum efficiency measurements over the same range

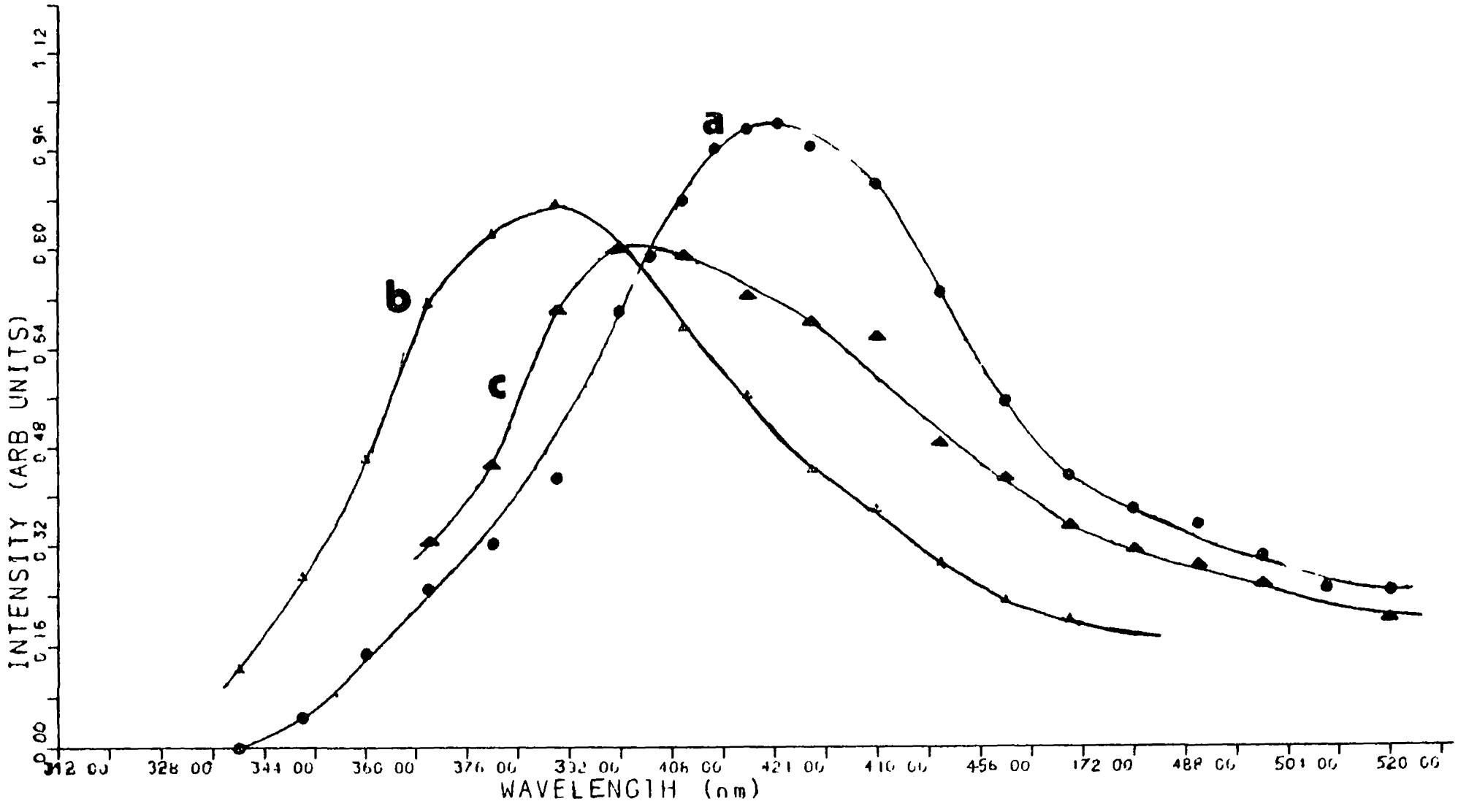

Fig (AP1 3) Luminescent emission curves obtained using a 1m integrating sphere The excitation wavelength used was 254nm Curve (a) is sodium salicylate, (b c) are cerium doped glasses

REFERENCES FOR APPENDIX ONE.

Carroll PK Kennedy ET and O'Sullivan G Appl Opt 19 PP 1454 - 1462 (1980)

Carroll PK Kennedy ET and O'Sullivan G J Quant Elect 19 12 (1983)

Dejardin G and Schwegler R Revue D'Optique 13 313 (1934)

Herb GK and Van Sciver WJ Rev Sci Instr 36 1650 (1965)

Johnson FS Watanabe K and Tousey R J Opt Soc Am 41 702 (1951)

Kuhne M Appl Opt 21 12 (1982)

Knapp RA and Smith AM Appl Opt 3 637 (1964)

Nygaard KJ and Sigmond RS Proc Roy Soc A 282 394 (1964)

Mythen C M Sc Thesis (to be completed)

Parkinson WW and Williams EE J Opt Soc Am 39 705 (1949)

Samson JAR J Opt Soc Am 56 6 (1964)

Slavin W Mooney RW and Palumbo DT J Opt Soc Am 51 93 (1961)

Spowart AR Nucl Instr and Meth 75 35 (1969)

Spowart AR Nucl Instr and Meth 135 PP 441 - 453 (1976)

Spowart AR J Phys C 12 PP 3369-3374 (1979)

Spowart AR J Phys C 12 PP 3375-3380 (1979)

Thornau DH J Opt Soc Am 46 346 (1956)

APPENDIX TWO COMPUTER PROGRAMS

APP2.1 INTRODUCTION.

This thesis has dealt with the development of a technique for recording absorption spectra of laser produced ionized species in the VUV/XUV wavelength region. In some sections of that work it was necessary to employ computer programs to, analyse data, carry out atomic theory calculations and in one instance to decide if transitions between excited states had been observed. This appendix deals only with those programs which were written as a part of that work and which have been refered to in previous sections of the thesis. The atomic theory programs (Dirac Fock and Hartree Fock) are not discussed here (although many modifications have been carried out on these programs as part of this work). Other software has also been written, to control the running of the Dirac Fock program as a batch job, and also to generate data for the Dirac Fock program when it was required to: for example, calculate energies of similar transitions along an isoelectronic sequence. Other programs for graph plotting and data analysis have also been written, these programs will also not be discussed here. Rather it is proposed to confine the discussion to the two programs specifically refered to in the preceeding chapters of this thesis.

APP2.2 THE POLLYFIT PROGRAM.

As discussed in chapter two (section 2.5) each photographic plate containing an absorption spectrum had an overlapping emission spectrum usually of aluminium or silicon which served to provide a series of reference wavelengths

from which wavelengths of unknown features in the absorption spectrum could be determined The photographic plates were measured on the photoelectric comparator in the Physics Dept of University College Dublin For each plate measured a series of data points in x y form is obtained The position of the feature along the plate is represented by x (measured to $\pm 1\mu m$) and its corresponding wavelength by y For each plate the positions of a series of known reference lines along the plate are noted, also noted are the positions of each unknown feature This data is then entered into data files in the computer (VAX 11/785) where it can be used by the POLLYFIT program which is described below

The POLLYFIT program (listed below) uses two routines taken from the NAG (Numerical Algrithms Group) software library The first E02ADF is called to fit the data points (contained in an input file) to an N^{th} order Chebychev polynomial The program uses four input/output data files NIN and NOUT are the numbers of the main input and output files and are given as input by the user when the program is run The first part of the program fits the data to the Chebychev polynomial and writes the results (a sample of which is given below after the program listing) to the output file NOUT The Chebychev coefficients (which are calculated for each order up to a maximum N spesified by the user at input) for which the best fit has been obtained are written to a second output file called CH DAT These coefficients are then used in the second part of the program to interpolate the wavelengths of the unknown features The interpolation part of the program calls the second NAG routine E02AEF which uses the coefficients stored in CH DAT and the x values (stored in the second input file called PTS DAT) of the unknown features to generate the wavelengths of these features A best fit is normally obtained for second or third order polynomials, higher order fits do not normally produce better accurecy The

program is listed below along with a typical set of input and output data Two other subroutines are also called in POLLYFIT the first TIMEDATE returns to the output file the time and date at which the program was run The second subroutine CPUTIMER (written to time the run of large atomic theory programs) returns a value of the cpu time used during the program run Both of these routines use VAX/VMS run time library (RTL) system routines which are called as needed in the program (see program listing for details)

```
C POLLYFIT is a program which carries out an Nth order regression
C     on a set of arbitrary data points which are given as input.
C     Nag library mark 5  release subroutenes  E02ADF and  E02AFF
C     are used to fit the data and also to interpolate.
C=============================================================
C=============================================================
C  The help  of Gerard O'Connor of  the computer serveces unit  ==
C  of the  National Institute  for Higher  Education in Dublin  ==
C  with the interpolation part of this program is acknowledged  ==
C=============================================================
C=============================================================
      character title*80
      COMMON NIN,NOUT,itime,idate
      INTEGER I,NROWS,M,K,IWGHT,KPLUS1,IFAIL,IPLUS,
     * JPLUS1,M2,R,R2,RPLUS1,MM,N,NPLUS,MPLUS1,MPLUS2
      DOUBLE PRECISION X1,XM,D,XARG,XCAPR,FIT,RES,X(200),Y(200),
     *W(200),A(50,50),AK(50),S(50),WORK1(3,200),WORK2(2,50),
     *FLM1,FLJ,XCAP,P,B(200),RANGE,MID,XPT,H,C,FNR,XAN
      LOGICAL MIDPT
C
      CALL CPUTIMER (-1)
C**********************************************************************
C Four input/output files are used NIN and NOUT are input and    *
C output file numbers specified at input by the user and         *
C contains the input and output data of the main program.        *
C PTS.DAT holds the points to be interpolated, CH.DAT holds      *
C the chebychev coeffs computed in the first part of the         *
C program and used in the interpolation section which starts at *
C 12345..................................................... *
C**********************************************************************

        OPEN(UNIT=3,FILE='CH.DAT',STATUS='NEW')
        WRITE (5,88886)
        READ(5,99997)NIN,NOUT
C
C    Put a date and time on the output
C
        CALL timedate
C
        WRITE (5,500)
  40.   write (nout,499 )
  499   format (//'*******************************
     ************************',
     */'                      P O L L Y F I T .',
     */'************************************************************')
  500   FORMAT (' Enter a title for the output ( up to 80 chrs )')
        READ (5,510) TITLE
        WRITE (NOUT,509) title
        WRITE ( 15,510 ) title
        NROWS = 50
  509   format (//// 1x,A80)
  510   format (1A80 )

      WRITE (5,88888)
   20 READ (5,99997) M
```

```
        MM=M
      IF (M.LE.0) STOP
      WRITE (5,88887)
      READ (5,99997) K
      IWGHT=1.0
      KPLUS1 = K + 1
      DO 60 R=1,M
         IF (IWGHT.EQ.1.0) GO TO 40
         READ (NIN,*) X(R), Y(R)
         GO TO 60
   40    READ (NIN,*) X(R), Y(R)
         W(R) = 1.0
   60 CONTINUE
      WRITE (NOUT,99994) M, K
      IF (IWGHT.NE.1) GO TO 80
      WRITE (NOUT,99993)
      GO TO 100
   80 WRITE (NOUT,99992)
  100 DO 140 R=1,M
         IF (IWGHT.NE.1) GO TO 120
         WRITE (NOUT,99991) R, X(R), Y(R)
         GO TO 140
  120    WRITE (NOUT,99991) R, X(R), Y(R), W(R)
         WRITE (15,99991) R,X(R),Y(R)
  140 CONTINUE
      IFAIL = 1
      CALL E02ADF(M,KPLUS1,NROWS,X,Y,W,WORK1,WORK2,A,S,IFAIL)
      IF (IFAIL.NE.0) GO TO 300
      WRITE (NOUT,99990)
C
C  The Chebyshev coeffs are put into a file called CH.DAT
C  and are  recalled into the  second part of the program
C  to be used in interpolation.....
C
      VAL=999.
      DO 160 IPLUS1=1,KPLUS1
         I = IPLUS1 - 1
         WRITE (NOUT,99989) I
         WRITE (NOUT,99988) (A(IPLUS1,JPLUS1),JPLUS1=1,IPLUS1)
         WRITE (4,99988) (A(IPLUS1,JPLUS1),JPLUS1=1,IPLUS1)
         WRITE (NOUT,99987) S(IPLUS1)
      IF ( ABS(S(IPLUS1)) .LT. VAL ) THEN
         III=IPLUS1
         VAL=S(IPLUS1)
      ENDIF
  160 CONTINUE
        II = III-1
        WRITE(NOUT,88885)VAL,II
        WRITE(3,555)III
        WRITE(3,556) (A(III,P),P=1,III)
555     FORMAT(I5)
556     FORMAT(F20.3)
        CLOSE(3)
C
Calculation of the chebychev coeffs is now complete.
```

```
      DO 180 IPLUS1=1,KPLUS1
      AK(IPLUS1) = A(KPLUS1,IPLUS1)
      write(3,556)ak(iplus1)
  180 CONTINUE
      X1 = X(1)
      XM = X(M)
      D = XM - X1
      WRITE (NOUT,99986) K
      WRITE (15,99986) K
      MIDPT = .FALSE.
      M2 = 2*M - 1
      R = 0
      DO 280 R2=1,M2+1
         IF(R2.EQ.M2+1)GOTO 12345
         IF (.NOT.MIDPT) GO TO 220
         XARG = 0.5D0*(X(R)+X(R+1))
         XCAPR = ((XARG-X1)-(XM-XARG))/D
         IFAIL = 1
         CALL E02AFF(KPLUS1, AK, XCAPR, FIT, IFAIL)
         IF (IFAIL.NE.0) GO TO 200
         WRITE (NOUT,99985) XARG, FIT
         GO TO 260
  200    WRITE (NOUT,99984) XARG
         GO TO 260
  220    R = R + 1
         XCAPR = ((X(R)-X1)-(XM-X(R)))/D
         IFAIL = 1
         CALL E02AFF(KPLUS1, AK, XCAPR, FIT, IFAIL)
         IF (IFAIL.NE.0) GO TO 240
         RES = FIT - Y(R)
         WRITE (NOUT,99991) R, X(R), FIT, RES
         WRITE (15,99991) R,X(R),FIT,RES
         GO TO 260
  240    WRITE (NOUT,99983) R, X(R)
  260    MIDPT = .NOT.MIDPT
  280 CONTINUE
      GO TO 20
  300 GO TO (320, 340, 360, 380, 400), IFAIL
  320 WRITE (NOUT,99982)
      GO TO 20
  340 WRITE (NOUT,99981)
      GO TO 20
  360 WRITE (NOUT,99980)
      GO TO 20
  380 WRITE (NOUT,99979)
      GO TO 20
  400 WRITE (NOUT,99978)
      GO TO 20
99998 FORMAT ('RESULTS'//)
99997 FORMAT (2I4)
99994 FORMAT (///'  Nth; order polynomial fit to an arbitrary
     * set of data points.',/'----------------------
     *----------------------------------------',
     * //' Input data ', /'-----------',//' Number of data
```

```
     *points =' ,I4, // ' Maximum degree = ',I4 )
99993 FORMAT (/ ' Unit weighting factors are used. ',
     *//3x, 'r',3x,' Position X(r)',6x, ' Wavelength Y(r)'/)
99992 FORMAT (//'   r      Abscissa X(r)       Ordinate Y(r)' )
99991 FORMAT (1x, I3,1x,F10.3,10x,F10.3,10x,F12.8)
99990 FORMAT (//' RESULTS',/' -------')
99989 FORMAT (/' DEGREE', I4,//' J  CHEBYSHEV COEFF A(J)'/)
99988 FORMAT (1x, F20.8)
99987 FORMAT (/' R.M.S. residual =', F20.8)
99986 FORMAT (/' POLYNOMIAL APPROXIMATION AND RESIDUALS FOR DEGREE',
     * I4,//'   R     POSITION            WAVELENGTH     ',
     * '      RESIDUAL',/)
99985 FORMAT (3x,F10.3,10x,F10.3)
99984 FORMAT (5x,F20.3,' Argument outside range. ')
99983 FORMAT (1x,I3, F10.3,'           ARGUMENT OUTSIDE RANGE')
99982 FORMAT (/ ' NON-POSITIVE WEIGHT')
99981 FORMAT (/'Values of independent variable not
     * increasing monotonically.')
99980 FORMAT (/' Values of independent variable all equal ')
99979 FORMAT (/'Too few distinct values of the independent variable.
99978 FORMAT (/' NROWS FAILS TO EXCEED MAXIMUM DEGREE')
88888 FORMAT(//,' Input the No of data points m.')
88887 FORMAT(//,' Input the maximum degree ')
88886 FORMAT(//,' Input and output file numbers (nin and nout )')
88885 FORMAT(////,' Minimum  R.M.S. residual is is. ',F10.7
     *,'   and occurs for degree ', I3)
12345 CONTINUE
C
          CALL CPUTIMER (1)
C
C     ****************************************************************
C       RANGE + MIDPT OF DATA TO BE INTERPOLATED  ARE CALCULATED
C       THESE ARE USED IN THE SCALING CALCULATIONS.............
C     ****************************************************************
         RANGE=X(MM)-X(1)
         MID=X(1)+(range/2)
         REWIND(3)
         OPEN(17,FILE='PTS.DAT',STATUS='O D')
         OPEN(UNIT=3,FILE='CH.DAT',STATUS='O D')
         NIN=3
         NOUT=7
        WRITE (NOUT,69995)
        IF (MM.LE.0) STOP
22      READ (NIN,69997,END=67) N
        NPLUS1 = N
        MPLUS1 = MM + 1
        MPLUS2 = MM + 2
        FLM1 = MM - 1
        READ (NIN,69996) (R(I),I=1,NPLUS1)
        write (nout,69994)
        WRITE (NOUT,69991)
          R=0
          IJK=1
          DO WHILE(IJK.EQ.1)
          R=R+1
```

```
        READ(17,7998,END=67)XCAP
C    ****************************************************************
C    SCALING CALCULATIONS ARE NOW DONE TO SCALE THE X(r) VALUES
C    SUCH THAT X(max) BECOMES +1 AND X(min) BECOMES -1...
C    I.E,       -1<X(r)<+1 ..........................................
C    ****************************************************************
         XPT=XCAP
         XCAP=(XCAP-MID)/(RANGE/2)
         IFAIL = 1
         CALL E02AEF(NPLUS1, B, XCAP, P, IFAIL)
                IF(IFAIL.NE.0)GOTO 44
C
C       WAVELENGTH TO  ENERGY CONVERSION.....
C
         Enr=12398.5415/P

         WRITE (NOUT,69990) R, XPT, P,Enr
C
C       END OF CONVERSION.....................
C
          if (p.eq.(0.0)) then
          go to 44
          else
          go to 66
          endif
   44     WRITE (NOUT,69989) R, XPT
   66 END DO
      GO TO 22
   67    close(3)
         close (17)
      CALL CPUTIMER (0)
      CALL CPUTIMER (1)
      WRITE (5,55555)
         WRITE (5,55554)
            WRITE (5,55553)
               write (nout,55555)
            write (nout,55554)
         write (nout,55553)
69999 FORMAT (6A4, 1A3)
69997 FORMAT (I5)
69996 FORMAT (F21.11)
69995 FORMAT (1F0)
69994 format (//'*********************************
     *********************************',
     */'            I N T E R P O L A T I O N
     *    F O L L O W S ',
     */'*********************************
     *********************************')
69991 FORMAT (//'   R    Position X(r)    Wavelength Y(r)',
     * '       Energy (eV)'/)

69990 FORMAT (1x, I3,2x,f10.3,7x,f10.3,12x,f10.3,3x,F10.3 )
69989 FORMAT (1x, I3,2x,F10.3, '       ARGUMENT outside RANGE.')
55555 format (///' ******************************
     ************************')
```

```
55554 format (//'              E N D     O F     D A T A .')
55553 format (//' ********************************
     **********************')

7998  FORMAT(F20.3)
      STOP' END OF PROGRAM'
      END
C*********************************************************************
C*********************************************************************
      SUBROUTINE CPUTIMER (I)
      INTEGER*4 LIBSINIT_TIMER,LIBSSHOW_TIMER,LIBSSTAT_TIMER,
     *VALUE,CODE,STATUS
      INTEGER  DAYS,HOURS,MINUIT
      REAL VALU,HRS,MINS,MIN,SECS,HURS,SIXTY,TFOUR,HUNDT
      COMMON NIN,NOUT
C
C THIS  SUBROUTINE CALCULATES  THE CPU  TIME  WHICH IS USED
C DURING THE PROGRAM RUN.
C IT HAS TWO MODES :
C (1) I=0   WRITES TO SYS$OUTPUT THE  TIME USED IN SECONDS
C           SINCE THE LAST CALL. UNLESS OTHERWISE ASSIGNED
C           SYS$OUTPUT IS THE SCREEN.
C
C     I=-1  USED TO INITIALISE  THE CPU TIME STORED STATUS.
C
C (2) I=1   RETURNS  THE CPU  TIME  USED SINCE LAST CALL TO
C           LIBSINIT_TIMER WAS MADE... THE RESULT IS WRITTEN
C           TO THE NOUT FILE....
C
C THE VAX/VMS RUN-TIME LIBRARY (RTL) ROUTINES LIBSINIT_TIMER
C LIBSSTAT_TIMER AND  LIBSSHOW_TIMER  ARE USED TO  CALCULATE
C THE CPU TIMES DISPLAYED....
C
C  ******INITIALIZE THE CPU TIMER********
C
      IF (I.EQ.-1) GO TO 1
      IF (I.EQ. 0) GO TO 2
      IF (I.EQ. 1) GO TO 3
C
C   MODE (1)
C
   1  CALL LIBSINIT_TIMER
      RETURN
C
C
   2  CODE = 0
      CALL LIBSSHOW_TIMER (,CODE,)
      CODE = 2
      CALL LIBSSHOW_TIMER (,CODE,)
      RETURN
C
C   MODE (2) *** PRINT OUT THE CPU TIME USED ***
C

   3   CODE=2
```

```
      HUNDT = 100.0
      STATUS= LIBSSTAT_TIMER(%REF(CODE),%REF(VALUE),)
C     IF (.NOT.STATUS) CALL LIBSSIGNAL(%VAL(STATUS))
      VALU  = VALUE/HUNDT
      SIXTY = 60.0
      TFOUR = 24.0
C
      IF (VALU .GE. SIXTY) THEN
      MINS = VALU/SIXTY
      SECS =(MINS - INT(MINS))*SIXTY
      else
      secs = valu
      END IF
C
      IF (MINS .GE. SIXTY) THEN
      HRS = MINS/SIXTY
      MIN = (HRS - INT(HRS))*SIXTY
      MINUIT = INT(MIN)
      else
      minuit = int(MINS)
      END IF
C
      IF (HRS .GE. TFOUR) THEN
      DAY = HRS/TFOUR
      HURS = (DAY- INT(DAY))*SIXTY
      HOURS = INT(HURS)
      DAYS = INT(DAY)
      else
      HOURS = int(HRS)
      END IF
C
      WRITE ( NOUT,222)DAYS,HOURS,MINUIT,SECS
  222 FORMAT (//4X,'ELAPSED CPU TIME FOR THIS PROCESS IS. ',//
     * 4X,I2,':',I2,':',I2,':',F5.2 )
      RETURN
      END
C*****************************************************************
C*****************************************************************
      SUBROUTINE timedate
C   timedate returns the time and date of execution of the program
C   IT USES THE UTILITY TIME AND DATE ROUTINES WHICH RETURNS
C   TIME AND DATE IN IN CHARACTER*12 FORMAT.
      CHARACTER*25 ITIME,IDATE
      COMMON NIN,NOUT
      CALL TIME (ITIME)
      CALL DATE (IDATE)
      write (nout,665) ITIME,IDATE
  665 format (////' This polyfit was run at ',1A8,
     * ' on the ',1A10, '.' )
      RETURN
      END
```

This polyfit was run at 21:31:58 on the 14-DEC-85 .

****

P O L Y F I T .

****

Nth; order polynomial fit to an arbitrary set of data points.

Input data

Number of data points = 9

Maximum degree = 3

Unit weighting factors are used.

r	Position X(r)	Wavelength Y(r)
1	54.534	161.686
2	56.374	160.073
3	91.120	131.441
4	107.353	118.984
5	120.059	109.514
6	132.498	100.616
7	143.675	92.875
8	147.641	90.200
9	159.881	82.082

RESULTS

DEGREE 0

J CHEBYSHEV COEFF A(J)

232.77133333

R.M.S. residual = 29.37941885

DEGREE 1

J CHEBYSHEV COEFF A(J)

240.93488821

-40.08936728

R.M.S. residual = 1.22693804

```
DEGREE   2

J  CHEBYSHEV COEFF A(J)

        240.94589588
        -39.78422333
          1.40995351

R.M.S. residual =          0.02364705

DEGREE   3

J  CHEBYSHEV COEFF A(J)

        240.93521107
        -39.77992637
          1.40997521
         -0.01565144

R.M.S. residual =          0.02158993


Minimum  R.M.S. residual is is.  0.0215899   and occurs for degree 3

POLYNOMIAL APPROXIMATION AND RESIDUALS FOR DEGREE   3

  R      POSITION            WAVELENGTH          RESIDUAL

  1      54.534              161.673          -0.00124144
        55.454              160.878
  2      56.374              160.085           0.01229207
        73.747              145.452
  3      91.120              131.458           0.00167535
        99.236              125.135
  4     107.353              118.948          -0.00310255
       113.706              114.198
  5     120.059              109.530           0.01637174
       126.279              105.039
  6     132.498              100.624           0.00751558
       138.087               96.721
  7     143.675               92.880           0.00514913
       145.658               91.532
  8     147.641               90.191          -0.00906282
       153.761               86.101
  9     159.881               82.082           0.00000293

   ELAPSED CPU TIME FOR THIS PROCESS IS.

    0: 0: 0: 0.71
```

****

I N T E R P O L A T I O N F O L L O W S

****

R	Position X(r)	Wavelength Y(r)	Energy (eV)
1	54.534	161.674	76.689
2	56.374	160.086	77.449
3	91.210	131.386	94.367
4	98.096	126.015	98.389
5	98.778	125.488	98.802
6	107.353	118.948	104.235
7	107.996	118.463	104.661
8	120.059	109.530	113.197
9	132.096	100.907	122.871
10	132.498	100.624	123.217
11	143.675	92.880	133.490
12	144.040	92.631	133.848
13	147.641	90.191	137.470
14	157.200	83.833	147.895
15	159.881	82.082	151.052
16	0.000	ARGUMENT outside RANGE.	
17	0.000	ARGUMENT outside RANGE.	
18	56.540	159.943	77.519
19	56.854	159.672	77.650
20	57.335	159.259	77.851
21	57.766	158.889	78.033
22	58.134	158.573	78.188
23	59.016	157.816	78.562
24	59.594	157.324	78.809
25	59.933	157.035	78.954
26	66.078	151.832	81.660
27	66.586	151.405	81.690
28	67.235	150.861	82.185
29	68.067	150.165	82.566
30	68.747	149.597	82.880
31	69.166	149.247	83.074
32	71.942	146.942	84.377
33	72.293	146.651	84.544
34	72.295	146.650	84.545
35	75.407	144.087	86.049
36	75.665	143.875	86.176
37	80.700	139.775	88.704
38	80.981	139.547	88.848
39	82.030	138.700	89.391
40	82.263	138.513	89.512
41	82.842	138.046	89.814
42	83.201	137.758	90.003
43	83.646	137.400	90.237
44	84.996	136.318	90.953
45	85.361	136.026	91.148
46	86.020	135.500	91.502
47	86.299	135.277	91.653
48	87.004	134.716	92.035

49	87.353	134.438	92.225
50	87.790	134.091	92.464
51	88.427	133.585	92.814
52	89.349	132.855	93.324
53	0.000	ARGUMENT outside RANGE.	
54	0.000	ARGUMENT outside RANGE.	
55	0.000	ARGUMENT outside RANGE.	
56	0.000	ARGUMENT outside RANGE.	
57	94.949	128.458	96.518
58	95.268	128.209	96.706
59	95.361	128.137	96.760
60	95.683	127.886	96.950
61	96.423	127.311	97.388
62	97.774	126.264	98.195
63	97.855	126.201	98.244
64	0.000	ARGUMENT outside RANGE.	
65	0.000	ARGUMENT outside RANGE.	
66	0.000	ARGUMENT outside RANGE.	
67	0.000	ARGUMENT outside RANGE.	
68	0.000	ARGUMENT outside RANGE.	
69	100.104	124.467	99.613
70	100.741	123.978	100.006
71	101.647	123.283	100.569
72	102.745	122.444	101.259
73	103.513	121.858	101.746
74	0.000	ARGUMENT outside RANGE.	
75	0.000	ARGUMENT outside RANGE.	
76	0.000	ARGUMENT outside RANGE.	
77	0.000	ARGUMENT outside RANGE.	
78	108.607	118.004	105.069
79	108.681	117.948	105.119
80	109.095	117.637	105.396
81	109.497	117.336	105.667
82	110.081	116.898	106.063
83	113.035	114.696	108.099
84	113.561	114.306	108.468
85	114.230	113.810	108.940
86	113.053	114.683	108.112
87	113.579	114.293	108.481
88	117.546	111.367	111.330
89	117.793	111.186	111.512
90	118.191	110.895	111.805
91	118.568	110.619	112.084
92	119.078	110.246	112.463
93	119.501	109.937	112.778
94	119.718	109.779	112.941
95	0.000	ARGUMENT outside RANGE.	
96	0.000	ARGUMENT outside RANGE.	
97	0.000	ARGUMENT outside RANGE.	
98	120.234	109.403	113.329
99	120.386	109.292	113.444
100	0.000	ARGUMENT outside RANGE.	
101	0.000	ARGUMENT outside RANGE.	
102	0.000	ARGUMENT outside RANGE.	
103	140.008	95.394	129.972

104	0.000	ARGUMENT outside RANGE.	
105	0.000	ARGUMENT outside RANGE.	
106	0.000	ARGUMENT outside RANGE.	
107	0.000	ARGUMENT outside RANGE.	
108	156.560	84.254	147.158
109	156.623	84.212	147.230
110	156.447	84.328	147.028
111	0.000	ARGUMENT outside RANGE.	
112	0.000	ARGUMENT outside RANGE.	
113	0.000	ARGUMENT outside RANGE.	
114	140.001	95.399	129.965
115	139.999	95.400	129.964
116	133.881	99.652	124.418

ELAPSED CPU TIME FOR THIS PROCESS IS.

0: 0: 0: 1.26

****

E N D O F D A T A .

****

APP2 3 THE ENERGY LEVELS PROGRAM.

This program was written in order to determine if any of the unknown absorption lines observed in the spectra of silicon and aluminium plasmas were due to transitions involving known excited states of ion stages likely to be contained in the plasma The program takes as input a series of energy levels and corresponding values of the quantum number J and by the application of the selection rule $\Delta J = 0 \pm 1$ determines the wavelengths of all allowed transitions between the levels given as input The program also restricts the output data to within two wavelength limits spesified as input The values of the energy levels (in cm^{-1}) are stored in a file called INPUT DAT along with the quantum number J and the term value The term value for each level is a non numerical character quantity which simply identifies the individual levels being used (eg $^1S_0$ or $^3P_1$ etc) The term value takes no part in the numerical calculations of the program and is simply used in the printed output for easy identification (see sample input/output data) Typical input and output data follows the listing of the program given below The sample input given below is the list of all known energy levels of the Al IV ion taken from Martin and Zalubas (1979) and the output is the list of all allowed conbinations of these levels A DCL (Digital Command Language) procedure (not included in the program) is then used to sort the output in order of decreacing wavelength

```
C*************************************************************
C                                                            *
C                                                            *
C   A  PROGRAM THAT CALCULATES ALL THE POSSIBLE  ALLOWED     *
C                                                            *
C   TRANSITIONS  BETWEEN A NUMBER OF KNOWN ENERGY LEVELS     *
C                                                            *
C     W H I C H   A R E   G I V E N   A S   I N P U T        *
C                                                            *
C              T O G E T H E R  W I T H                      *
C                                                            *
C     C O R R I S P O N D I N G  V A L U E S  O F            *
C                                                            *
C        T H E  Q U A N T U M  N U M B E R  J.               *
C*************************************************************
      CHARACTER*11 TITLE*50,TERM(1000)
      REAL L(1000),J(1000),E(1000),A(1000),JIK,WLIM1,WLIM2
      INTEGER I,K,N
      Common itime,idate
C*************************************************************************
C  INPUT AND OUTPUT FILES ARE OPENED.  'INPUT.DAT' CONTAINS THE           *
C                                                                         *
C  LEVELS AND J VALUES WHICH THE PROGRAM USES TO CALCULATE ALL            *
C                                                                         *
C    OF THE POSSIBLE  LEVELS ACCORDING TO THE SELECTION RULES             *
C                                                                         *
C   THE CALCULATED LEVELS ARE STORED IN THE OUTPUT FILE WHICH             *
C                                                                         *
C            HAS  BEEN GIVEN THE NAME 'LEVELS.DAT'                        *
C*************************************************************************
      OPEN (UNIT=4,FILE='LEVELS2.DAT',STATUS='NEW')
      OPEN (UNIT=3,FILE='INPUT.DAT',STATUS='OLD')
      OPEN (UNIT=7,FILE='LEVELS.DAT',STATUS='NEW')
C
C    Read a title for the output .
C

      WRITE (5,555)
         READ (5,554) TITLE
            WRITE (4,551)  TITLE
               WRITE (5,551)  TITLE
  555 FORMAT (2X,////////// ' Input a title for the output.'///)
  554 FORMAT( 1A50 )
  551 FORMAT (1X,1A50 // )
C
C      Read a date for the output
C
      call timeadate
C
C  Define as inputs the longwavelength limit
C  and the short wavwlength limit of the
C  output wavelengths range.
C
      WRITE(5,663)
          READ (5,661) WLIM1
```

```
            WRITE ( 5,662)
                READ (5,661) WLIM2
  663  FORMAT ( // ' Input the long-wavelength limit.')
  662  FORMAT ( // ' Input the short-wavelength limit.' )
  661  FORMAT (1F13.0)
C
C      Read in the energy levels and the 'J' values.
C
       read (3,155,end=98 ) ( L(N),J(N),TERM(N),N=1,1000)
  155  format ( f13.3,f5.2,a11 )
   98  CLOSE (3)
C
C      write wavelength limits to output file
C
        write ( 5,660 ) wlim1,wlim2
        write ( 4,660 ) wlim1,wlim2
 660    FORMAT (//1X,'Wavelength output is restricted to between',
     * / F8.3,' and ',F7.3, '  angstroms ' // )
        WRITE (5,120)
        WRITE (4,125)
        WRITE (5,130)
        WRITE (4,135)
 120    FORMAT( 4X,' LEVEL 1',8X,'LEVEL 2',6X,'J(1)',3X,'J(2)',
     *  2X, 'DELTA J', 3X ' NEW LEVEL',8X, 'WAVELENGTH'  )
 130    FORMAT ( 9X,'CM(-1)',12X,'CM(-1)',46X,'CM(-1)',20X,'(A,'/ )
 125    FORMAT(2X,'TERM(1)',9X,'LEVEL(1)',6X,'TERM(2)',4X,'LEVEL(2)',
     *  10X,'J(1)',5X,'J(2)',4X,'DELTA(J)', 3X,'NEW LEVEL',
     *  6X, 'WAVELENGTH'  )
 135    FORMAT ( 18X,'CM(-1)',19X,'CM(-1)',40X,'CM(-1)',13X,'(A)'/ )
C
C   The selection rules are now applied by using the nested do loops
C    below.
C
       DO 77 I=1,N-1
       DO 88 K=I+1,N-1
       IF ( J(I) .EQ. 0. .AND. J(K) .EQ. 0. ) GO TO 88
       JIK = ABS( J(I)-J(K) )
       IF ((JIK.EQ.0.).OR.(JIK.EQ.1.)) THEN
            GO TO 100
                 ELSE
            GO TO 88
                 END IF
 100   E(I)= ABS(L(I)-L(K))
        A(I)= 1./(E(I)/1.E8)
       IF (( A(I) .LE. WLIM1 ).AND.( A(I) .GE. WLIM2 )) THEN
            GO TO  95
                 ELSE
            GO TO 88
                 END IF
  95   WRITE (4,175 )TERM(I),L(I),TERM(K),L(K),J(I),J(K),JIK,E(I),A(I)
       WRITE (7,175 )TERM(I),L(I),TERM(K),L(K),J(I),J(K),JIK,E(I),A(I)
       WRITE (5,185 ) L(I),L(K),J(I),J(K),JIK,E(I),A(I)
 175   FORMAT (X,A11,2X,F13.3,4X,A11,2X,F13.3, 3X, F5.2,
     *  3X, F5.2, 5X, F5.2, 3X, F13.3, 1X, F13.3  )
 185   FORMAT ( F13.3,3X,F13.3,3X,F5.2,3X,F5.2,
```

```
     *  2X,F5.2,3X,F13.3,3X,F13.3 )
  88  CONTINUE
  77  CONTINUE
C
C   selection rules are applied and levels calculated.
C
                              WRITE (5,777)
                         WRITE (5,778)
                    WRITE (5,779)
          WRITE (4,777)
                WRITE (4,778)
                      WRITE (4,779)
                            WRITE (4,880)
                            WRITE (4,881)
                      WRITE (4,882)
                WRITE (4, 991)
          WRITE (4, 990)
  777    FORMAT (// ' ********************************************** '//)
  778    FORMAT ( '              E N D   O F   D A T A    ' //)
  779    FORMAT ( ' ********************************************** '//)
  880    FORMAT( //' ==========================================
     *==================================================='//)
  881    FORMAT( '  OUTPUT IS ARRANGED IN ORDER OF DECENDING
     * WAVELENGTH BELOW.'//)
  882    FORMAT ('==========================================
     *==================================================='//)
  991    FORMAT(2X,'TERM(1)',9X,'LEVEL(1)',6X,'TERM(2)',4X,'LEVEL(2)',
     *   10X,'J(1)',5X,'J(2)',4X,'DELTA(J)', 3X,'NEW LEVEL',
     *   6X, 'WAVELENGTH'  )
  990    FORMAT ( 18X, 'CM(-1)',19X, 'CM(-1)', 40X,'CM(-1)',13X,'(A)'// )
  888    CLOSE(3)
         CLOSE(4)
  999    CLOSE(7)
          STOP 'END OF JOB'
          END
C*********************************************************************
C*********************************************************************
       SUBROUTINE timedate
C    timedate returns the time and date of execution of the program
C    IT USES THE UTILITY TIME AND DATE ROUTINES WHICH RETURNS
C    TIME AND DATE IN IN CHARACTER*12 FORMAT.
        CHARACTER*25 ITIME,IDATE
        COMMON NIN,NOUT
        CALL TIME (ITIME)
        CALL DATE (IDATE)
        write (4,665) ITIME,IDATE
        write (5,665) ITIME,IDATE
  665   format (////' This program was run at ',1A8,
     *  ' on the ',1A10, '.' )
        RETURN
        END
```

Input data for the energy levels program

```
000000.00,0.0,1S0 IV
616644.20,2.0,3P2 IV
618473.90,1.0,3P1 IV
620060.10,0.0,3P0 IV
624717.50,1.0,1P1 IV
671632.50,1.0,3S1 IV
671632.00,1.0,3D3 IV
680859.80,3.0,3D2 IV
681683.30,2.0,3D1 IV
682981.80,1.0,1D1 IV
685728.20,2.0,1D2 IV
686959.10,1.0,1P1 IV
687830.50,2.0,3P2 IV
688309.60,0.0,3P0 IV
688649.40,1.0,3P1 IV
714096.90,0.0,1S0 IV
759193.40,0.0,3P0 IV
759596.80,1.0,3P1 IV
760472.30,2.0,3P2 IV
761688.40,4.0,3F4 IV
762272.50,3.0,3F3 IV
763613.60,2.0,3F2 IV
764297.10,3.0,1F3 IV
766880.80,1.0,3D1 IV
767345.50,3.0,3D3 IV
767750.60,2.0,3D2 IV
767035.70,2.0,1D2 IV
770836.90,1.0,1D1 IV
801882.30,2.0,2[3/2]2 IV
802907.50,1.0,2[3/2]1 IV
805309.70,0.0,2[1/2]0 IV
806234.90,1.0,2[1/2]1 IV
821408.90,1.0,2[1/2]1 IV
827799.50,0.0,2[1/2]0 IV
824080.00,3.0,2[5/2]3 IV
824544.70,2.0,2[5/2]2 IV
825277.90,1.0,2[3/2]1 IV
825739.60,2.0,2[3/2]2 IV
827845.90,1.0,2[3/2]1 IV
828439.20,2.0,2[3/2]2 IV
828498.80,1.0,2[1/2]1 IV
836666.50,0.0,2[1/2]0 IV
851722.10,0.0,2[1/2]0 IV
852007.50,1.0,2[1/2]1 IV
852570.50,2.0,2[3/2]2 IV
855272.70,1.0,2[3/2]1 IV
852706.80,4.0,2[7/2]4 IV
853039.10,3.0,2[7/2]3 IV
853749.40,2.0,2[5/2]2 IV
853971.50,3.0,2[5/2]3 IV
856625.40,2.0,2[5/2]2 IV
856859.90,3.0,2[5/2]3 IV
856843.10,2.0,2[3/2]2 IV
858642.00,1.0,2[3/2]1 IV
857409.60,1.0,2[3/2]1 IV
857436.70,2.0,2[3/2]2 IV
857642.70,5.0,2[9/2]5 IV
857645.90,4.0,2[9/2]4 IV
857810.50,3.0,2[5/2]3 IV
857835.10,2.0,2[5/2]2 IV
858051.40,3.0,2[7/2]3 IV
858055.60,4.0,2[7/2]4 IV
861246.90,3.0,2[7/2]3 IV
861252.40,4.0,2[7/2]4 IV
861257.70,3.0,2[5/2]3 IV
861274.80,2.0,2[5/2]2 IV
870991.90,2.0,2[3/2]2 IV
871512.20,1.0,2[3/2]1 IV
874422.90,0.0,2[1/2]0 IV
874756.80,1.0,2[1/2]1 IV
894610.00,1.0,2[1/2]1 IV
896140.00,1.0,2[3/2]1 IV
897197.10,1.0,2[3/2]1 IV
897217.60,2.0,2[3/2]2 IV
897324.70,5.0,2[9/2]5 IV
897328.40,4.0,2[9/2]4 IV
897416.80,3.0,2[5/2]3 IV
897435.70,2.0,2[5/2]2 IV
897470.30,2.0,2[5/2]2 IV
897471.00,3.0,2[5/2]3 IV
897506.50,5.0,2[11/2]5 IV
897506.00,6.0,2[11/2]6 IV
897537.50,3.0,2[7/2]3 IV
897540.10,4.0,2[7/2]4 IV
897571.00,3.0,2[7/2]3 IV
897572.11,4.0,2[7/2]4 IV
897608.50,4.0,2[9/2]4 IV
897610.00,5.0,2[9/2]5 IV
899310.00,1.0,2[3/2]1 IV
900836.90,3.0,2[5/2]3 IV
900854.10,2.0,2[5/2]2 IV
900843.60,3.0,2[7/2]3 IV
900847.70,4.0,2[7/2]4 IV
900988.40,4.0,2[9/2]4 IV
900989.00,5.0,2[9/2]5 IV
900990.22,3.0,2[7/2]3 IV
900991.35,4.0,2[7/2]4 IV
917250.00,1.0,2[1/2]1 IV
918160.00,1.0,2[3/2]1 IV
921440.00,1.0,2[3/2]1 IV
931360.00,1.0,2[3/2]1 IV
934670.00,1.0,2[3/2]1 IV
967804.00,1.0,2P3/2[IM IV
971246.00,1.0,2P1/2[IM IV
1045200.00,1.0,3P1 IV
1046500.00,1.0,1P1 IV
1183700.00,1.0,3P1 IV
1185100.00,1.0,1P1 IV
1241000.00,1.0,1P1 IV
1269200.00,1.0,1P1 IV
```

TEST DATA FOR APPENDIX TWO

This program was run at 18:74:38 on the 14-DEC-85 .

Wavelength output is restricted to between
200.000 and 10 000 angstroms

TERM(1)	IFVFI(1) CM(-1)	TERM(2)	IFVFI(2) CM(-1)	J(1)	J(2)	DELTA(J)	NEW IFVFI CM(-1)	WAVELENGTH (A)
1S0 IV	0.000	3P1 IV	618473.875	0 00	1.00	1.00	618473.875	161.688
1S0 IV	0 000	1P1 IV	624717.500	0 00	1.00	1 00	624717 500	160.072
1S0 IV	0.000	3S1 IV	671632.500	0 00	1.00	1.00	671632.500	148.891
1S0 IV	0 000	3D3 IV	671632.000	0 00	1.00	1.00	671632.000	148.891
1S0 IV	0.000	1D1 IV	682981.813	0 00	1.00	1.00	682981.813	146.417
1S0 IV	0.000	1P1 IV	688959.125	0.00	1 00	1.00	688959.125	145.569
1S0 IV	0.000	3P1 IV	688649.375	0.00	1.00	1.00	688649.375	145.212
1S0 IV	0.000	3P1 IV	759596.813	0 00	1.00	1.00	759596.813	131 649
1S0 IV	0 000	3D1 IV	766880.8 3	0.00	1 00	1.00	766880 813	130 398
1S0 IV	0.000	1D1 IV	770836 875	0 00	1 00	1.00	770836.875	129.779
1S0 IV	0 000	2[3/2]1 IV	802907.500	0 00	1 00	1.00	802907.500	124 547
1S0 IV	0 000	2[1/2]1 IV	806234.875	0 00	1 00	1.00	806234 875	124 033
1S0 IV	0.000	2[1/2]1 IV	821408.875	0 00	1 00	1.00	821408 875	121.742
1S0 IV	0 000	2[3/2]1 IV	825277.875	0 00	1 00	1.00	825277.875	121.171
1S0 IV	0.000	2[3/2]1 IV	827845.875	0.00	1 00	1.00	827845.875	120.795
1S0 IV	0 000	2[1/2]1 IV	828498.813	0 00	1 00	1.00	828498.813	120 700
1S0 IV	0.000	2[1/2]1 IV	852007.500	0.00	1.00	1.00	852007.500	117.370
1S0 IV	0.000	2[3/2]1 IV	855272.688	0 00	1.00	1.00	855272.688	116.922
1S0 IV	0.000	2[3/2]1 IV	858642.000	0 00	1.00	1.00	858642.000	116 463
1S0 IV	0.000	2[3/2]1 IV	857409.625	0.00	1.00	1.00	857409.625	116.630
1S0 IV	0.000	2[3/2]1 IV	871512.188	0 00	1.00	1.00	871512.188	114.743
1S0 IV	0 000	2[1/2]1 IV	874756.813	0.00	1 00	1.00	874756.813	114.317
1S0 IV	0.000	2[1/2]1 IV	894610.000	0.00	1.00	1.00	894610.000	111.781
1S0 IV	0.000	2[3/2]1 IV	896140.000	0.00	1.00	1.00	896140.000	111.590
1S0 IV	0 000	2[3/2]1 IV	897197.125	0 00	1 00	1.00	897197.125	111.458
1S0 IV	0.000	2[3/2]1 IV	899310 000	0 00	1 00	1.00	899310 000	111 196
1S0 IV	0 000	2[1/2]1 IV	917250.000	0 00	1.00	1.00	917250 000	109.022
1S0 IV	0.000	2[3/2]1 IV	918160.000	0 00	1.00	1.00	918160.000	108 913
1S0 IV	0.000	2[3/2]1 IV	921440.000	0.00	1.00	1.00	921440.000	108.526
1S0 IV	0.000	2[3/2]1 IV	931360.000	0 00	1.00	1.00	931360 000	107.370
1S0 IV	0.000	2[3/2]1 IV	934670.000	0.00	1.00	1.00	934670.000	106.990
1S0 IV	0.000	2P3/2[1 IM IV	967804.000	0 00	1 00	1.00	967804.000	103.327
1S0 IV	0 000	2P1/2[1 IM IV	971246.000	0 00	1.00	1.00	971246.000	102.961
1S0 IV	0.000	3P1 IV	1045200.000	0 00	1.00	1.00	1045200.000	95.675
1S0 IV	0 000	1P1 IV	1046500.000	0.00	1.00	1.00	1046500.000	95.557
1S0 IV	0.000	3P1 IV	1183700.000	0.00	1.00	1.00	1183700.000	84 481
1S0 IV	0.000	1P1 IV	1185100.000	0 00	1.00	1.00	1185100.000	84 381
1S0 IV	0 000	1P1 IV	1241000.000	0 00	1.00	1.00	1241000.000	80.580
1S0 IV	0 000	1P1 IV	1269200.000	0 00	1.00	1.00	1269200.000	78 790
1S0 IV	0.000	2S1/2[IM IV	1326620.000	0 00	1.00	1.00	1326620 000	75.380
3P2 IV	616644 188	3P1 IV	1183700.000	2.00	1.00	1.00	567055.813	176.349
3P2 IV	616644 188	1P1 IV	1185100.000	2.00	1.00	1.00	568455.813	175.915
3P2 IV	616644 188	1P1 IV	1241000.000	2 00	1.00	1.00	624355 813	160.165
3P2 IV	616644.188	1P1 IV	1269200.000	2.00	1 00	1.00	652555.813	153.244

3P2 IV	616644.188	2S1/2(IM IV	1326620.000	2.00	1.00	1.00	709975.813	140.850
3P1 IV	618473.875	3P1 IV	1183700.000	1.00	1.00	0.00	565226.125	176.920
3P1 IV	618473.875	1P1 IV	1185100.000	1 00	1.00	0.00	566626.125	176.483
3P1 IV	618473.875	1P1 IV	1241000.000	1.00	1.00	0.00	622526.125	160.636
3P1 IV	618473.875	1P1 IV	1269200.000	1.00	1.00	0.00	650726.125	153.674
3P1 IV	618473.875	2S1/2(IM IV	1326620.000	1.00	1.00	0.00	708146.125	141.214
3P0 IV	620060.125	3P1 IV	1183700 000	0 00	1.00	1.00	563639 875	177.418
3P0 IV	620060.125	1P1 IV	1185100.000	0 00	1.00	1.00	565039.875	176.979
3P0 IV	620060 125	1P1 IV	1241000.000	0.00	1.00	1.00	620939 875	161.046
3P0 IV	620060 125	1P1 IV	1269200.000	0.00	1.00	1.00	649139.875	154.050
3P0 IV	620060.125	2S1/2(IM IV	1326620 000	0.00	1.00	1.00	706559.875	141.531
1P1 IV	624717.500	3P1 IV	1183700.000	1 00	1.00	0.00	558982.500	178.896
1P1 IV	624717.500	1P1 IV	1185100.000	1.00	1.00	0.00	560382.500	178.450
1P1 IV	624717 500	1P1 IV	1241000.000	1.00	1.00	0.00	616282.500	162.263
1P1 IV	624717.500	1P1 IV	1269200.000	1.00	1.00	0.00	644482.500	155.163
1P1 IV	624717.500	2S1/2(IM IV	1326620.000	1.00	1.00	0.00	701902.500	142.470
3S1 IV	671632.500	3P1 IV	1183700.000	1.00	1.00	0.00	512067.500	195.287
3S1 IV	671632.500	1P1 IV	1185100.000	1.00	1 00	0.00	513467.500	194.754
3S1 IV	671632.500	1P1 IV	1241000.000	1.00	1.00	0.00	569367.500	175.633
3S1 IV	671632.500	1P1 IV	1269200.000	1.00	1.00	0.00	597567.500	167.345
3S1 IV	671632.500	2S1/2(IM IV	1326620 000	1.00	1.00	0.00	654987 500	152.675
3D3 IV	671632.000	3P1 IV	1183700.000	1.00	1 00	0.00	512068 000	195.287
3D3 IV	671632.000	1P1 IV	1185100.000	1.00	1.00	0.00	513468 000	194.754
3D3 IV	671632.000	1P1 IV	1241000.000	1.00	1.00	0.00	569368.000	175.633
3D3 IV	671632.000	1P1 IV	1269200.000	1.00	1 00	0.00	597568.000	167.345
3D3 IV	671632.000	2S1/2(IM IV	1326620.000	1.00	1.00	0.00	654988 000	152.675
3D1 IV	681683.313	3P1 IV	1183700.000	2 00	1.00	1.00	502016.688	199 197
3D1 IV	681683.313	1P1 IV	1185100.000	2.00	1.00	1.00	503416.688	198.643
3D1 IV	681683.313	1P1 IV	1241000.000	2.00	1.00	1 00	559316.688	178.790
3D1 IV	681683.313	1P1 IV	1269200.000	2.00	1 00	1.00	587516.688	170.208
3D1 IV	681683.313	2S1/2(IM IV	1326620.000	2.00	1.00	1.00	644936.688	155.054
1D1 IV	682981 813	3P1 IV	1183700.000	1 00	1.00	0.00	500718.188	199.713
1D1 IV	682981 813	1P1 IV	1185100.000	1.00	1.00	0.00	502118.188	199.156
1D1 IV	682981.813	1P1 IV	1241000.000	1.00	1 00	0 00	558018 188	179.206
1D1 IV	682981.813	1P1 IV	1269200.000	1.00	1 00	0.00	586218.188	170.585
1D1 IV	682981.813	2S1/2(IM IV	1326620.000	1.00	1.00	0.00	643638.188	155.367
1D2 IV	685728.188	1P1 IV	1241000.000	2.00	1.00	1.00	555271.813	180.092
1D2 IV	685728.188	1P1 IV	1269200 000	2.00	1.00	1.00	583471.813	171 388
1D2 IV	685728 188	2S1/2(IM IV	1326620.000	2.00	1 00	1 00	640891.813	156 033
1P1 IV	686959 125	1P1 IV	1241000.000	1.00	1 00	0.00	554040.875	180.497
1P1 IV	686959 125	1P1 IV	1269200.000	1.00	1.00	0.00	582240.875	171 750
1P1 IV	686959.125	2S1/2(IM IV	1326620.000	1.00	1.00	0.00	639660 875	156.333
3P2 IV	687830.500	1P1 IV	1241000.000	2.00	1.00	1.00	553169.500	180.776
3P2 IV	687830.500	1P1 IV	1269200.000	2.00	1.00	1.00	581369.500	172.008
3P2 IV	687830.500	2S1/2(IM IV	1326620.000	2.00	1.00	1.00	638789.500	156.546
3P0 IV	688309.625	1P1 IV	1241000.000	0 00	1.00	1.00	552690.375	180.933
3P0 IV	688309.625	1P1 IV	1269200.000	0.00	1 00	1 00	580890.375	172.150
3P0 IV	688309 625	2S1/2(IM IV	1326620.000	0.00	1 00	1 00	638310.375	156.664
3P1 IV	688649.375	1P1 IV	1241000.000	1.00	1.00	0 00	552350.625	181.044
3P1 IV	688649.375	1P1 IV	1269200.000	1.00	1 00	0.00	580550.625	172.250
3P1 IV	688649.375	2S1/2(IM IV	1326620.000	1.00	1.00	0.00	637970.625	156.747
1S0 IV	714096 875	1P1 IV	1241000.000	0.00	1.00	1 00	526903.125	189.788
1S0 IV	714096 875	1P1 IV	1269200 000	0.00	1.00	1.00	555103 125	180.147
1S0 IV	714096 875	2S1/2(IM IV	1326620.000	0.00	1 00	1.00	612523.125	163.259
3P0 IV	759193.375	1P1 IV	1269200.000	0.00	1 00	1.00	510006.625	196 076

3P0 IV	759193.375	2S1/2(IM IV	1326620.000	0.00	1 00	1.00	567426.625	176.234
3P1 IV	759596.813	1P1 IV	1269200.000	1.00	1.00	0.00	509603.188	196.231
3P1 IV	759596 813	2S1/2(IM IV	1326620.000	1.00	1 00	0.00	567023.188	176.360
3P2 IV	760472.313	1P1 IV	1269200.000	2 00	1.00	1.00	508727.688	196.569
3P2 IV	760472.313	2S1/2(IM IV	1326620.000	2.00	1.00	1.00	566147.688	176.632
3F2 IV	763613.625	1P1 IV	1269200.000	2.00	1.00	1.00	505586.375	197.790
3F2 IV	763613.625	2S1/2(IM IV	1326620.000	2.00	1 00	1.00	563006.375	177.618
3D1 IV	766880.813	1P1 IV	1269200.000	1.00	1.00	0.00	502319.188	199.077
3D1 IV	766880.813	2S1/2(IM IV	1326620.000	1.00	1.00	0.00	559739.188	178.655
3D2 IV	767750.625	1P1 IV	1269200.000	2.00	1.00	1.00	501449.375	199.422
3D2 IV	767750.625	2S1/2(IM IV	1326620.000	2.00	1.00	1.00	558869.375	178.933
1D2 IV	767035.688	1P1 IV	1269200.000	2.00	1.00	1.00	502164.313	199.138
1D2 IV	767035.688	2S1/2(IM IV	1326620.000	2.00	1.00	1 00	559584.313	178.704
1D1 IV	770836.875	2S1/2(IM IV	1326620.000	1.00	1.00	0.00	555783.125	179.926
2[3/2]2 IV	801882.313	2S1/2(IM IV	1326620.000	2.00	1.00	1.00	524737.688	190.571
2[3/2]1 IV	802907.500	2S1/2(IM IV	1326620.000	1.00	1.00	0.00	523712.500	190.944
2[1/2]0 IV	805309.688	2S1/2(IM IV	1326620.000	0.00	1.00	1.00	521310.313	191.824
2[1/2]1 IV	806234.875	2S1/2(IM IV	1326620.000	1.00	1.00	0.00	520385.125	192.165
2[1/2]1 IV	821408 875	2S1/2(IM IV	1326620.000	1.00	1.00	0.00	505211.125	197.937
2[5/2]2 IV	824544.688	2S1/2(IM IV	1326620.000	2.00	1.00	1.00	502075.313	199 173
2[3/2]1 IV	825277.875	2S1/2(IM IV	1326620.000	1.00	1.00	0.00	501342.125	199.465
2[3/2]2 IV	825739.625	2S1/2(IM IV	1326620.000	2.00	1.00	1.00	500880.375	199.648

OUTPUT IS ARRANGED IN ORDER OF DECENDING WAVELENGTH BELOW.

TERM(1)	LEVEL(1) CM(-1)	TERM(2)	LEVEL(2) CM(-1)	J(1)	J(2)	DELTA(J)	NEW LEVEL CM(-1)	WAVELENGTH (A)
1D1 IV	682981.813	3P1 IV	1183700.000	1.00	1.00	0.00	500718.188	199.713
2[3/2]2 IV	825739.625	2S1/2(IM IV	1326620.000	2.00	1.00	1.00	500880.375	199.648
2[3/2]1 IV	825277.875	2S1/2(IM IV	1326620.000	1.00	1.00	0.00	501342.125	199.465
3D2 IV	767750.625	1P1 IV	1269200.000	2.00	1 00	1.00	501449.375	199.422
3D1 IV	681683.313	3P1 IV	1183700.000	2.00	1.00	1.00	502016.688	199.197
2[5/2]2 IV	824544.688	2S1/2(IM IV	1326620.000	2.00	1.00	1 00	502075 313	199.173
1D1 IV	682981 813	1P1 IV	1185100.000	1 00	1 00	0.00	502118 188	199 156
1D2 IV	767035.688	1P1 IV	1269200.000	2.00	1.00	1.00	502164.313	199.138
3D1 IV	766880.813	1P1 IV	1269200.000	1.00	1 00	0.00	502319.188	199.077
3D1 IV	681683.313	1P1 IV	1185100.000	2.00	1.00	1.00	503416.688	198.643
2[1/2]1 IV	821408.875	2S1/2(IM IV	1326620.000	1.00	1.00	0.00	505211 125	197.937
3F2 IV	763613.625	1P1 IV	1269200.000	2.00	1 00	1.00	505586.375	197.790
3P2 IV	760472 313	1P1 IV	1269200.000	2.00	1 00	1.00	508727.688	196.569
3P1 IV	759596.813	1P1 IV	1269200.000	1.00	1.00	0.00	509603 188	196.231
3P0 IV	759193.375	1P1 IV	1269200.000	0.00	1.00	1.00	510006.625	196.076
3S1 IV	671632.500	3P1 IV	1183700.000	1.00	1 00	0.00	512067.500	195.287
3D3 IV	671632.000	3P1 IV	1183700.000	1.00	1.00	0.00	512068.000	195.287
3D3 IV	671632.000	1P1 IV	1185100.000	1.00	1.00	0.00	513468.000	194.754
3S1 IV	671632.500	1P1 IV	1185100.000	1.00	1 00	0.00	513467.500	194.754
2[1/2]1 IV	806234.875	2S1/2(IM IV	1326620.000	1.00	1.00	0.00	520385.125	192.165
2[1/2]0 IV	805309.688	2S1/2(IM IV	1326620.000	0.00	1.00	1.00	521310.313	191 824

2[3/2]1 IV	802907 500	2[1/2[IM IV	1326620 000	1.00	1 00	0 00	523712 500	190 944
2[3/2]2 IV	801882 313	2[1/2[IM IV	1326620 000	2 00	1.00	1 00	524737.688	190 571
1B0 IV	714096 875	1P1 IV	1241000 000	0.00	1 00	1 00	526903 125	189.788
3P1 IV	688649 375	1P1 IV	1241000 000	1 00	1 00	0 00	552350 625	181 044
3P0 IV	688309 625	1P1 IV	1241000 000	0.00	1 00	1 00	552690 375	180 933
3P2 IV	687830 500	1P1 IV	1241000 000	2 00	1 00	1 00	553169 500	180 776
1P1 IV	686959 125	1P1 IV	1241000 000	1.00	1 00	0 00	554040 875	180 497
1B0 IV	714096 875	1P1 IV	1269200 000	0.00	1 00	1 00	555103 125	180 147
1D2 IV	685728 188	1P1 IV	1241000 000	2 00	1 00	1 00	555271 813	180 092
1D1 IV	770836 875	2[1/2[IM IV	1326620 000	1 00	1 00	0 00	555783 125	179 926
1D1 IV	682981 813	1P1 IV	1241000.000	1 00	1 00	0 00	558018 188	179 206
3D2 IV	767750 625	2[1/2[IM IV	1326620 000	2 00	1 00	1 00	558869 375	178 933
1P1 IV	624717 500	3P1 IV	1183700 000	1 00	1 00	0 00	558982 500	178 896
3D1 IV	681683 313	1P1 IV	1241000 000	2.00	1 00	1 00	559316 688	178 790
1D2 IV	767035 688	2[1/2[IM IV	1326620 000	2 00	1 00	1 00	559584 313	178 704
3D1 IV	766880 813	2[1/2[IM IV	1326620 000	1 00	1 00	0 00	559739.188	178 655
1P1 IV	624717 500	1P1 IV	1185100 000	1 00	1 00	0 00	560382 500	178 450
3P2 IV	763013 625	2[1/2[IM IV	1326620 000	2 00	1 00	1 00	563006 375	177 618
3P0 IV	620060.125	3P1 IV	1183700 000	0 00	1 00	1 00	563639 875	177 418
3P0 IV	620060 125	1P1 IV	1185100 000	0.00	1 00	1 00	565039 875	176 979
3P1 IV	618473 875	3P1 IV	1183700 000	1 00	1 00	0 00	565226 125	176 920
3P2 IV	760472.313	2[1/2[IM IV	1326620 000	2 00	1 00	1 00	566147 688	176 632
3P1 IV	618473 875	1P1 IV	1185100 000	1.00	1 00	0 00	566626 125	176 483
3P1 IV	759596 813	2[1/2[IM IV	1326620 000	1 00	1 00	0 00	567023 188	176 360
3P2 IV	616644 188	3P1 IV	1183700 000	2 00	1 00	1 00	567055 813	176 349
3P0 IV	759193 375	2[1/2[IM IV	1326620 000	0 00	1 00	1 00	567426 625	176 234
3P2 IV	616644 188	1P1 IV	1185100.000	2 00	1 00	1 00	568455 813	175 915
3D3 IV	671632 000	1P1 IV	1241000 000	1 00	1 00	0 00	569368 000	175 631
3B1 IV	671632.500	1P1 IV	1241000 000	1 00	1 00	0 00	569367 500	175 631
3P1 IV	688649.375	1P1 IV	1269200 000	1 00	1 00	0.00	580550 625	172 250
3P0 IV	688309 625	1P1 IV	1269200 000	0 00	1 00	1 00	580890 375	172 150
3P2 IV	687830 500	1P1 IV	1269200 000	2 00	1 00	1 00	581369 500	172 008
1P1 IV	686959 125	1P1 IV	1269200 000	1 00	1 00	0 00	582240 875	171 750
1D2 IV	685728 188	1P1 IV	1269200 000	2.00	1 00	1 00	582471 813	171 588
1D1 IV	682981 813	1P1 IV	1269200 000	1 00	1 00	0 00	586218 188	170 585
3D1 IV	681683.313	1P1 IV	1269200 000	2 00	1 00	1 00	587516 688	170 208
3D3 IV	671632.000	1P1 IV	1269200 000	1 00	1 00	0.00	597568 000	167 345
3B1 IV	671632.500	1P1 IV	1269200 000	1 00	1 00	0 00	597567.500	167 345
1B0 IV	714096.875	2[1/2[IM IV	1326620.000	0 00	1 00	1.00	612523 125	163 259
1P1 IV	624717 500	1P1 IV	1241000.000	1.00	1 00	0 00	616282 500	162 263
1B0 IV	0 000	3P1 IV	618473 875	0.00	1.00	1 00	618473 875	161 688
3P0 IV	620060 125	1P1 IV	1241000 000	0.00	1 00	1 00	620939 875	161 046
3P1 IV	618473 875	1P1 IV	1241000 000	1 00	1 00	0 00	622526 125	160 636
3P2 IV	616644.188	1P1 IV	1241000.000	2.00	1 00	1 00	624355 813	160 165
1B0 IV	0 000	1P1 IV	624717 500	0.00	1 00	1 00	624717 500	160 077
3P1 IV	688649 375	2[1/2[IM IV	1326620 000	1 00	1 00	0 00	637970 625	156 747
3P0 IV	688309 625	2[1/2[IM IV	1326620 000	0 00	1 00	1 00	638310 375	156 664
3P2 IV	687830 500	2[1/2[IM IV	1326620 000	2.00	1 00	1 00	638789 500	156 546
1P1 IV	686959 125	2[1/2[IM IV	1326620.000	1 00	1 00	0 00	639660 875	156 333
1D2 IV	685728.188	2[1/2[IM IV	1326620 000	2.00	1 00	1 00	640891 813	156 033
1D1 IV	682981 813	2[1/2[IM IV	1326620 000	1.00	1 00	0 00	643638 188	155 367
1P1 IV	624717 500	1P1 IV	1269200.000	1 00	1 00	0 00	644462 500	155 163
3D1 IV	681683 313	2[1/2[IM IV	1326620 000	2 00	1 00	1 00	644936 688	155 054
3P0 IV	620060 125	1P1 IV	1269200 000	0 00	1 00	1 00	649139 875	154 050
3P1 IV	618473 875	1P1 IV	1269200 000	1.00	1 00	0 00	650726 125	153 674

3P2 IV	616644.188	1P1 IV	1269200.000	2.00
3D3 IV	671632.000	2S1/2(IM IV	1326620.000	1.00
3S1 IV	671632.500	2S1/2(IM IV	1326620.000	1.00
180 IV	0.000	3S1 IV	671632.500	0.00
180 IV	0.000	3D3 IV	671632.000	0.00
160 IV	0.000	1D1 IV	682981.813	0.00
180 IV	0.000	1P1 IV	686959.125	0.00
180 IV	0.000	3P1 IV	688649.375	0.00
1P1 IV	624717.500	2S1/2(IM IV	1326620.000	1.00
3P0 IV	620060.125	2S1/2(IM IV	1326620.000	0.00
3P1 IV	618473.875	2S1/2(IM IV	1326620.000	1.00
3P2 IV	616644.188	2S1/2(IM IV	1326620.000	2.00
180 IV	0.000	3P1 IV	759596.813	0.00
160 IV	0.000	3D1 IV	766880.813	0.00
180 IV	0.000	1D1 IV	770836.875	0.00
160 IV	0.000	2P3/2)1 IV	802907.500	0.00
160 IV	0.000	2P1/2)1 IV	806234.875	0.00
160 IV	0.000	2P1/2)1 IV	821408.875	0.00
160 IV	0.000	2P3/2)1 IV	825277.875	0.00
160 IV	0.000	2P3/2)1 IV	827845.875	0.00
180 IV	0.000	2P1/2)1 IV	828498.813	0.00
160 IV	0.000	2P1/2)1 IV	852007.500	0.00
180 IV	0.000	2P3/2)1 IV	855272.688	0.00
160 IV	0.000	2P3/2)1 IV	857409.625	0.00
160 IV	0.000	2P3/2)1 IV	858642.000	0.00
160 IV	0.000	2P3/2)1 IV	871512.188	0.00
180 IV	0.000	2P1/2)1 IV	874756.813	0.00
160 IV	0.000	2P1/2)1 IV	894610.000	0.00
160 IV	0.000	2P3/2)1 IV	896140.000	0.00
160 IV	0.000	2P3/2)1 IV	897197.125	0.00
160 IV	0.000	2P3/2)1 IV	899310.000	0.00
180 IV	0.000	2P1/2)1 IV	917250.000	0.00
160 IV	0.000	2P3/2)1 IV	918160.000	0.00
180 IV	0.000	2P3/2)1 IV	921440.000	0.00
180 IV	0.000	2P3/2)1 IV	931360.000	0.00
180 IV	0.000	2P3/2)1 IV	934670.000	0.00
160 IV	0.000	2P3/2(IM IV	967804.000	0.00
180 IV	0.000	2P1/2(IM IV	971246.000	0.00
160 IV	0.000	3P1 IV	1045200.000	0.00
180 IV	0.000	1P1 IV	1046500.000	0.00
180 IV	0.000	3P1 IV	1183700.000	0.00
180 IV	0.000	1P1 IV	1185100.000	0.00
180 IV	0.000	1P1 IV	1241000.000	0.00
160 IV	0.000	1P1 IV	1269200.000	0.00
180 IV	0.000	2S1/2(IM IV	1326620.000	0.00

****

F N D O F D A T A

****

1.00	1.00	652555.813	153.244
1.00	0.00	654988.000	152.675
1.00	0.00	654987.500	152.675
1.00	1.00	671632.500	148.891
1.00	1.00	671632.000	148.891
1.00	1.00	682981.813	146.417
1.00	1.00	686959.125	145.569
1.00	1.00	688649.375	145.212
1.00	0.00	701902.500	142.470
1.00	1.00	706559.875	141.531
1.00	0.00	708146.125	141.214
1.00	1.00	709975.813	140.850
1.00	1.00	759596.813	131.649
1.00	1.00	766880.813	130.398
1.00	1.00	770836.875	129.729
1.00	1.00	802907.500	124.547
1.00	1.00	806734.875	124.033
1.00	1.00	821408.875	121.742
1.00	1.00	825277.875	121.171
1.00	1.00	827845.875	120.795
1.00	1.00	828498.813	120.700
1.00	1.00	852007.500	117.370
1.00	1.00	855772.688	116.922
1.00	1.00	857409.625	116.630
1.00	1.00	858642.000	116.463
1.00	1.00	871512.188	114.743
1.00	1.00	874756.813	114.317
1.00	1.00	894610.000	111.781
1.00	1.00	896140.000	111.590
1.00	1.00	897197.125	111.458
1.00	1.00	899310.000	111.196
1.00	1.00	917250.000	109.022
1.00	1.00	918160.000	108.913
1.00	1.00	921440.000	108.526
1.00	1.00	931360.000	107.370
1.00	1.00	934670.000	106.990
1.00	1.00	967804.000	103.327
1.00	1.00	971246.000	102.961
1.00	1.00	1045200.000	95.675
1.00	1.00	1046500.000	95.557
1.00	1.00	1183700.000	84.481
1.00	1.00	1185100.000	84.381
1.00	1.00	1241000.000	80.580
1.00	1.00	1269200.000	78.790
1.00	1.00	1326620.000	75.380

REFERENCES FOR APPENDIX TWO

The NAG (Numerical Algrithms Group) reference/user manual Vol 2

Martin WC and Zalubas R J Phys Chem Ref Data 8 pp 817 - 864 (1979)

ACKNOWLEDGEMENTS

I am grateful to a number of people for assistance received during the course of this work

I would firstly like to thank my research supervisor Dr Eugene T Kennedy for his constant and sustained interest in the project as well as for his patience and attention to detail My thanks also go to the other members of the laser applications group at N I H E D, Gerard O'Sullivan John Costello and Ciaran Mythen for useful and helpful discussions over the course of this work I would also like to express my thanks to Professor P K Carroll of the Physics Department University College Dublin, for allowing me the use of the photoelectric comparator to measure photographic plates during this work

I am also grateful to the technical staff of the School of Physical Sciences at N I H E D for much valuable assistance while this work was in progress I also offer my thanks to Dr J Vos and the technical staff of the School of Chemical Sciences for the use of equipment in that department Lastly I would like to thank David O'Callaghan for help received in the preparation of the prints which appear in this thesis and also to Jos Evertson of the I I R S for the use of the microdensitometer